

UCSF

UC San Francisco Electronic Theses and Dissertations

Title

Migratory and adhesive cues controlling innate-like lymphocyte surveillance of the pathogen-exposed surface of the lymph node

Permalink

<https://escholarship.org/uc/item/9tk9j1qx>

Author

Zhang, Yang

Publication Date

2016

Peer reviewed|Thesis/dissertation

Migratory and adhesive cues controlling innate-like lymphocyte
surveillance of the pathogen-exposed surface of the lymph node

by

Yang Zhang

DISSERTATION

Submitted in partial satisfaction of the requirements for the degree of

DOCTOR OF PHILOSOPHY

in

Biomedical Sciences

in the

GRADUATE DIVISION

of the

UNIVERSITY OF CALIFORNIA, SAN FRANCISCO

**Migratory and adhesive cues controlling innate-like lymphocyte
surveillance of the pathogen-exposed surface of the lymph node**

Yang Zhang

University of California,

San Francisco

2016

This dissertation is dedicated to my parents, Tianxiang Zhang and Xingyun Shao, and my graduate mentor Jason Cyster. They have supported me through all that I have chosen to do and have made me confident in my competency to make an impact toward improved healthcare in society.

Acknowledgements

First, I would like to thank my graduate mentor Jason Cyster, who allowed me to study in his lab. It is a great honor and privilege to work with Jason. In the past 3 years, I have gained numerous insights from conversation with him. With his dedicated guidance, I was able to perform experiments appropriately and do the data analysis carefully. He was always so passionate about science and provided me with a lot of new angles for my graduate study. His passion inspired me to try to keep up with his pace, but later I found it was impossible for me to perform at his level. Without Jason's guidance, it would have been impossible to finish this study done such short period. After staying in Jason's lab for 3 years, I definitely deepened my understanding of biology and formed my own views of immunology, especially in regards to barrier immunity. The concept of barrier immunity became more popular after the characterization of memory resident T cells in the skin starting in the early 2000s. This concept later extended to secondary lymphoid tissue, with further teams characterizing the importance of strategically positioned antigen presenting cells (SCS macrophages and dendritic cells) in the skin draining lymph nodes. In this study, we characterized a group of innate-like lymphocytes closely associated with SCS macrophages in addition to identifying cues and adhesive molecules that establish the specialized positioning of those innate-like lymphocytes. I am sure the field of barrier immunity in lymph node will keep evolving. Some of the most important questions remaining are: 1) what are the requirements for establishing barrier immunity? 2) how do rapid barrier immune responses differ per tissue?

I would also like to thank members of the Cyster lab. Francisco Ramire-Valle was very patient and showed me a lot of techniques applied in this study. He was an extremely neat and careful person. It was great fun to do experiments with him. Mark Ansel, as a past Cyster lab trainee and my graduate advisor, was always supportive and enthusiastic about new ideas and new things. I enjoyed hanging out with his lab members at Arnold, and it brings good memories when I recall my time doing rotational work with him. Jiayi Wu, a recent member of the Cyster lab, inspired in me many new thoughts and grew me in having a deeper understanding of science. I am very much a fan of his graduate work and he always gave me fresh ideas and perspectives about science and life. It is a fortune to be able to work with Jiayi. Michael Barnes, a postdoc of the Cyster lab, was very nice and gentle. He was always open-minded and very kind to everyone. I learned a lot from him about immunology. Jinping An, the lab manager of the Cyster lab, helped so much with the mice breeding and she always brought me positive energy and a happy mood. I wish the best for her and her family. Finally I would like to thank a rotational student, Theodore Roth. As an extremely talented and bright student, he helped a lot in the study. He did far more work than a normal student would be able to complete in a short time period. It is definitely a privilege to work with such a fascinating student.

To Tianxiang Zhang, and Xingyun Shao, my parents, I would like to give my best thanks to them. Since my childhood, my parents have supported me a lot by letting me pursue whatever I was interested in. When I was a child, they worked so hard to help the family and they always tried their best to provide me with the best opportunities for education. They always told me I should learn as much as possible when I was young

and contribute back to society when I grow older. In addition, my mom has influenced me so deeply by always telling me to be kind to help and to share with others because life is short. She also told me I should treasure all my friendships since it is small chance for two random people to meet on earth. Besides my parents, I would like to thank Yike Zhang, Mengyun Ni, Weiwei Zhou, Yongjie Tao, Shilun Zhang, Jian Zhou and Beilei Feng. Those are my best friends since childhood, and they are always so supportive. We will always be a big family. Ying Zou, was one of my best friends working as a market analyst, I enjoy her companionship in the bay area when experiments don't work well. She brought a lot of comfort and understanding. Finally, I would like to thank Junliang Shen, Jingwei Zhang, Haoyu Wang, Jinbo Ma, Menghan Chen. Those are the people I developed friendships since high school, and all of them are pursuing incredible careers in their own sectors. I wish their best success and thank them for their support throughout my undergraduate and graduate studies. I feel confident to move on because of all the support I get from all these great people.

Contribution to presented work

Chapter 2 of this dissertation is a reprint of the material as it appears in a manuscript accepted by eLIFE. Yang Zhang, Theodore L. Roth, Elizabeth E. Gray, Hsin Chen, Lauren B. Rodda, Yin Liang, Patrick Ventura, Saul Villeda, Paul R. Crocker and Jason G. Cyster. Migratory and adhesive cues controlling innate-like lymphocyte surveillance of the pathogen-exposed surface of the lymph node. I contributed to most of the data in all the figures and supplemental figures in addition to helping write and revise the manuscript. Theodore L. Roth contributed to most of imaging data. Elizabeth E. Gray provided unpublished data, and helped read and revise the manuscript. Lauren B. Rodda and Yin Liang helped sort different stromal population from mouse lymph nodes and get RT-qPCR data for CCL20. Patrick Ventura and Sal Villeda performed the parabiosis surgery. Paul R. Crocker provided us with purified CD169-Fc protein used for the adhesion assay. Jason G. Cyster was involved in concept design, data analysis, and manuscript writing and revision.

Migratory and adhesive cues controlling innate-like lymphocyte surveillance of the pathogen-exposed surface of the lymph node

by

Yang Zhang

Barrer immunity in skin has been well characterized and revealed that strategically positioned antigen presenting cells and skin resident memory T cells are critical for mediating rapid innate immune response against acute pathogen invasion. In this study, we found that a similar scenario could be applied to skin-draining lymph nodes. We identified a group of $IL7R\alpha^{hi}CCR6^{+}$ innate-like lymphocytes that survey the subcapsular sinus (SCS) and associated macrophages. Acute bacterial and fungal challenge could cause SCS macrophages to activate innate-like lymphocytes to rapidly produce rapid IL17. This process depended upon intact functionality of ASC. Through dynamic analysis, we show that these innate-like lymphocytes are LN resident continually cross into and out of the SCS, which can be observed in real time. By positional analysis, CCR6 was found to be required for innate-like lymphocyte positioning near the SCS. S1PR1 is critical for innate-like lymphocytes migration into SCS from the parenchyma. Innate-like lymphocytes express high level of LFA1 and their movement from the SCS into the parenchyma is controlled by LFA1 and its ligand ICAM1. As a sialic acid-binding lectin, CD169 plays a novel role in mediating retention of innate-like lymphocytes in

SCS against shear force from lymph flow. This study defined molecular requirements for lymphocyte surveillance of the pathogen-exposed surface of the LN and identified novel roles of LFA1 and CD169 in mediating shear-resistant adhesion to keep innate-like lymphocytes resident within the lymph node.

Table of Contents

	Page
Chapter 1	
Introduction	1
References	12
Chapter 2	
Mechanism of innate-like lymphocyte surveillance of the subcapsular sinus to provide lymph node barrier immunity	19
References	55
Chapter 3	
Conclusion and discussion	95
References	105

List of Figures

	Page
Chapter 1	
Figure 1	Barrier immunity in skin 16
Figure 2	Barrier immunity in lymph node 17
Figure 3	Innate-like lymphocyte surveillance of sinus macrophages 18
Chapter 2	
Figure 1	Rapid induction of IL17 expression by IL7R α^{hi} CCR6 $^{+}$ innate-like lymphocytes in a CD169 $^{+}$ macrophage-dependent manner following bacterial and fungal challenge 79
Figure 2	IL7R α^{hi} CCR6 $^{+}$ innate-like lymphocytes are mostly LN resident 80
Figure 3	Migration dynamics, sinus exposure and CD169 $^{+}$ macrophage interaction of LN innate-like lymphocytes 81
Figure 4	CCR6 promotes innate-like lymphocyte positioning near the SCS 82
Figure 5	S1PR1 is required for innate-like lymphocyte movement into the SCS 83
Figure 6	LFA1 and ICAM1 control innate-like lymphocyte access to the LN parenchyma from the SCS 84
Figure 7	CD169 mediates SCS retention of innate-like lymphocytes 85
Figure 3-figure supplement 1	Example of automatically generated tracks for 86

	CXCR6-GFP+ cells in a CXCR6 ^{GFP/+} mouse LN	
Figure 4-figure supplement 1	CCL20 distribution in inguinal LN	87
Figure 4-figure supplement 2	Movement of CXCR6-GFP+ cells to SCS location following CCL20 injection	88
Chapter 2		
Figure 4-figure supplement 3	CCR6 is required for positioning of CCR6 ⁺ cells at the SCS	89
Figure 4-figure supplement 4	CCR6 is required for positioning of Scart2+ $\gamma\delta$ T cells at the SCS	90
Figure 5-figure supplement 1	FTY720 treatment depletes SCART2+ $\gamma\delta$ T cells from the SCS	91
Figure 5-figure supplement 2	Frequency of CXCR6 ^{GFP/+} cells plotted against their depth from the surface of the LN capsule	92
Figure 6-figure supplement 1	Effect of α L blockade on innate-like lymphocyte distribution	93
Figure 7-figure supplement 1	Effects of CD169 blockade on innate-like lymphocyte properties and distribution	94

Chapter 1

Introduction

Innate immunity at barrier surface

Barrier immunity is the rapid immune response in peripheral tissue against acute pathogenic challenge without triggering the adaptive immune response. The skin is where barrier immunity has been best established. As the primary interface between the human body and the environment, skin provides a first line of defense against physical/chemical insults and pathogens. Barrier immunity requires specialized antigen presenting cells and effector lymphocytes positioned in the frontline to mediate rapid immune response against insults. In the skin epidermis and dermis layers, keratinocytes, Langerhans and CD103+ dendritic cells are the main populations playing critical roles in sensing danger signals breaching the skin surface. In the epidermis, keratinocytes (Kalali et al., 2008; Feldmeyer et al., 2007) express various TLRs and NLRs which sense different pattern associated molecular patterns. Langerhans cells (Hunger, R. E. et al., 2004), also in the epidermis, take up lipid and microbial antigens and present them to effector T cells. Strategically positioned within the dermis, CD103+ dendritic cells present antigen from skin-tropic pathogens to activate skin resident T cells They also participate in the immune response by secreting cytokines and chemokines (Bursch, L. S. et al., 2007; Ginhoux et al., 2007; Poulin et al., 2007).

Closely positioned with these specialized antigen presenting cells are lymphocytes exerting effector function and are present in both the epidermis and dermis layer. These lymphocytes include skin resident memory T cells and innate-like lymphocytes. Moreover, the skin resident memory T cells are comprised of both memory CD4+ and/or CD8+ cells. A recent study in the model of HSV infection (Wakim, L. M., et al., 2008) has shown that both CD4+ and CD8+ memory T cells activated by skin DCs are critical

for HSV clearance in peripheral tissues. Innate-like lymphocytes, including $\gamma\delta$ T cells and NKT cells, are also present in this model. They express surface receptors to sense infected pathogens and can participate in mediating the innate immune response by secreting effector cytokines and anti-microbial peptides.

In summary, upon pathogen invasion through the skin lesion, strategically positioned antigen presenting cells (keratinocytes, Langerhans cells and dermal DCs) in both epidermis and dermis layers can rapidly sense and produce inflammatory mediators required for skin resident T cell and innate-like lymphocyte activation, resulting in pathogen clearance. Rather than relying on circulating T cells (Nestle, O. F. et al., 2008) to control bacterial invasion in the skin, rapid immune responses mediated by skin resident memory T cells (CD4+ and CD8+) and innate-like lymphocytes ($\gamma\delta$ T cells and NKT cells) are critical in skin barrier immune response against acute pathogen invasion (Figure 1).

Lymph nodes can be viewed as extensional space of lymphatic vessels from dermal space, so presumably pathogens breaching the dermis could be exposed to lymph node very rapidly as well. This opens the question whether similar barrier immunity exists in lymph nodes. Understanding of skin barrier immunity lays down important basis for the field of barrier immunity in lymph nodes.

Conventional view of LN as sites for adaptive immune response

Lymph nodes are most commonly known for their importance in generating adaptive immune responses. As a critical component of secondary lymphoid organs (spleen, lymph nodes, tonsils and peyer's patches), LNs act as filters (Cyster, 1999) that

actively concentrate antigen to be sampled by recirculating lymphocytes. Lymph nodes are throughout the mammalian body and are an integral part of lymph drainage from both skin and visceral organs, sampling antigen in the passing lymph fluid before it is returned to the bloodstream through the thoracic duct.

Coordinated by stromal structural cells and the master chemokines CCL21 and CXCL13, lymph nodes are segregated into a central T zone and B cell regions (follicles), with naïve T and B cells continuously arriving from blood through HEVs and leaving the lymph nodes through the efferent lymphatic vessel. Classic adaptive immune responses are initiated when dendritic cells pick up antigen upon pathogen entry. After activation through pattern recognition receptor systems, DCs become highly migratory and utilize lymphatic vessels as highways to reach draining lymph nodes. Upon arriving, DCs (Braun, et al., 2011) cross the subcapsular sinus floor and migrate towards the T zone .

Approximately 1 in 100,000 naïve T cells with cognate TCR will recognize and be activated by antigen presented as a peptide-MHC complex from incoming DCs. Activation of T cells promotes their differentiation into T helper cells. Through the down-modulation of CCR7 and the upregulation of CXCR5 and the recently identified EBI2, activated T cells migrate towards the B-T boundary and interfollicular area to promote cognate T cell-B cell interaction. With T cell help and costimulation through CD40L, B cells upregulate EBI2 (Pereira, P. J, et al., 2009) and down-modulate CCR7 (Cyster, 2010). By an unknown mechanism, some B cells down-modulate EBI2 and upregulate Bcl-6 to form the initial germinal center cluster. With help from T follicular helper cells and FDCs carrying particulate antigen, germinal center B cells transit through the Dark

Zone and Light Zone by coordinated functionality of the chemokine receptors CXCR4, CXCR5 and S1PR2 (Cyster, 2015; Green, A. J., et al., 2011). Through the upregulation of AID, germinal center B cells mature and differentiate into high-affinity plasma cells and memory B cells by mechanisms such as somatic hypermutation and isotype class switching. Terminally differentiated B cells (Qi, H, et al., 2014) and T helper cells then participate to clear the infection

Identification of innate immunity in LN orchestrated by SCS macrophages

The skin contains immune effector cells that help keep pathogen replication in check, in a process referred to as 'barrier immunity' (Belkaid and Segre, 2014). Despite this, in many cases, intact pathogens travel within minutes via lymph fluid to draining LNs. Indeed some pathogens, such as *Yersinia pestis* (St John et al., 2014), appear to have evolved to undergo marked expansion only after arrival in the LN. *Y. pestis*-infected draining lymph nodes displayed a characteristic pathology of swollen sinuses, and sinus macrophages appeared to be the major population *Y. pestis* infected. To ask whether barrier immunity in lymph nodes exists, the first question to ask is whether lymph node has specialized antigen presenting cells that are strategically positioned in close proximity to both incoming pathogens in the lymph and the effector memory cells.

Recent work identified the existence of resident antigen presenting cells (SCS macrophages and DCs) within lymph nodes that rapidly coordinate an innate immune response after pathogen challenge. Lymph node resident DCs have been classified as CD11c^{hi} MHCII^{int}. These DCs are composed of CD11b⁺ and CD8⁺ subsets. The majority of CD11b⁺ are resident DCs (Gerner, Y. M. et al., 2012) positioned closely to lymphatic

sinuses, and the CD8⁺ DCs are located both near lymphatic sinuses and in the T cell zone. Independent of migratory DCs, LN-resident CD11b⁺ DCs, which reside along the lymphatic sinus endothelium, were observed to scan lymph using motile dendrites. They could capture lymph-borne antigens and present them to cognate T cells, leading to rapid T cell activation (Gerner, Y. M. et al., 2015). Upon footpad immunization of microspheres covalently conjugated with OVA protein, TCR-transgenic (OT-II) CD4⁺ and (OT-I) CD8⁺ T cells could be identified to form clusters with CD11c⁺ lymphatic sinus resident dendritic cells near the SCS. Lymphatic sinus resident DCs are also important for OT-II and OT-I T cell early cellular expansion and OT-II T cell T_{fh} differentiation in response to particulate antigens. In addition to LN-resident DCs, sialoadhesin (CD169) positive macrophages have been identified along the subcapsular sinus in lymph nodes and marginal zone sinuses in spleen (Martinez-Pomares, L. et al., 1999; Van den Berg, K. T. et al., 1992; Crocker, R. P. et al., 1991). It has long been reported that footpad injected HRP/anti-HRP immune complex (Szakal, K. A. et al., 1983) can deposit on SCS macrophages and unknown non-phagocytic cells are responsible for transporting and depositing the immune complex onto FDCs in follicles. Recently it is more and more accepted that SCS macrophages in lymph nodes are act as “flypapers” to trap lymph-borne antigen and pathogens. Using intravital two-photon microscopy, SCS macrophages are confirmed to be able to capture subcutaneously injected PE-immune complexes (Phan, G. T. et al., 2007). Complement receptor 1/2 on follicular B cell are responsible for transporting PE-IC from SCS macrophages onto FDCs. Furthermore, after subcutaneous injection of PE into mice passively immunized with PE-specific rabbit polyclonal antibodies, rapid PE-immune complex depositing on

SCS macrophages can be observed and the PE-immune complex is conveyed along macrophage cell processes from subcapsular sinus into lymph node parenchyma. After adoptive transfer of Hy10 B cells or OT-II T cells into recipient mice with either wild type or CR1/2-deficient non-cognate B cells, the magnitude of the germinal center response mediated by Hy10 B cells against HEL is approximately half in the mice with CR1/2-deficient noncognate B cells compared with WT B cells (Phan, G. T. et al., 2009).

Besides immune complex, SCS macrophages also play critical roles in capturing viral particles and presenting them to B cells. Upon footpad challenge of ultraviolet-inactivated vesicular stomatitis virus (VSV), VSV deposited on SCS macrophages within minutes (Junt, T. et al., 2007). Ablation of SCS macrophages by injection of clodronate liposomes (CLL) into the footpad caused less local capture of VSV virus in the popliteal lymph nodes but more dissemination of the virus into the blood and spleen. In addition, VSV specific B cells are able to interact with SCS macrophages after virus challenge, direct activation of VSV specific B cells could be observed, and these B cells participate in the germinal center response. In a later study, the same authors also find that VSV infected SCS macrophages are able to cause relocalization of plasmacytoid dendritic cells (pDCs) (Iannacone, M. et al., 2010) towards the SCS and medullary area. SCS macrophages together with pDCs are able to produce IFN-I, which is critical for protecting VSV from infecting LN peripheral nerves. Upon SCS macrophage ablation, VSV is able to infect and replicate in the peripheral nerves leading to mice developing ascending CNS pathology starting with ipsilateral hindleg paralysis and progressing to death. It has also been reported that SCS macrophages can directly activate CD8+ T cells. Challenge of mice with vaccinia virus or VSV leads to infection of SCS

macrophages, resulting in CD8+ T cell relocation to the peri-SCS area and interaction with virus infected SCS macrophages (Hickman, D. H. et al., 2007). In addition, SCS macrophages are critical for NK and NKT cell accumulation and activation in response to lymph-borne pathogen or antigen. Following earflap infection of *Toxoplasma gondii* (*T. gondii*), a five fold increase of NK cells (Coombes, J. L. et al., 2012) in the cervical lymph node is observed at 24 hours post infection. NK cells mainly accumulate and interact with macrophages at the SCS and medulla areas. Ablation of sinus macrophages by clodronate liposomes abolishes NK activation, suggesting a role of sinus macrophages in activating NK cells in *T. gondii* infection model. A similar study by a different group has shown footpad challenge of recombinant modified vaccinia virus Ankara (MVA) (Garcia, Z. et al., 2012) is able to cause the rapid accumulation of NK cells near subcapsular sinus areas of the draining popliteal lymph node. MVA-infected SCS macrophages are able to produce type I IFNs, which is critical for NK cell activation. Upon ablation of SCS macrophages, both NK cell accumulation and activation are abolished in the draining lymph nodes. Furthermore, it has been shown that invariant NKT cells (Barral, P. et al., 2010) can relocate to close to the SCS to interact with CD169+ macrophages, and CD169+ macrophages are able to present lipid antigens presented by CD1d to directly activate iNKT cells.

In conclusion, lymph nodes exist specialized antigen presenting dendritic cells and macrophages near SCS, those SCS macrophages and DCs are important in capturing lymph-borne antigen/pathogens to limit their systemic spread and they play a pivotal role in presenting antigen to and activation of a variety of immune cell populations.

Identification of innate-like lymphocytes as potential effectors for mediating innate immunity at LN

Like the skin barrier immunity, in which effector memory cells could be found in close proximity to dermal antigen presenting cells, innate-like lymphocytes have been identified in close proximity to SCS sentinel macrophages (Figure 2). Rapid virus and bacteria challenge through the footpad lead to the release of IL18 from SCS macrophages (Kastenmuller, W. et al., 2012) in LNs, which in turn activated closely positioned innate-like lymphocytes to produce IFN γ as early as 4 hours post challenge. The IFN γ ⁺ innate-like lymphocytes were composed of 15% NK cells, 20% $\gamma\delta$ T cells plus NKT cells, and about 65% CD8⁺ $\alpha\beta$ TCR⁺ cells. Anti-IFN γ blockade substantially increased bacterial titers in draining lymph nodes and the blood early after challenge, suggesting a critical role of innate-like lymphocytes in mediating barrier innate immunity in LNs.

Besides IFN γ ⁺ innate-like lymphocytes, there also exists IL17-producing innate-like lymphocytes (Gray, E. E. et al., 2012). Those innate-like lymphocytes have been identified as IL7R α ^{hi}CCR6⁺CXCR6⁺ lymphocytes and are composed of ~20% $\gamma\delta$ T cells (majority are V γ 4⁺ cells) and 70% $\alpha\beta$ T cells. They are positioned near SCS macrophages and rapidly produce IL17 upon in vitro stimulation. In this study, we show that after acute challenge of *Yersinia pestis*, *Staphylococcus aureus* bioparticles and heat inactivated *Candida albicans* through the footpad, IL7R α ^{hi}CCR6⁺CXCR6⁺ innate-like lymphocytes are able to rapidly produce IL17 as early as 3 hours post challenge. SCS macrophage ablation abolishes the capacity for IL7R α ^{hi}CCR6⁺CXCR6⁺ innate-like

lymphocytes to produce IL17 in response to *Staphylococcus aureus* bioparticles. And IL7R α^{hi} CCR6⁺CXCR6⁺ innate-like lymphocytes from ASC deficient mice mediate a diminished IL17 response against challenge, suggesting a potential role of SCS macrophages in producing IL1 β to activate IL7R α^{hi} CCR6⁺CXCR6⁺ innate-like lymphocytes to produce effector cytokine, IL17.

Organization cues for innate-like lymphocytes in LN

In this study, we focused on identifying cues in positioning IL17-producing innate-like lymphocytes at the LN SCS. Through photoconversion and parabiosis experiments, we find these innate-like lymphocytes are lymph node resident. Innate-like lymphocytes can be found near subcapsular sinus area and CCR6 contributes to their subcapsular sinus localization, and CCR6 intact functionality was important for innate-like lymphocytes' IL17 response against acute bacterial challenge (Figure 3A). Intravital two photon microscopy analysis revealed their capacity to cross into the sinus and back into lymph node parenchyma side. S1PR1 controlled their access into the subcapsular sinus and integrin LFA1 controlled their crossing back into lymph node parenchyma. In addition, innate-like lymphocytes expressed high levels CD169 ligand to mediate SCS macrophage-innate lymphocytes interaction. LFA1 together with CD169 ligand are critical for keeping these innate-like lymphocytes resident within the lymph node (Figure 3B).

Although IL7R α^{hi} CCR6⁺ innate-like lymphocytes from lymph nodes have been shown to rapidly produce IL17 upon in vitro stimulation, no study has directly shown a role for their capacity to produce IL17 against microbial challenge in vivo. Here we

demonstrated LN IL7R α^{hi} CCR6 $^{+}$ innate-like lymphocytes are able to rapidly produce IL17 upon attenuated *Yersinia pestis*, *Candida albicans*, and *Staphylococcus aureus* challenge. Intact CCR6 functionality on IL7R α^{hi} CCR6 $^{+}$ innate-like lymphocytes is important for their full IL17 production upon acute challenge. Another surprising finding is that although IL7R α^{hi} CCR6 $^{+}$ innate-like lymphocytes could be readily identified in lymphatic sinus (SCS) in the lymph nodes, they are lymph node resident. This observation leads us to find a role for LFA1 in promoting sinus-exposed innate-like lymphocytes to cross through the SCS lymphatic to enter the lymph node parenchyma, and it reveals a novel role for CD169 as lymph node sinus retention factor. This lymph node retention mechanism of LFA1 and CD169 may apply to other cell types in other peripheral tissues as well.

References

- Barral, P. et al. CD169+ macrophages present lipid antigens to mediate early activation of iNKT cells in lymph nodes. *Nature Immunology*. 11. 303-312. (2010)
- Belkaid, Y, Segre, A. J. Dialogue between skin microbiota and immunity. *Science*. 346. 954-959. (2014)
- Braun, A. et al. Afferent lymph-derived T cells and DCs use different chemokine receptor CCR7-dependent routes for entry into the lymph node and intranodal migration. *Nature Immunology*. 12. 879-887 (2011)
- Bursch, L. S. et al. Identification of a novel population of Langerin+ dendritic cells. *J. Exp. Med*. 204. 3147-3156 (2007)
- Coombes, J. L. et al. Infection-induced regulation of natural killer cells by macrophages and collagen at the lymph node subcapsular sinus. *Cell Report*. 2. 124-135. (2012)
- Crocker, R. P. et al. Purification and properties of sialoadhesin, a sialic acid-binding receptor of murine tissue macrophages. *EMBO J*. 10. 1661-1669. (1991)
- Cyster. Chemokines and cell migration in secondary lymphoid organs. *Science*. 286. 2098-2102 (1999)
- Cyster. B cell follicles and antigen encounters of the third kind. *Nature Immunology*. 11. 989-996 (2010)
- Cyster. Germinal centers: gaining strength from the dark side. *Immunity*. 43. 1026-1028 (2015)
- Feldmeyer, L. et al. The inflammasome mediates UVB-induced activation and secretion of interleukin-1 β by keratinocytes. *Curr. Biol*. 17, 1140-1145 (2007)

Garcia, Z. et al. Subcapsular sinus macrophages promote NK cell accumulation and activation in response to lymph-borne viral particles. *Blood*. 120. 4744-4750. (2012)

Gerner, Y. M., Kastenmuller, W., Ifrim, I., Kabat, J., Germain, N. R. Histo-Cytometry: A method for highly multiplex quantitative tissue imaging analysis applied to dendritic cell subset microanatomy in lymph nodes. *Immunity*. 37. 364-376.

Gerner, Y. M., Torabi-Parizi, P., Germain, N. R. Strategically localized dendritic cells promote rapid T cell responses to lymph-borne particulate antigens. *Immunity*. 42. 172-185. (2015)

Ginhoux, F. et al. Blood-derived dermal langerin+ dendritic cells survey the skin in the steady state. *J. Exp. Med.* 204. 3133-3146 (2007)

Gray, E. E., Friend, S., Suzaki, K., Phan, G. T., Cyster, G. J. Subcapsular sinus macrophages fragmentation and CD169+ bleb acquisition by closely associated IL17-committed innate-like lymphocytes. *Plos One*. 7. e38258. (2012)

Green, A. J. et al. The sphingosine 1-phosphate receptor S1PR2 maintains the homeostasis of germinal center cells and promotes niche confinement. *Nature Immunology*. 12. 672-680 (2011)

Hickman, D. H. et al. Direct priming of antiviral CD8+ T cells in the peripheral interfollicular region of lymph nodes. *Nature Immunology*. 9. 155-165 (2007)

Hunger, R. E. et al. Langerhans cells utilize CD1a and langerin to efficiently present nonpeptide antigens to T cells. *J. Clin. Invest.* 113. 701-708 (2004)

Iannacone, M. et al. Subcapsular sinus macrophages prevent CNS invasion on peripheral infection with a neurotropic virus. *Nature*. 465. 1079-1083. (2010)

Junt, T. et al. Subcapsular sinus macrophages in lymph nodes clear lymph-borne viruses and present them to antiviral B cells. *Nature*. 450. 110-114. (2007)

Kalali, B. N. et al. Double-stranded RNA induces an antiviral defense status in epidermal keratinocytes through TLR3-, PKR- and MDA5/RIG-I-mediated differential signaling. *J. Immunol.* 181, 2694-2704 (2008).

Kastenmuller, W., Torabi-Parizi, P., Subramanian, N., Lammermann, T., Germain, N. R. A spacially-organized multicellular innate immune response in lymph nodes limits systemic pathogen spread. *Cell*. 150. 1235-1248. (2012)

Martinez-Pomares, L. et al. Fc chimeric protein containing the cysteine-rich domain of the murine mannose receptor binds to macrophages from splenic marginal zone and lymph node subcapsular sinus and to germinal centers. *J. Exp. Med.* 184. 1927-1937. (1999)

Nestle, O. F. et al. Skin immune sentinels in health and disease. *Nature Rev Immunology*. 9. 679-691 (2009)

Pereira, P. J. et al. EB12 mediates B cell segregation between the outer and centre follicle. *Nature*. 460. 1122-1126 (2009)

Phan, G. T., Grigorova, I., Okada, T., Cyster, G. J. Subcapsular encounter and complement-dependent transport of immune complexes by lymph node B cells. *Nature Immunology*. 8. 992-1000. (2007)

Phan, G. T. et al. Immune complex relay by subcapsular sinus macrophages and noncognate B cells drives antibody affinity maturation. *Nature Immunology*. 10. 786-793. (2009)

Poulin, L. F. et al. The dermis contains langerin+ dendritic cells that develop and function independently of epidermal Langerhans cells. *J. Exp. Med.* 204. 3119-3131 (2007)

Qi, H. et al. Spatiotemporal basis of innate and adaptive immunity in secondary lymphoid tissue. *Annual review of cell and development biology.* 30. 141-167. (2014)

St John, A.L., Ang, W.X., Huang, M.N., Kunder, C.A., Chan, E.W., Gunn, M.D., and Abraham, S.N. S1P-Dependent trafficking of intracellular yersinia pestis through lymph nodes establishes Buboes and systemic infection. *Immunity.* 41, 440-450. (2014)

Szakai, K. A. et al. Transport of immune complexes from the subcapsular sinus to lymph node follicles on the surface of nonphagocytic cells, including cells with dendritic morphology. *The Journal of Immunology.* 131. 1714-1727. (1983)

Van den Berg, K. T. et al. Sialoadhesin on macrophages: its identification as a lymphocyte adhesion molecule. *J. Exp. Med.* 176. 657-655. (1992)

Wakim, L. M. et al. Dendritic cell-induced memory T cell activation in nonlymphoid tissues. *Science.* 319. 198-202. (2008)

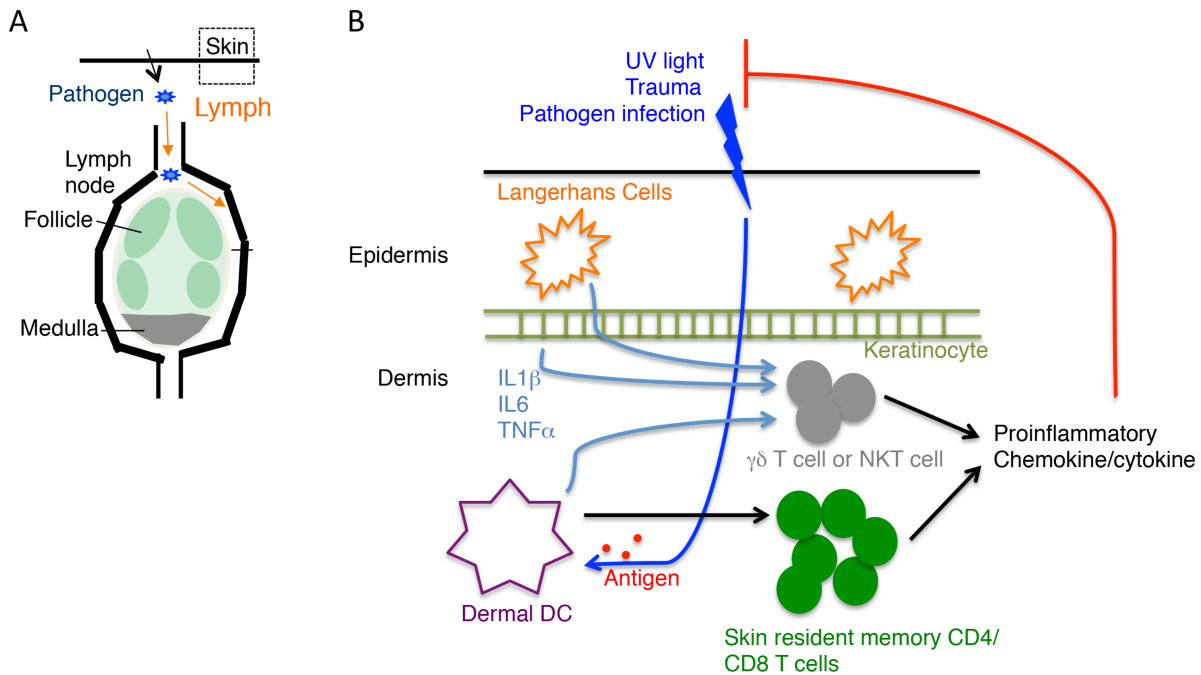


Figure 1. Barrier immunity in skin. (A) Diagram of pathogenic challenge breaching the skin barrier. Skin draining lymph node is shown as well. (B) Skin barrier immunity (Zoom in of the box content in panel (A)). UV light, trauma or pathogenic infection breaches skin barrier and cause a rapid immune response. Strategically positioned Langerhans cells and keratinocytes in the skin epidermis and dermal DCs in the dermis become rapidly activated, which in turn activates skin effector resident cells (skin resident memory CD4/CD8+ T cells, $\gamma\delta$ T cells and NKT cells) through cytokine dependent or antigen dependent manner. Activation of skin effector resident cells causes rapid secretion of proinflammatory chemokine and cytokine, which is critical to clear pathogen and resolve immune response.

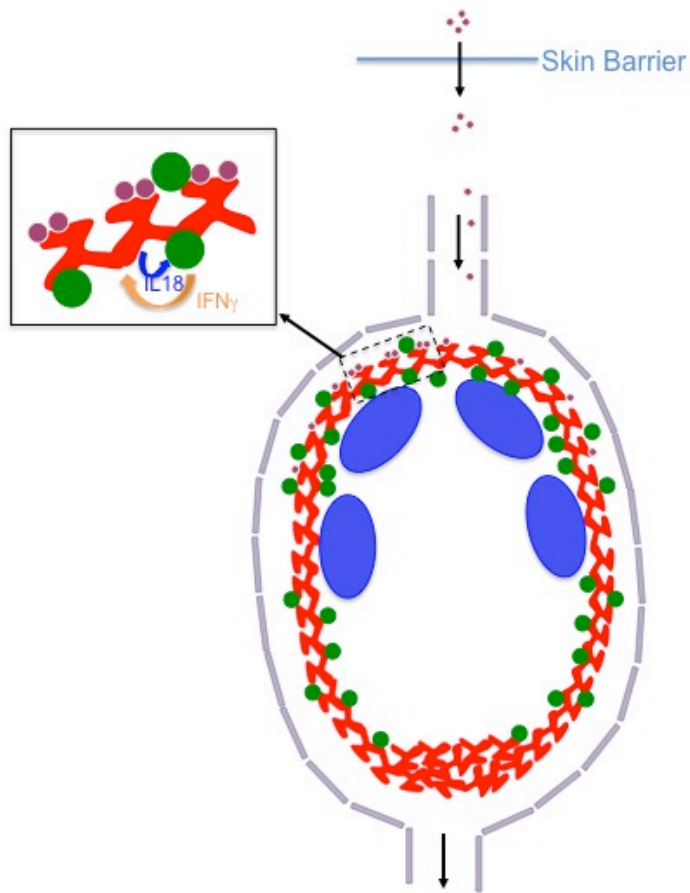


Figure 2. Barrier immunity in lymph node. Subcapsular sinus (SCS) itself as a second barrier layer. Pathogens breached primary skin barrier are carried into SCS area by lymph through afferent lymphatic vessels. SCS macrophages (Red) are uniquely positioned to rapidly detect antigen (Purple) and produce mature IL18 (Blue). CD44hi innate-like lymphocytes (Green) near SCS macrophages sense the cytokine and crosstalk back to macrophages by secreting IFN γ (Orange).

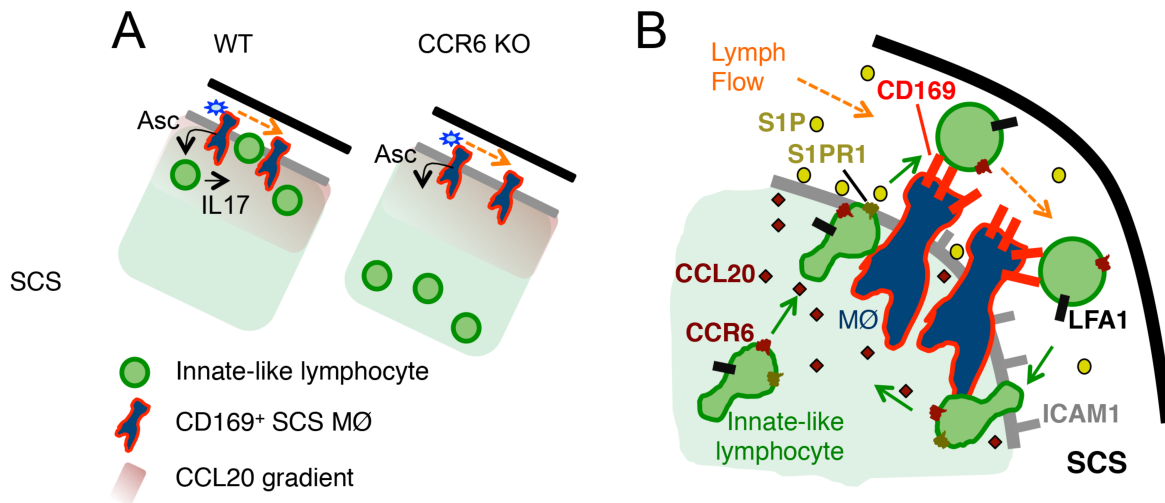


Figure 3. (A) Model showing effect of CCR6 deficiency on innate-like lymphocyte positioning and associated defect in ability to upregulate IL17 in response to IL1-family cytokines produced by SCS macrophages in an ASC-dependent manner. (B) Model showing Innate-like lymphocyte surveillance of sinus macrophages. Model shows role of CCR6-CCL20 in guiding innate-like lymphocyte to lymphatic sinus, S1PR1-S1P in promoting trans-cellular migration into sinus, and CD169 on macrophage (MØ) mediating retention of CD169-ligand^{hi} lymphocyte (green) against lymph flow. Green arrows show cell migration and orange arrows show lymph flow.

Chapter 2

Migratory and adhesive cues controlling innate-like lymphocyte surveillance of the pathogen-exposed surface of the lymph node

Migratory and adhesive cues controlling innate-like lymphocyte surveillance of the pathogen-exposed surface of the lymph node

Yang Zhang¹, Theodore L. Roth¹, Elizabeth E. Gray^{1*}, Hsin Chen¹, Lauren B. Rodda¹, Yin Liang¹, Patrick Ventura², Saul Villeda², Paul R. Crocker³ and Jason G. Cyster¹

¹Howard Hughes Medical Institute and Department of Microbiology and Immunology, University of California San Francisco, CA 94143, USA; ²The Eli and Edythe Broad Center of Regeneration Medicine and Stem Cell Research University of California, San Francisco, School of Medicine; ³Division of Cell Signalling and Immunology, Wellcome Trust Building, College of Life Sciences, University of Dundee, Dundee DD1 5EH, UK.

*Present address: Department of Immunology, University of Washington School of Medicine, Seattle, WA, 98195, USA

Address correspondence to Jason G Cyster, Department of Microbiology and Immunology, University of California San Francisco, CA 94143, USA, (415) 502-6427, Jason.Cyster@ucsf.edu

Abstract

Lymph nodes (LNs) contain innate-like lymphocytes that survey the subcapsular sinus (SCS) and associated macrophages for pathogen entry. The factors promoting this surveillance behavior have not been defined. Here we report that IL7R^{hi}Ccr6⁺ lymphocytes in mouse LNs rapidly produce IL17 upon bacterial and fungal challenge. We show that these innate-like lymphocytes are mostly LN resident. Ccr6 is required for their accumulation near the SCS and for efficient IL17 induction. Migration into the SCS intrinsically requires S1pr1 whereas movement from the sinus into the parenchyma involves the integrin LFA1 and its ligand ICAM1. CD169, a sialic acid-binding lectin, helps retain the cells within the sinus, preventing their loss in lymph flow. These findings establish a role for Ccr6 in augmenting innate-like lymphocyte responses to lymph-borne pathogens, and they define requirements for cell movement between parenchyma and SCS in what we speculate is a program of immune surveillance that helps achieve LN barrier immunity.

Introduction

Our ability to mount adaptive immune responses against skin-invading pathogens depends on the delivery of antigens to lymph nodes (LNs) for encounter by naïve lymphocytes (Cyster, 2010; Qi et al., 2014). However, activation, clonal expansion and effector lymphocyte differentiation takes several days whereas pathogens can undergo marked replication in a matter of hours. The skin contains immune effector cells that help keep pathogen replication in check, in a process referred to as 'barrier immunity'

(Belkaid and Segre, 2014). Despite this, in many cases, intact pathogens travel within minutes via lymph fluid to draining LNs. Indeed some pathogens, such as *Yersinia pestis*, appear to have evolved to undergo marked expansion only after arrival in the LN (St John et al., 2014). Recently, there has been evidence indicating the existence of barrier immunity within LNs. The first LN cells exposed to lymph-borne antigens include the CD169⁺ macrophages that extend between the subcapsular sinus (SCS) or medullary sinuses and the underlying parenchyma (Barral et al., 2010; Iannacone et al., 2010; Phan et al., 2009). Crosstalk between sinus-associated macrophages and IFN γ precommitted CD8 T cells and NK cells is important for mounting rapid Th1-like and NK cell responses against acute infection by *Pseudomonas aeruginosa*, *Salmonella typhimurium* and *Toxoplasma gondii* (Coombes et al., 2012; Kastenmuller et al., 2012). IL17 is a cytokine with roles in anti-bacterial and anti-fungal defense that is made abundantly by effector T cells at epithelial surfaces (Littman and Rudensky, 2010). Whether IL17 is produced rapidly during responses to subcapsular sinus-invaders in LNs is unclear.

In recent work, our group and others identified populations of innate-like (pre-formed effector) lymphocytes that are enriched near the SCS in peripheral LNs and are pre-committed to produce IL17 (Do et al., 2010; Doisne et al., 2009; Gray et al., 2012; Roark et al., 2013). These cells express high amounts of the chemokine receptors Ccr6 and Cxcr6 as well as the cytokine receptor IL7R, and they include a majority of ab T cells but also considerable numbers of gd T cells as well as non-T cells (Gray et al., 2012). Within the IL17-committed gd T cell population a major subset expresses a Vg4-containing TCR (according to the nomenclature of (Heilig and Tonegawa, 1986)), and

undergoes expansion in response to challenge with imiquimod or complete Freund's adjuvant (Gray et al., 2013; Ramirez-Valle et al., 2015; Roark et al., 2013). In previous work we found that innate-like lymphocytes isolated from peripheral LNs were heavily coated with CD169⁺ macrophage-derived membrane fragments ('blebs') (Gray et al., 2012). This observation suggested there may be strong adhesive interactions between these cells and the CD169⁺ macrophages. CD169 is the founding member of the Siglec family of sialic acid-binding lectins (Crocker et al., 2007; Macauley et al., 2014).

Although CD169 is a defining feature of LN SCS macrophages and targeting antigens to CD169 can promote antibody responses (Macauley et al., 2014), the function of CD169 on these cells is not fully understood.

Pre-enrichment of innate-like lymphocytes near LN sinuses is thought to be important for allowing very rapid responses against lymph-borne invaders (Gray et al., 2012; Kastenmuller et al., 2012). Despite this, it is not known whether IL17-committed innate-like lymphocytes in LNs respond rapidly upon pathogen challenge, and little is understood about how these cells localize to or move in the subcapsular region. In this study, we found IL7Ra^{hi}Ccr6⁺ innate-like lymphocytes were mostly LN resident and they produced IL17 within hours of bacterial or fungal challenge. Their proximity to the SCS was mediated by Ccr6 and was important for the rapid induction of IL17 following bacterial challenge. Real time intravital two photon microscopy and *in vivo* labeling procedures revealed that innate-like lymphocytes exchanged between the LN parenchyma and the SCS. Movement into the SCS was S1pr1 dependent whereas return to the parenchyma involved LFA1 and ICAM1. Within the SCS, CD169 mediated adhesive interactions that helped retain the cells, presumably against the shear

stresses exerted by lymph flow. This requirement was most prominent for the Vg4⁺ gd T cell subset of innate-like lymphocytes. These observations provide a model for understanding the mechanism by which innate-like lymphocytes survey the pathogen-exposed surface of the LN to protect the organ from infection.

Results

IL7Ra^{hi}Ccr6⁺ innate-like lymphocytes near the SCS respond rapidly to pathogens

IL7Ra^{hi}Ccr6⁺ innate-like lymphocytes within peripheral LNs express high amounts of Cxcr6 and they include ~70% ab T cells, ~20% gd T cells and 5-10% non-T cells (Fig. 1A, B)(Gray et al., 2012). Consistent with previous findings, the IL7Ra^{hi}Ccr6⁺ gd T cell subset produced IL17 rapidly upon treatment with PMA and ionomycin or with the cytokines IL1b and IL23 (Fig. 1C, lower graph) (Cai et al., 2014; Gray et al., 2012; Gray et al., 2011). These treatments also triggered rapid IL17 production from the IL7Ra^{hi}Ccr6⁺ ab T cells (Fig. 1C). We therefore tested whether both the ab and gd subsets of IL7Ra^{hi}Ccr6⁺ T cells produce IL17 in skin draining LNs following bacterial or fungal challenge. IL17 is known to play a role in host defense against cutaneous *Candida albicans* and *Staphylococcus aureus* infection (Cho et al., 2010; Conti and Gaffen, 2015) and to be induced in rats by *Y. pestis* (Comer et al., 2010). Three hrs after heat-killed *C. albicans*, *S. aureus* bioparticle, or attenuated *Y. pestis* footpad challenge, IL17 production in draining popliteal LNs was observed (Fig. 1D). IL7Ra^{hi}Ccr6⁺ lymphocytes were the dominant IL17 producers at this early time point after challenge (Fig. 1D). The induction of IL17 expression in IL7Ra^{hi}Ccr6⁺ cells upon bacterial challenge was dependent on CD169⁺ SCS macrophages as the response was

greatly blunted in CD169-DTR mice (Miyake et al., 2007) pretreated with DT to ablate these cells (Fig. 1E). Since IL1b and IL23 induced IL17 production from IL7Ra^{hi}Ccr6⁺ T cells *in vitro*, we looked for expression of these cytokines after *S. aureus* bioparticle challenge. Transcripts for both *Il1b* and *Il23a* were upregulated (Fig. 1F). Induction of IL17 following *S. aureus* bioparticle challenge was compromised in mice lacking the ASC (Apoptosis-associated speck-like protein containing a CARD) inflammasome subunit (Fig. 1G), consistent with a role for IL1b in activating IL7Ra^{hi}Ccr6⁺ cells during the response to these bacteria.

IL7Ra^{hi}Ccr6⁺ innate-like lymphocytes are mostly LN resident

IL7Ra^{hi}Ccr6⁺ lymphocytes make up ~0.5 % of peripheral LN cells yet they represent only ~0.1 % of cells in blood (Fig. 2A), suggesting that the cells are largely non-recirculatory under homeostatic conditions. To test this more directly we ‘time stamped’ cells in inguinal LNs of KikGR photoconvertible protein-expressing transgenic mice by brief violet light exposure (Gray et al., 2013). At 24 hrs after photoconversion almost three quarters of the IL7Ra^{hi}Ccr6⁺ cells and a similar fraction of the Vg4⁺Ccr6⁺ cells remained resident in the LN whereas more than 80% of the conventional $\alpha\beta$ T cells and Ccr6⁻ Vg4⁺ T cells had left the LN and been replaced by newly arriving cells. At 48 hrs the innate-like lymphocyte pool showed little further exchange whereas naïve $\alpha\beta$ T cells were 90% replaced (Fig. 2B). In a further approach we examined the amount of cell exchange that occurred in parabiotic mice. Two weeks following surgery the naïve $\alpha\beta$ T cell compartment and the Ccr6⁻ Vg4⁺ T cells had achieved full chimerism whereas the innate-like lymphocytes showed only limited exchange between the paired mice (Fig. 2C). Taken together, these findings indicate that most IL7Ra^{hi}Ccr6⁺ cells are resident in

the LN for multiple days and are not extensively recirculating under homeostatic conditions.

Migration dynamics of innate-like lymphocytes at the SCS

Cxcr6-GFP is highly expressed by all IL7Ra^{hi}Ccr6⁺ cells (Fig. 1A) and in previous work we observed that Cxcr6^{GFP/+} cells migrate extensively in outer and inter-follicular regions, often in close association with CD169⁺ SCS macrophages (Gray et al., 2012). A closer examination of Cxcr6^{GFP/+} cell behavior in this region revealed that the cells frequently made contact with CD169⁺ macrophages, and occasionally lymphocytes could be observed crossing the layer of macrophages to reach the SCS (Fig. 3A and Movies 1 and 2). Reciprocally, cells that were initially detected within the SCS could be observed migrating across the thick CD169⁺ macrophage layer into the LN parenchyma (Fig. 3A and Movies 1 and 2). To quantify the crossing events, cell tracks were generated automatically (Figure 3-figure supplement 1) and tracks crossing the SCS floor were manually enumerated. Among all the tracks of Cxcr6^{GFP/+} cells within 50µm of the capsule, ~25% were in the SCS (Fig. 3B). Cell tracking analysis showed that about 3% of the cells in the SCS region traveled from the parenchyma into the sinus, and 3% of the cells traveled in the reverse direction, in the 30 min imaging periods (Fig. 3C). To quantitate the proportion of cells in the LN lymphatic sinuses at a given moment in time we optimized an *in vivo* procedure to label lymph-exposed cells based on the established method of antibody pulse-labeling of blood-exposed cells (Cinamon et al., 2008). We targeted Thy1 since this marker is expressed by all the IL7Ra^{hi}Ccr6⁺ cells while not being present on SCS macrophages (not shown). PE-conjugated antibody was used as the large size of PE (250 kD) reduces the rate at which the antibody

accesses the lymphoid tissue parenchyma (Pereira et al., 2009). Thy1-PE antibody (0.2 μ g) was injected into the footpad, the draining popliteal LN was isolated 5 min later and the frequency of labeled cells determined by flow cytometry. Approximately 10% of the total IL7Ra^{hi}Ccr6⁺ cells were brightly labeled with Thy1-PE antibody compared with about 0.3% of naive T cells (Fig. 3D). Among the innate-like lymphocytes, gd T cells (predominantly Vg4⁺Ccr6⁺ cells) were preferentially labeled, with around 15-20% of these cells being antibody exposed. By immunofluorescence microscopy, Thy1-PE labeled CD3e⁺ cells were observed in the SCS and in nearby lymphatic sinuses, and few labeled cells were detected within the LN parenchyma, confirming that footpad injection of PE-conjugated antibody led to preferential labeling of lymph-exposed LN cells (Fig. 3E). The broader labeling of the sinus by Thy-1 than by CD3 reflects the expression of Thy1 by lymphatic endothelial cells (Jurisic et al., 2010).

We also obtained information about lymphocyte-SCS macrophage proximity by following up on our finding that isolated innate-like lymphocytes are heavily coated with CD169⁺ macrophage-derived membrane fragments ('blebs') (Gray et al., 2012). This coating is thought to occur at the time of LN cell dissociation, possibly because the SCS macrophages are tightly bound to the extracellular matrix and become fragmented during mechanical preparation of the tissue. Importantly, the blebs only become bound to cells that are associated with the macrophages at the time of isolation since co-preparation of LN cells from congenically distinct animals did not lead to cross acquisition of macrophage-derived blebs by innate-like lymphocytes from the different LNs (Gray et al., 2012). In accord with previous findings, 30-40% of the IL7Ra^{hi}Ccr6⁺ innate-like lymphocytes isolated from control mice were CD169 macrophage-derived

membrane bleb positive (Fig. 3F). A higher frequency (40-55%) of the Vg4⁺ gd T cells were CD169 bleb positive, suggesting these cells may be preferentially associated with SCS macrophages (Fig. 3F). Combining this analysis with Thy1-PE labeling showed that lymph-exposed innate-like lymphocytes, but not total ab T cells, were enriched for CD169-bleb positive cells (Fig. 3G). The Thy1-PE⁺ CD169⁻ cells amongst total ab T cells most likely correspond to recirculating cells that are exiting the LN via cortical and medullary sinuses.

Ccr6 promotes innate-like lymphocyte positioning near the SCS

Given the high Ccr6 expression on the innate-like lymphocyte population we asked whether this CCL20 receptor had a role in guiding innate-like lymphocytes to the subcapsular region. Although CCL20 is not abundantly expressed in LNs, it is expressed in LN lymphatic endothelial cells (LECs) at levels more than 100-fold higher than other LN lymphoid stromal cells (Fig. 4A). Immunofluorescence microscopy showed evidence of CCL20 protein in the subcapsular sinus region (overlying follicular and interfollicular regions) but not in the medullary sinus region (Fig. 4B, Figure 4-figure supplement 1) consistent with findings in primate LNs (Choi et al., 2003; Pegu et al., 2007). Innate-like lymphocytes were responsive to CCL20 by *in vitro* migration assays (Fig. 4C). When CCL20 was injected subcutaneously into Cxcr6^{GFP/+} mice, IL7Ra^{hi}Ccr6⁺Cxcr6^{hi} lymphocytes became clustered near and within the SCS in the draining LNs (Fig. 4D, Figure 4-figure supplement 2). Cells from these LNs showed reduced surface Ccr6, and increased CD169 staining and Thy1 labeling, consistent with their having been exposed to increased amounts of CCL20 and localizing near and within the SCS (Fig. 4E).

We next examined the distribution of Ccr6-deficient (KO) cells in Ccr6^{GFP/GFP} mice and found that the cells were reduced in density near the SCS (Fig. 4F, Figure 4-figure supplement 3) despite being slightly increased in total frequency in the LN (not shown). Instead, the cells were often distributed along the B-T zone interface (Fig. 4F, Figure 4-figure supplement 3). In Thy1-PE labeling experiments Ccr6 KO mice showed reduced frequencies of labeled cells, a result that was most significant for the Vg4⁺ population (Fig. 4G). Consistent with reduced proximity to SCS macrophages, Ccr6-GFP⁺ IL7Ra^{hi} cells and the Vg4⁺ subset from Ccr6 KO mice were associated with less CD169⁺ blebs compared with Ccr6-sufficient controls (Fig. 4H). The CD169⁺ macrophage population in LN sections was unaffected by Ccr6-deficiency (not shown).

Given that the Vg4⁺Ccr6⁺ cell population was most dependent on Ccr6 for Thy1 labeling and macrophage bleb acquisition (Fig. 4G, H), we further studied the properties of these cells. Vg4⁺Ccr6⁺ T cells uniquely express the surface marker Scart2 (Fig. 4I) (Gray et al., 2013; Kisielow et al., 2008). In a complementary approach to Thy1 labeling, Scart2 antibody treatment was found to label fewer Vg4⁺ cells in LNs from Ccr6-deficient mice than from wild-type mice (Fig. 4I). By immunofluorescence microscopy, Scart2⁺ gd T cells were underrepresented in the SCS region in LN sections from Ccr6-deficient mice compared with those from control mice (Fig. 4J, Figure 4-figure supplement 4).

Together these data support the conclusion that Ccr6 plays a role in guiding innate-like lymphocytes towards the SCS region. Importantly, when Ccr6 KO mice were immunized with *S. aureus* bioparticles, the IL7Ra^{hi}Ccr6⁺ cells mounted a diminished IL17 response (Fig. 4K) whereas they responded normally to activation stimuli *in vitro* (not shown).

These data provide further evidence that proximity to SCS macrophages is important for innate-like lymphocytes to mount rapid IL17 responses following pathogen exposure.

S1pr1 is required for innate-like lymphocyte movement into the SCS

S1pr1 is needed in naïve lymphocyte for access to cortical and medullary lymphatic sinuses during LN egress (Cyster and Schwab, 2012). S1pr1 is also required for marginal zone (MZ) B cell shuttling between the S1P high MZ and the S1P low lymphoid follicle (Arnon et al., 2013). We therefore tested whether S1pr1 played a role in guiding innate-like lymphocytes into the SCS. The innate-like lymphocytes had detectable surface S1pr1 (Fig. 5A) and they responded to S1P by *in vitro* migration in a Transwell assay (Fig. 5B). Pretreatment of mice for 6 hrs with FTY720, a functional antagonist of S1pr1, greatly diminished *in vivo* Thy1-PE labeling on IL7Ra^{hi}Ccr6⁺ lymphocytes (Fig. 5C). Similarly, *in vivo* Scart2 antibody labeling of Vg4⁺ gd T cells was decreased after FTY720 treatment (Fig.5D). FTY720 also decreased the CD169 membrane bleb positive fraction to 20-25 % in both the total IL7Ra^{hi}Ccr6⁺ population and the gd T cell subpopulation (Fig. 5C). The reductions in Thy1-PE labeled cells (from ~10 to ~1 %) and in CD169-bleb⁺ cells (from ~35 to ~25%) were similar, representing ~10% of the total IL7Ra^{hi}Ccr6⁺ population in both cases (Fig. 5C), suggesting that the reduced frequency of CD169-bleb⁺ cells was due to the loss of cells accessing the sinus. Comparable findings were made after treatment with the more selective S1pr1 functional antagonist, AUY954 (Fig. 5E). These data provided evidence that S1pr1 was required for the cells to have normal access to the SCS. Examination of tissue sections by immunofluorescence microscopy showed a loss of Cxcr6^{GFP/+} cells from the SCS following FTY720 treatment (Fig. 5F). FTY720 treatment also caused a depletion of

Scart2⁺ cells from the SCS (Fig. 5G, Figure 5-figure supplement 1). When FTY720-treated mice were challenged with *S. aureus* bioparticles the IL7Ra^{hi}Ccr6⁺ population mounted an IL17 response of normal magnitude (not shown). We speculate that SCS access is needed for other types of responses.

In mice unable to produce lymphatic S1P due to generalized Sphk2 deficiency and ablation of Sphk1 in lymphatic endothelium, innate-like lymphocytes had less CD169⁺ macrophage-derived membrane blebs and less *in vivo* Thy1-PE antibody labeling compared with control mice (Fig. 5H). These observations are consistent with the conclusion that the S1P-S1pr1 axis plays a role in guiding innate-like lymphocytes into the SCS.

In accord with S1pr1 having an intrinsic role in promoting SCS access of IL7Ra^{hi}Ccr6⁺ cells, staining for S1pr1 and CD169 showed the macrophage-derived bleb coating was restricted to the S1pr1⁺ cells (Fig. 5I). This analysis required use of an unconjugated rat antibody to detect S1pr1. Since the Thy1-PE is a rat antibody, it was not possible to combine the S1pr1 stain with the *in vivo* Thy1-PE labeling procedure. To further test whether S1pr1 in innate-like lymphocytes was required for SCS access, S1pr1^{f/-} mice were bred. Tamoxifen treatment of adult mice for 5 days caused a loss of S1pr1 in innate-like lymphocytes (Fig. 5J). Analysis in separate mice showed that the loss of S1pr1 was associated with reduced *in vivo* Thy1-PE labeling and reduced CD169 on IL7Ra^{hi}Ccr6⁺ cells (Fig. 5J). However, this approach could not exclude a role for S1pr1 in other cell types. Attempts to test the intrinsic role of S1pr1 using BM chimeras were unsuccessful due to difficulties in achieving efficient reconstitution of IL7Ra^{hi}Ccr6⁺ cells and our finding that many of the cells developing in the chimeric mice appeared

activated based on CD69 expression (not shown). In another approach, mice were treated with tamoxifen for a short time to cause a ~50% reduction in the fraction of cells that were S1pr1⁺ (Fig. 5K). We reasoned that if S1pr1 were acting cell intrinsically in IL7Ra^{hi}Ccr6⁺ cells then under conditions of partial ablation the S1pr1-deleted cells should lose their CD169 association whereas this would not occur if the receptor were acting in another cell type. Consistent with an intrinsic role, there was little CD169 staining of S1pr1-negative cells in the tamoxifen treated mice (Fig. 5K). These data support the conclusion that S1pr1 acts intrinsically in innate-like lymphocytes to promote close associations with SCS macrophages.

We also examined the effect of S1pr1 antagonism on innate-like lymphocyte migration dynamics using intravital two photon microscopy. Visual inspection of the imaging data for FTY720 treated versus control LNs suggested that there were fewer Cxcr6^{GFP/+} innate-like lymphocytes in the SCS after FTY720 treatment and less examples of cells migrating into the sinus (Movie 3). Quantification of the number of tracks present in the SCS and the parenchyma in four imaging experiments confirmed that there were fewer cells in the sinus (Fig. 5L) and there was a significant reduction in the number of tracks that crossed from the parenchyma into the sinus (Fig. 5M). We also plotted the frequency of cells versus distance from the LN capsule for multiple experiments determined using a computational approach (see Methods) and this confirmed that FTY720 caused a depletion of Cxcr6^{GFP/+} cells from the sinus region (Figure 5-figure supplement 2). These data are consistent with the conclusion that S1pr1 antagonism prevents innate-like lymphocyte access to the sinus.

Involvement of LFA1 and ICAM1 in innate-like lymphocyte access to the LN parenchyma from the SCS

Cell movement from vascular locations into the tissue parenchyma often involves integrin-mediated adhesion. Innate-like lymphocytes express high levels of LFA1 (αLβ2) integrin (Fig. 6A) and ICAM1 is highly expressed by LECs lining the SCS (Cohen et al., 2014) (Fig. 6B). ICAM1 is also expressed by CD169⁺ SCS macrophages (not shown). In adhesion assays, IL7Ra^{hi}Ccr6⁺ cells bound avidly to ICAM1 (Fig. 6C). The Vg4⁺ subset had slightly lower LFA1 than the total IL7Ra^{hi}Ccr6⁺ population and adhered less strongly to ICAM1 (Fig. 6A, C). Given these findings, we hypothesized that LFA1-ICAM1 interaction may have a role in innate-like lymphocyte movement from the SCS into the LN parenchyma. Consistent with this model, 6hr αL blocking antibody treatment caused increased Thy1-PE labeling on total IL7Ra^{hi}Ccr6⁺ lymphocytes and on the Vg4⁺ gd T cell subset, without influencing their total number in the LN (Fig. 6D, Figure 6-figure supplement 1A). A similar increase in the frequency of Thy1-PE labeled innate-like lymphocytes was observed in *Icam1*^{-/-} mice compared to littermate controls (Fig. 6E). However, *Icam1*^{-/-} mice had less IL7Ra^{hi}Ccr6⁺ and Vg4⁺Ccr6⁺ cells compared with ICAM1 sufficient control mice whereas the cells were present at an increased frequency in blood (Fig. 6F, G). When mice were treated with αL blocking antibody for 3 days, there was a similar reduction in IL7Ra^{hi}Ccr6⁺ cell number in LNs and a marked increase in their numbers in blood (Figure 6-figure supplement 1B). These data indicate that, unlike short-term integrin blockade, long-term deficiency of ICAM1 or sustained blockade of LFA1 causes a loss of innate-like lymphocytes from the LN.

By immunofluorescence microscopy, IL7Ra^{hi} cells were found enriched in the SCS in α L blocked mice (Fig. 6H). These data suggested that innate-like lymphocytes were trapped in the SCS following α L blockade, leading to their increased exposure to the lymph-borne Thy1-PE antibody. To further examine this possibility, intravital two photon microscopy was performed, comparing control and 6hr α L blocked Cxcr6^{GFP/+} mice. Visual inspection of the movies revealed many Cxcr6^{GFP/+} cells that appeared to be 'stuck' to the SCS floor with their cell bodies 'fluttering' in the sinus, possibly being moved by passing lymph (Fig. 6I and Movie 4). These cells had an elongated morphology compared to the rounded shape of cells in the SCS of control mice (Fig. 6I and Movie 4). Consistent with the *in vivo* Thy1-PE labeling and IF microscopy, quantitative analysis of the imaging experiments by enumerating cell tracks and by a computational approach revealed that α L treatment caused an increase of cells in the sinus in association with the macrophage layer (Figure 6J, Figure 6-figure supplement 1C). Moreover, the cell tracking analysis showed that while there was not a significant change in the frequency of tracks crossing from the parenchyma into the SCS, there was a significant reduction in cells traveling from the SCS into the parenchyma (Fig. 6K). These data support the conclusion that LFA1-ICAM1 mediated adhesion is required for innate-like lymphocytes to migrate from the SCS into the LN parenchyma.

CD169 mediates SCS retention of innate-like lymphocytes

Our finding that innate-like lymphocytes are coated with CD169⁺ macrophage-derived membrane blebs (Gray et al., 2012) together with *in vitro* evidence that CD169 can support adhesion of certain cell types (Crocker et al., 1995; Crocker and Gordon, 1989; van den Berg et al., 2001) led us to test whether CD169 contributed to innate-like

lymphocyte migration or adhesion in the SCS. CD169 binds α 2-3 linked sialic acid on surface glycoproteins (Macauley et al., 2014). By CD169-Fc staining, we found IL7Ra^{hi}Ccr6⁺ lymphocytes had a high amount of CD169 ligand on their surface, and neuraminidase treatment of the cells abolished their ability to bind CD169 (Fig. 7A). The acquisition of abundant macrophage membrane fragments by innate-like lymphocytes was dependent on CD169, since in mice in which CD169 was blocked with a neutralizing antibody (Crocker and Gordon, 1989) or in mice deficient in CD169, there were no CD11b⁺ macrophage membrane fragments on innate-like lymphocytes (Fig. 7B and Figure 7-figure supplement 1A).

By real time two photon microscopy, CD169 blockade in Cxcr6^{GFP/+} mice appeared to increase the amount of innate-like lymphocyte migration within the SCS and between parenchyma and sinus (Movie 5). Quantitation of the cell tracks crossing between compartments confirmed that there was an increase in bidirectional exchange (Fig. 7C). We also examined Cxcr6-GFP⁺ cells in CD169 KO mice and here too the cells seemed to move extensively in the SCS region (Movie 5). These data are consistent with the idea that CD169 blockade or deficiency disrupts stable interactions between innate-like lymphocytes and SCS macrophages.

We therefore asked whether CD169 plays a role in mediating lymphatic sinus retention of innate-like lymphocytes. After 30 hrs of treatment with CD169-blocking antibody there was no change in total IL7Ra^{hi}Ccr6⁺ cell frequency, but there was a two-fold loss of Vg4⁺Ccr6⁺ cells in the LN (Fig. 7D). We speculated that if this loss was occurring due to inhibited adherence of cells in the SCS then the lymph exposed cells might be lost rapidly following CD169-blockade. Indeed, in 6 hr blockade experiments there was a

significant reduction in the fraction of $Vg4^{+}Ccr6^{+}$ cells that were Thy1-PE labeled (Fig. 7E). There was only a slight reduction in the total numbers of $Vg4^{+}Ccr6^{+}$ cells after this short period (Figure 7-figure supplement 1B) consistent with only a low fraction of the total population being in the sinus at a given time. These observations suggest that CD169 blockade caused a loss of cells in lymphatic sinuses and this in turn led to a loss of cells from the LN over time. A loss of $Vg4^{+}Ccr6^{+}$ cells was also observed following CD169⁺ macrophage ablation using CD169-DTR mice (Fig. 7F). In considering explanations for why these effects were mostly selective to the $Vg4^{+}Ccr6^{+}$ subpopulation, we found it notable that in ICAM1 adhesion assays, $Vg4^{+}Ccr6^{+}$ cells were less capable of binding ICAM1 compared with other innate-like lymphocytes (Fig. 6C). Taking this observation together with the finding that a higher fraction of $Vg4^{+}Ccr6^{+}$ cells were lymph-exposed in the steady state (Fig. 3D), we speculated that the non-gdT innate-like lymphocytes – but not the $Vg4^{+}Ccr6^{+}$ cells – in the SCS were able to travel back into the LN parenchyma even in the absence of CD169.

In an effort to reveal a role of CD169 in sinus retention of the total innate-like lymphocyte population, we blocked αL prior to blocking CD169. In the first 4 hrs following αL treatment, we observed a gradual increase in the fraction of cells that were Thy1-PE⁺ (Fig. 7G), consistent with the accumulation of cells in the sinus (Fig. 6). Within 2 hrs of anti-CD169 treatment this enhanced Thy1 labeling was lost, indicating loss of innate-like lymphocytes from the sinus, and there was a reduction in $IL7Ra^{hi}Ccr6^{+}$ cell frequency (Fig. 7G). $IL7Ra^{hi}Ccr6^{+}$ cell frequency declined further after 4 and 6 hrs of double blockade (Fig. 7G). When αL and CD169 were both blocked continually for 6 hrs there was a 50% loss of total innate-like lymphocytes in LNs, and this was accompanied

by an increase of the cells in blood (Fig. 7H). In CD169 Het and KO mice there were comparable starting frequencies of IL7Ra^{hi}Ccr6⁺ cells (Figure 7-figure supplement 1C), but after aL blocking antibody treatment there was a loss of Thy1-PE labeling and in total IL7Ra^{hi}Ccr6⁺ cells in the CD169 KO mice compared with the Het controls (Fig. 7I). The decrease in innate-like lymphocytes in LNs 6 hrs after aL and CD169 double blockade was also evident in intact LNs visualized by real time two photon microscopy (Movie 6). Importantly, unlike aL blockade, which caused many innate-like lymphocytes to become non-migratory and apparently stuck to the SCS floor (Movie 4), applying anti-CD169 in addition to anti-aL led to innate-like lymphocyte detachment from CD169⁺ macrophages and loss in the lymph flow (Movie 7). In some regions it was also possible to observe cells moving from the parenchyma into the sinus, but then failing to attach and being carried away in the lymph flow (Movie 7). By quantitative analysis of three imaging experiments CD169-blockade or deficiency was found to have little effect on the density of Cxcr6^{GFP/+} cells in the SCS, but combined aL and anti-CD169 treatment caused a decrease of cells from the sinus region (Figure 7-figure supplement 1D, Figure 7-figure supplement 1E). These data provide evidence that CD169 has a role in mediating lymphatic sinus retention of most innate-like lymphocytes.

Finally we examined the sufficiency of CD169 to support adhesive interactions of innate-like lymphocytes. In adhesion assays, IL7Ra^{hi}Ccr6⁺ lymphocytes showed binding to plates coated with recombinant WT but not a binding site mutant of CD169 (Fig. 7J). By contrast, naïve ab T cells showed minimal binding to CD169 (Fig. 7J).

Discussion

The above findings show that the Ccr6-dependent positioning of IL7R^{hi}Ccr6⁺ innate-like lymphocytes near the LN SCS is important for their rapid cytokine production following bacterial or fungal challenge. The data support a model where lymphatic endothelial-derived CCL20 acts on Ccr6 to attract the innate-like lymphocytes into proximity with SCS macrophages. This enhances their exposure to macrophage-derived cytokines that promote IL17-production and likely other effector functions of the lymphocytes

Our findings also reveal an unusual migratory behavior of innate-like lymphocytes in the SCS region that involves exchange of cells between the parenchyma and SCS.

Movement across the CD169⁺ macrophage layer into the sinus is promoted by S1pr1 and lymphatic endothelial cell-derived S1P. Within the sinus CD169 on macrophages binds to sialylated ligands on the innate-like lymphocytes and helps prevent loss of the cells in lymph flow, with the Vg4⁺ subset of innate-like lymphocytes being most dependent on this adhesive system. LFA1 binding to ICAM1 also contributes to retaining innate-like lymphocytes in the sinus. Finally, return of cells to the parenchyma involves LFA1 and ICAM1, presumably to support transmigration across the lymphatic endothelium. Although this local migratory behavior was not essential for mounting IL17 responses against the pathogens tested in this study (data not shown), we propose that this surveillance program allows innate like lymphocytes to interrogate the CD169⁺ macrophages and SCS for pathogen- or commensal-derived molecules for which they have appropriate receptors.

The cues required for homeostatic positioning of cells in LN T zone and follicles have been well studied, with CCL21/CCL19 and CXCL13 having dominant roles (Cyster,

2005). Our findings add CCL20 as an additional homeostatic organizer, acting to recruit Ccr6⁺ IL17-committed cells to the LN SCS region. As well as expression by innate-like lymphocytes, Ccr6 is abundant on Th17 cells (Littman and Rudensky, 2010) and we speculate that Th17 effector cells that remain in the LN following immunization or infection may position in proximity with the SCS. Although Cxcr6 is also abundantly expressed by innate-like lymphocytes, Cxcr6-deficiency also did not appear to affect their distribution in the LN (unpubl. obs.). The expression of CCL20 in a subcapsular region in primate LNs (Choi et al., 2003; Pegu et al., 2007) makes it likely that our findings with Ccr6 in mice will extend to humans. Ccr6 antagonism was suggested to reduce the egress of Ccr6⁺ effector CD4 T cells from LNs in a mouse EAE model (Liston et al., 2009). CCL20 can be strongly induced in inflamed tissue (Mabuchi et al., 2013) and we speculate that under the inflammatory condition associated with EAE, CCL20 travels to LNs from the inflamed site and attracts Ccr6⁺ cells into the sinus lumen as we observed following CCL20 injection. In the case of Ccr6⁺ CD4 effector T cells, this might then favor their exit from the LN.

S1P and S1pr1 have a critical role in promoting egress of T and B cells from LNs, acting at the step of transmigration into cortical and medullary sinuses (Grigorova et al., 2009; Sinha et al., 2009). We describe here a further function for this ligand-receptor pair in promoting cell migration into the SCS. As for movement into cortical and medullary sinuses, this response involves S1P production by lymphatic endothelial cells. S1pr1 on naïve lymphocytes is required during the egress commitment step and did not appear to have a role in promoting chemotaxis to the sinus (Grigorova et al., 2009). Consistent with those findings, we did not observe an obvious effect of S1pr1 antagonism on

innate-like lymphocyte density near the SCS, only a loss of cells from within the sinus. We therefore favor the model that the cells approach the sinus-lining lymphatic endothelial cells in a CCL20-dependent manner and S1pr1 commits some of the cells to cross the lymphatic endothelium (and associated CD169⁺ macrophage layer) and enter the sinus. Within the sinus we anticipate that the cells are exposed to high amounts of S1P that cause rapid, GRK2-dependent (Arnon et al., 2011), internalization and desensitization of S1pr1, allowing the cells to respond to cues (possibly including CCL20) that can promote their return to the parenchyma. This type of shuttling behavior has been described in the spleen for another population of innate-like lymphocytes, the MZ B cells, with movement into the blood-rich MZ being S1pr1 dependent and return to the parenchyma being CXCL13 dependent (Arnon et al., 2013). One function of MZ B cell shuttling is to deliver immune complexes from blood to B cell follicles (Cinamon et al., 2008). It will be interesting to see if cell shuttling in LNs contributes to cargo delivery from lymph to the LN parenchyma.

CD169 is abundantly expressed on the lymph-exposed heads of SCS macrophages as well as on the tails that extend into the LN parenchyma (Phan et al., 2007). We show that CD169 supports adhesion of innate-like lymphocytes in the sinus and helps restrain them against lymph flow. A number of *in vitro* studies have shown an ability of CD169 to support cell-cell adhesion (Crocker et al., 1995; Crocker and Gordon, 1989; van den Berg et al., 2001). Recent work has also revealed that CD169 on LN SCS macrophages can play a role in the capture of lymph-borne exosomes (Saunderson et al., 2014) and retroviruses (Sewald et al., 2015). The present work builds upon those observations to provide *in vivo* evidence that this Siglec family member can support shear stress-

resistant adhesion of cells. Although lymph flow rates in the mouse popliteal LN have not been directly measured, a modeling study estimated wall shear stresses of several dyn/cm² in the SCS close to afferent lymphatic vessels (Jafarnejad et al., 2015). These shear stresses are similar to those in blood vessels that support leukocyte adhesion (Finger et al., 1996). A recent genomics study found that high endothelial venules in Peyer's patches highly express *St6gal1*, an enzyme that can generate ligands for CD22 (Siglec-2) (Lee et al., 2014). In transfer experiments CD22-deficient B cells showed reduced homing to Peyer's patches (Lee et al., 2014). CD22 also contributes to B cell homing to the bone marrow (Nitschke et al., 1999). These studies together with our work provide evidence that Siglecs are a second class of lectin, after the selectins, that functions in mediating shear-resistant adhesion of cells. A key feature that facilitates selectin function is the high density of glycosylated ligands on the target cell and the very rapid on- and off-rates of lectin-ligand interactions (Rosen, 2004). We suggest that similar features contribute to the function of CD169 as a shear-resistant adhesion receptor. The long ectodomain of CD169 (with 17 Ig-domains) also seems likely to contribute to an ability to 'capture' cells that have become dislodged by lymph flow and to allow their re-adhesion and subsequent transmigration. A similar activity may be involved in capturing CD169-ligand high cells arriving in the SCS from the afferent lymphatic.

Our study provides evidence that LFA1 and ICAM1 are required for retaining IL7Ra^{hi}Ccr6⁺ innate-like lymphocytes in the SCS and supporting their return from the sinus to the parenchyma. These findings are in accord with the well-established roles of LFA1 and ICAM1 in supporting adhesion to and transmigration of lymphocytes across

blood vessel endothelium into tissues (Rot and Von Andrian, 2004). However, they are in discord with a study showing that migration of BM-derived DCs from the SCS into the LN parenchyma was integrin independent (Lammermann et al., 2008). The basis for this discrepancy is not yet clear but might reflect general differences in the properties of lymphocytes and BM-derived DCs. Moreover, integrins may contribute to DC trafficking into LNs under conditions of inflammation (Teijeira et al., 2013). Our conclusion that LFA1 and ICAM1 function during innate-like lymphocyte movement from the SCS into the LN parenchyma is based on four sets of observations in mice treated with aL blocking antibody: (1) innate-like lymphocytes transiently accumulate in the SCS; (2) the accumulated cells exhibit an unusual elongated morphology (suggesting a less adhesive state); (3) tracking analysis shows reduced numbers of cells migrating from the SCS into the parenchyma; (4) the cells are more sensitive to dislodgement by CD169 blocking antibody. We feel that the most parsimonious explanation for these data is that LFA1 supports adhesive interactions between innate-like lymphocytes and ICAM1⁺ sinus associated cells (lymphatic endothelial cells, macrophages) that are needed for movement into the parenchyma. However, given the heterogeneity of the innate-like lymphocyte population, we cannot exclude the possibility that LFA1 blockade also decreases retention of some cells within the LN parenchyma, thereby increasing their movement into the SCS. A study of naïve lymphocyte egress from LNs showed that LFA1 and ICAM1 can contribute to promoting retention of cells in the LN and this was suggested to reflect a role for LFA1 in limiting the rate of cell movement across the endothelium into the sinus lumen (Reichardt et al., 2013). More studies will be needed

to fully address all the functions of LFA1 and ICAM1 in innate-like lymphocyte migration dynamics.

The migration of innate-like lymphocytes in close association with SCS macrophages seems likely to ensure that factors made by the macrophages, such as IL1-family cytokines, can rapidly engage the lymphocytes. It presumably also ensures that signaling in the reverse direction, from the innate-like lymphocyte to the CD169⁺ cells, can take place efficiently. Such signaling may serve to augment the anti-bacterial, anti-fungal or anti-viral activities of the macrophages. The importance of cell movement into the lumen of the SCS is not yet clear but might allow prompt surveillance of pathogens and endogenous cells (e.g. cancer cells) arriving via the lymph, prior to their accessing the LN parenchyma. The greater CD169 coating of Vg4⁺ gdT cells and their stronger dependence on CD169 for retention in the SCS than the other innate-like lymphocytes suggests these cells interact more strongly or in a more selective way with CD169⁺ macrophages. This likely reflects requirements for recognizing and responding to unique ligands beyond IL1b and IL23.

Following *Toxoplasma* infection or after vaccinia virus injection, NK cell interaction with CD169⁺ macrophages is induced (Coombes et al., 2012; Garcia et al., 2012). These studies observed NK cell movement on collagen fibers and of NK cells slowing or stopping in contact with CD169⁺ cells. Whether collagen fibers guide the movement of IL7Ra^{hi}Ccr6⁺ cells needs further study though in contrast to NK cells, the IL7Ra^{hi}Ccr6⁺ cells had minimal expression of the collagen binding α 2 integrin (not shown and (Gray et al., 2012)). Another distinction between these cell types is that LN NK cells lack Ccr6 (unpubl. obs.). A previous study showed that NK1.1⁺ cells in the LN are concentrated in

medullary regions (Kastenmuller et al., 2012), consistent with their homeostatic positioning being controlled by cues other than CCL20. NK cell movement to the SCS might occur in response to inflammation-induced chemoattractants such as CXCR3 ligands that can be upregulated in this region and function in recruiting activated CD4 T cells and CD8 central memory cells (Garcia et al., 2012; Groom et al., 2012; Sung et al., 2012). NKT cell interaction with SCS macrophages was observed following immunization with α -galactosylceramide (Barral et al., 2010). Since 15-20% of the IL7R^{hi}Ccr6⁺ innate-like lymphocytes are NKT cells (Gray et al., 2012), it is likely that these cells are continually surveying the SCS macrophages in a manner similar to the bulk Cxcr6⁺ population studied here. As well as macrophages, there are DCs in the SCS region (Gerner et al., 2015) and the migration behavior we describe may help ensure efficient surveillance of SCS-associated DCs. Following exposure to strong inflammatory signals, SCS macrophages move into the follicle (Gaya et al., 2015). It will be interesting to examine how this reorganization modifies the innate-like lymphocyte trafficking behavior.

Previous work has shown that the IL7R^{hi}Ccr6⁺ gdT cells in peripheral LNs and related cells in the dermis are precommitted to IL17 production, with stimulation by IL1b and IL23 being sufficient to strongly promote IL17 production by these cells (Cai et al., 2011; Gray et al., 2011; Haas et al., 2009; O'Brien and Born, 2015; Ramirez-Valle et al., 2015). Our studies here show that the IL7R^{hi}Ccr6⁺ abT cell population also readily produces IL17 upon IL1b and IL23 stimulation. These cells are double negative for CD4 and CD8 (Gray et al., 2012). LN DN T cells highly express IL23R and respond to this cytokine (Mizui et al., 2014; Riol-Blanco et al., 2010). Our findings in ASC-deficient mice

provide *in vivo* evidence that IL1-family cytokines are involved in activating the cells. These observations are reminiscent of findings for innate-like CD8 T cells in LNs that rapidly make IFN γ upon cytokine (IL18 and IL12 or IL18 and IFN α) stimulation, and for various types of memory T cells that make IFN γ upon IL12 and IL18 exposure (Jameson et al., 2015; Kastenmuller et al., 2012). While our data suggest cytokines may be sufficient to activate the innate-like T cells under some conditions, this does not exclude a role for TCR stimulation in promoting activation or augmenting responses under other conditions.

In summary, we demonstrate that IL17-committed innate-like lymphocytes survey the pathogen-exposed surface of peripheral LNs and respond rapidly upon challenge with bacterial and fungal pathogens. Ccr6-guided proximity to the SCS is important for these cytokine driven responses. S1pr1, CD169 and LFA1 function to promote migration between parenchyma and SCS in close association with CD169⁺ macrophages in a program that we suggest allows innate-like lymphocytes to survey for a range of pathogen- and commensal-derived antigens and mount appropriately tailored responses.

Acknowledgements

We thank members of the Cyster laboratory for helpful discussions and comments on the manuscript, Ying Xu for help with QPCR analysis, Gang Wu for help preparing CD169-Fc, K Karjalainen for SCART2 antibody, J Hinnebusch for attenuated *Y. pestis*, and R Proia, S Coughlin, A.-K. Hadjantonakis and M Tanaka for mice. J.G.C. is an investigator of the Howard Hughes Medical Institute. Y.Z. was supported by the BMS

graduate program and H.C. is a CRI Irvington postdoctoral fellow. This work was supported in part by grant NIH AI074847.

Materials and Methods

Mice

Wild-type C57BL/6NCr mice of 7-9 weeks of age were purchased from the National Cancer Institute (Frederick, MD, USA). *Cxcr6*^{GFP/+} (RRID:MGI:3616633), *Ccr6*^{GFP/+} (RRID:MGI:3852186), *Ccr6*^{+/-} (RRID:MGI:4359785), *Pycard*^{+/-}, *CAG-KiKGR*⁺, *S1pr1*^{ff}, *CreERT2*⁺, *Lyve1-Cre*⁺*Sphk1*^{ff} *Sphk2*^{-/-} mice (RRID:MGI:4421697), and *Icam1*^{+/-} mice were previously described and were from JAX or from an internal colony. CD169-DTR mice were provided by Masato Tanaka (Miyake et al., 2007). Littermate mice were evenly distributed into control or treatment groups and mice of both groups were co-caged whenever possible. All mice were adult and were studied between 7 and 20 weeks of age. Animals were housed in a specific-pathogen free environment in the Laboratory Animal Research Center at the University of California, San Francisco, and all experiments conformed to ethical principles and guidelines approved by the Institutional Animal Care and Use Committee, protocol approval number: AN107975-02.

FTY720 and AUY954 treatment

Mice were treated with FTY720 in saline at a dose of ~1ug/g i.p. Mice were analyzed for Thy1-PE labeling or CD169 bleb association at 6hrs or O/N post treatment. Control mice were treated with saline i.p. AUY954 in saline was given i.p. in 300ul at 300uM.

Mice were analyzed for CD169 bleb association O/N post treatment. Control mice were treated with saline i.p.

aL and anti-CD169 blocking

100ug aL blocking antibody (clone M17/4) or anti-CD169 blocking antibody (Ser4) or both antibodies was injected i.v. Mice were analyzed 6hrs or 30hrs post treatment. For 3 day experiments, mice were injected with 100ug aL blocking antibody at day-3 and day-1, and experiments were done at Day 0.

Footpad bacterial challenge

Mice were challenged with 2×10^7 CFU of heat inactivated *Candida albicans*, attenuated *Yersinia pestis*, or 150ug *Staphylococcus aureus* bioparticle (Invitrogen, Cat S2859) through the footpad. Control mice were treated with 25ul saline. Draining popliteal LNs were dissected and analyzed 3hrs post challenge. For IL17 staining, popliteal LN cells were incubated in Golgi plug for 2hrs at 37°C, stained for surface antigens, treated with BD Cytofix Buffer and Perm/Wash reagent (BD Biosciences), and stained with anti-IL-17A.

Footpad Thy1-PE labeling

0.2ug Thy1.2-PE antibody (30-H12) was injected through the footpad in 25ul saline. Labeling was done for 5min. Draining popliteal LNs were harvested for flow cytometric or immunofluorescence analysis.

Diphtheria toxin treatment

WT and CD169-DTR/+ were treated with 0.75ug DT on Day-5 and Day-2. Experiments were performed and the mice analyzed on Day 0.

Tamoxifen treatment

For full deletion, WT and S1pr1^{f/-} ERcre⁺ mice were treated with tamoxifen at Day -5 to Day -1 and analyzed on Day 0. For transient deletion, mice were treated with one dose on Day -2 and analyzed on Day 0. Tamoxifen was dosed at 5mg/mouse/day orally.

Flow cytometry

Cells were stained in “FACS buffer” (PBS with 0.1% sodium azide, 2% FBS and 1uM EDTA) with antibodies to TCRgd (GL3), TCRb (H57-597), IL17A (eBio17B7), Ccr6 (140706), IL7Ra (A7R34), CD3e (clone 145-2C11), CD11b (clone Mac-1), Vg4 (clone UC3-10A6), CD90.2 (30-H12), S1pr1 (R&D, MAB7089, clone 713412), anti-CD169 (clone MOMA-1 and clone Ser4); anti-scart2 antibody was kindly provided by Dr. Klaus Karjalainen. Molecular Probes® Monoclonal Antibody Labeling Kits (Invitrogen) were used to directly conjugate antibody to Alexafluor647 or Pacific Blue dyes. During analysis, singlets were gated based on peak FSC-H/FSC-W and SSC-H/SSC-W. These gates encompassed more than 90% of total events and were set sufficiently wide to include singlet events of variable size while avoiding the main doublet peak.

To detect IL-17A, cells were stimulated for 3h with 50 ng/ml PMA (Sigma) and 1 µg/ml Ionomycin (I, EMD Biosciences) or 3h with 10ng/ml IL1b and 10ng/ml IL23 in Golgi plug

(BD Biosciences) at 37°C, stained for surface antigens, treated with BD Cytifix Buffer and Perm/Wash reagent (BD Biosciences), and stained with anti-IL-17A.

CD169-Fc/R97A CD169-Fc FACS staining

1ug/ml CD169-Fc or R97A CD169-Fc and 3ug/ml anti-human IgG-PE antibody (Jackson Immunoresearch, Cat 109-116-098) was preincubated at 4°C for 1hour. After pre-binding, the mixture was added to lymphocytes from LNs and staining was done for 1hour on ice. Cells were then stained as normal for FACS analysis.

Scart2 antibody labeling

5ug Scart2 antibody in 100ul volume of saline was injected s.c, draining inguinal lymph node was analyzed by flow cytometry 1hr post antibody injection.

Surgery and photoconversion

The mouse was anesthetized with ketamine, shaved and antiseptically prepared with 0.02% chlorhexidine gluconate. The mouse was then draped and a ~1.5cm incision was made in the abdominal skin to expose the left inguinal LN. A silver LED 415 (Prizmatix), set to maximum intensity, with a high numerical aperture polymer optical fiber (core diameter, 1.5mm) light guide and fiber collimator, was used as a 415nm violet light source. During the 15min exposure period the tissue was kept moist with saline. After photoconversion, the skin was closed with two autoclips (Thermo Fisher Scientific). ~0.1mg/kg buprenorphine in saline was given i.p immediately before and after surgery, and every 4-12 h as needed thereafter. The mice were closely monitored for signs of

pain. Mice were analyzed immediately before and after photoconversion, and 24 h and 48 h post photoconversion. Flow cytometry was used to analyze left and right inguinal LN cells as previously described (Gray et al., 2013). The staining was done with antibodies against Vg4, IL7Ra, Ccr6, and TCRb.

Parabiosis

Parabiosis surgery followed previously described procedures (Smith et al., 2015). Mirror-image incisions at the left and right flanks were made through the skin and shorter incisions were made through the abdominal wall. The peritoneal openings of the adjacent parabionts were sutured together. Elbow and knee joints from each parabiont were sutured together and the skin of each mouse was stapled (9mm Autoclip, Clay Adams) to the skin of the adjacent parabiont. Each mouse was injected subcutaneously with Baytril antibiotic and Buprenex as directed for pain and monitored during recovery. For overall health and maintenance behavior, several recovery characteristics were analyzed at various times after surgery, including paired weights and grooming behavior. Mice were sacrificed for flow cytometric analysis two weeks post parabiotic surgery.

Intravital two-photon laser-scanning microscopy of popliteal LNs

Mice were anaesthetized by intraperitoneal injection of 10 ml kg^{-1} saline containing xylazine (1 mg ml^{-1}) and ketamine (5 mg ml^{-1}). Maintenance doses of intramuscular injections of 4 ml kg^{-1} of xylazine (1 mg ml^{-1}) and ketamine (5 mg ml^{-1}) were given approximately every 30 min. To image the popliteal LN, the mouse's hind leg was

immobilized using thermal putty to a Biotherm stage warmer at 37 °C (Biogenics) for the duration of the surgery and subsequent imaging. A small incision was made directly behind the knee, and a ~0.5 cm square region of underlying tissue was exposed. The fat pad surrounding the popliteal LN was carefully dissected away without damaging surrounding vasculature and the afferent and efferent lymphatic vessels. After visualization of the popliteal LN, a 3D-printed plastic tissue mount was attached to the surrounding tissue using Vetbond. The tissue mount was immobilized with additional thermal putty, and the area above the LN was submerged in PBS for imaging. Images were acquired with ZEN2009 (Carl Zeiss) using a 7MP two-photon microscope (Carl Zeiss) equipped with a Chameleon laser (Coherent). For video acquisition, a series of planes of 3 µm z-spacing spanning a depth of 90 µm were collected every 30 s. Excitation wavelengths were 905 nm. Emission filters were 500–550 nm for GFP, 570–640 nm for PE, and 450–490 for second harmonic signal. Videos were made and analysed with Imaris 7.4.2 ×64 (Bitplane). Two hrs prior to all imaging experiments, 2µg CD11b-PE or 3µg MOMA1-TxRed antibody was injected through footpad. Cell tracking was performed using Imaris Bitplane software. Tracks generated using the software were manually confirmed and tracks that were a minimum of 5 min in duration were grouped according to whether they were exclusively in the parenchyma, exclusively in the SCS or crossed between compartments. Each movie contained a total of between 100-300 tracks in the region of interest. Approximately 15% of the Imaris generated tracks could not be confirmed as representing the migration path of a single cell and these were excluded. To quantify the depth of cells from the LN capsule in the imaging data we used a computational procedure. First a surface object was created in Imaris

over the LN capsule. The positions of both Cxcr6⁺ cells and CD11b⁺ subcapsular macrophages were determined using spots objects in Imaris. The minimum distance between each spot and the capsule was determined using a custom MATLAB (MathWorks) script and the ImarisXT interface. These data were exported into the R programming environment for analysis and plotting (ggplot2 package). The depth of the subcapsular sinus in individual LNs varied, and for each experiment was computationally determined as the peak frequency on a plot of CD11b⁺ subcapsular macrophage's depth below the LN capsule, minus 2 μm , which agreed across experiments with visual estimates of the subcapsular sinus site. As the sinus size varied across experiments from 15-40 μm , for the graphs of cell frequency against depth below the capsule the size of the sinus was normalized across experiments to 20 μm . Only the region within the sinus was normalized. Axis ratio was calculated as the ratio of ellipticity (prolate)/ellipticity (oblate). These dimensions were obtained by first creating a surface object for each cell using Imaris Bitplane software. Final videos were annotated and exported in Premiere (Adobe).

Transwell migration assay

Lymphocytes from LN were allowed to transmigrate for 4 hours across 5 μm transwell filters (Corning Costar, Corning, NY, USA) towards medium or SDF, CCL20, or S1P and enumerated by flow cytometry as described (Ramirez-Valle et al., 2015).

Immunofluorescence microscopy

7um sections were prepared from paraformaldehyde-fixed tissue, prepared as previously described (Besty). In some cases, sections were fixed by acetone (Besty). Sections were stained with the following antibodies: anti-Lyve1-A647, anti-CD3e-bio (clone 145-2C11), Goat anti-CCL20 (AF760), Polyclonal Rabbit anti-GFP (Thermo Fisher Scientific), anti-B220-A647 (RA3-6B2), anti-ICAM1-bio (3E2), anti-IL7Ra-A647 (A7R34), rat anti-scart2, Hamster anti-TCRgd (GL3), Donkey anti-Goat-biotin (Jackson immunoresearch), Goat anti-Armenian Hamster-bio (Jackson immunoresearch), Donkey anti-Rat-bio (Jackson immunoresearch), Anti-biotin-A488 (Jackson immunoresearch), Anti-biotin-Cy3 (Jackson immunoresearch). Images were captured with a Zeiss AxioObserver Z1 inverted microscope.

Cxcr6-GFP cell enrichment

Isolated LN cells from 2-4 Cxcr6^{GFP/+} mice in complete RPMI media (with 2% FBS) were washed twice and resuspended in 200~400ul PBS (with 2% FBS). Cells were stained with anti CD62L-bio (clone MEL-14), anti CD19-bio (clone MB19-1), anti CD11c-bio (clone N418), anti NK1.1-bio (clone PK136) for 30min on ice, washed twice, resuspended in 300ul PBS (2% FBS) with 10~20ul anti-Biotin MACS beads (5ul per mouse) and incubated on ice for 30min. Cells were then washed with and resuspended in 2ml MACS buffer (PBS, 2% FBS, 2mM EDTA, pH 7.2), filtered and loaded onto a MACS column, following manufacturer instructions to negatively select Cxcr6^{GFP/+} cells. FACS was used to check enrichment and yield.

In vitro adhesion assay

ICAM1 adhesion assay: 96 Well Costar Assay Plates (High binding polystyrene, Corning) were coated with ICAM1 at 10ug/ml concentration in 0.1M Na₂CO₃/NaHCO₃ pH9.5 buffer at 4 °C O/N. Plates were then blocked with 1% BSA in RPMI for 30min at room temp. Plates were washed twice with RPMI with 0.5% BSA. 1 million Lymphocytes were added and adhesion assays performed at 37 °C for 30min. A 200ul pipette was used to wash cells (3x 12 o'clock, 3x 6 o'clock, 1x 12 o'clock, 3 o'clock, 6 o'clock and then 9 o'clock). After washing, cells were eluted with 5mM EDTA in RPMI with 0.5% BSA and incubation on ice for 15min. Cells were stained and analyzed by FACS.

CD169-Fc/R97A CD169-Fc adhesion assay: Goat Anti-human IgG antibody (Jackson Immunoresearch) was coated on 96 Well Costar Assay Plate (High binding polystyrene, Corning) at 15ug/ml in 0.1M Na₂CO₃/NaHCO₃ pH9.5 buffer at 4 degree O/N. After coating, plates were washed twice with PBS. After washing, 0.5ug CD169-Fc or R97A CD169-Fc in 100ul PBS was added. After 30min binding, plates were washed twice with PBS, and then blocked with RPMI with 1% BSA for 30min at room temp. After blocking, plates were washed twice with RPMI with 0.5% BSA. Enriched Cxcr6^{GFP/+} cells or total LN cells (in RPMI with 0.5% BSA) were added to the plates. Adhesion assays were performed at 37 °C for 30min. After binding, cells were washed once (carefully using a 200ul pipette to remove the medium) with RPMI with 0.5% BSA solution and adherent cells were analyzed by immunofluorescence microscopy or bright field microscopy for quantification.

Quantitative RT-PCR

Total RNA from sorted LECs or whole LN was isolated and reverse-transcribed, and quantitative PCR was performed for IL1b, IL23a and CCL20 as described. Data were analyzed using the comparative C_T ($2^{-\Delta\Delta C_t}$) method using *Hprt* as the reference.

Statistical analysis

Prism software (GraphPad) was used for all statistical analysis. Statistical comparisons were performed using a two-tailed Student's t-test. *P* values were considered significant when less than 0.05.

References

Arnon, T.I., Horton, R.M., Grigorova, I.L., and Cyster, J.G. (2013). Visualization of splenic marginal zone B-cell shuttling and follicular B-cell egress. *Nature* 493, 684-688.

Arnon, T.I., Xu, Y., Lo, C., Pham, T., An, J., Coughlin, S., Dorn, G.W., and Cyster, J.G. (2011). GRK2-dependent S1pr1 desensitization is required for lymphocytes to overcome their attraction to blood. *Science* 333, 1898-1903.

Barral, P., Polzella, P., Bruckbauer, A., van Rooijen, N., Besra, G.S., Cerundolo, V., and Batista, F.D. (2010). CD169(+) macrophages present lipid antigens to mediate early activation of iNKT cells in lymph nodes. *Nat. Immunol.* 11, 303-312.

Belkaid, Y., and Segre, J.A. (2014). Dialogue between skin microbiota and immunity. *Science* 346, 954-959.

Cai, Y., Shen, X., Ding, C., Qi, C., Li, K., Li, X., Jala, V.R., Zhang, H.G., Wang, T., Zheng, J., and Yan, J. (2011). Pivotal Role of Dermal IL-17-Producing gammadelta T Cells in Skin Inflammation. *Immunity*.

Cai, Y., Xue, F., Fleming, C., Yang, J., Ding, C., Ma, Y., Liu, M., Zhang, H.G., Zheng, J., Xiong, N., and Yan, J. (2014). Differential developmental requirement and peripheral regulation for dermal Vgamma4 and Vgamma6T17 cells in health and inflammation. *Nature communications* 5, 3986.

Cho, J.S., Pietras, E.M., Garcia, N.C., Ramos, R.I., Farzam, D.M., Monroe, H.R., Magorien, J.E., Blauvelt, A., Kolls, J.K., Cheung, A.L., *et al.* (2010). IL-17 is essential for host defense against cutaneous *Staphylococcus aureus* infection in mice. *J. Clin. Invest.* 120, 1762-1773.

Choi, Y.K., Fallert, B.A., Murphey-Corb, M.A., and Reinhart, T.A. (2003). Simian immunodeficiency virus dramatically alters expression of homeostatic chemokines and dendritic cell markers during infection in vivo. *Blood* 101, 1684-1691.

Cinamon, G., Zachariah, M., Lam, O., and Cyster, J.G. (2008). Follicular shuttling of marginal zone B cells facilitates antigen transport. *Nat. Immunol.* 9, 54-62.

Cohen, J.N., Tewalt, E.F., Rouhani, S.J., Buonomo, E.L., Bruce, A.N., Xu, X., Bekiranov, S., Fu, Y.X., and Engelhard, V.H. (2014). Tolerogenic properties of lymphatic endothelial cells are controlled by the lymph node microenvironment. *PLoS One* 9, e87740.

Comer, J.E., Sturdevant, D.E., Carmody, A.B., Virtaneva, K., Gardner, D., Long, D., Rosenke, R., Porcella, S.F., and Hinnebusch, B.J. (2010). Transcriptomic and innate

immune responses to *Yersinia pestis* in the lymph node during bubonic plague. *Infect. Immun.* **78**, 5086-5098.

Conti, H.R., and Gaffen, S.L. (2015). IL-17-Mediated Immunity to the Opportunistic Fungal Pathogen *Candida albicans*. *J. Immunol.* **195**, 780-788.

Coombes, J.L., Han, S.J., van Rooijen, N., Raulet, D.H., and Robey, E.A. (2012). Infection-induced regulation of natural killer cells by macrophages and collagen at the lymph node subcapsular sinus. *Cell Rep* **2**, 124-135.

Crocker, P.R., Freeman, S., Gordon, S., and Kelm, S. (1995). Sialoadhesin binds preferentially to cells of the granulocytic lineage. *J. Clin. Invest.* **95**, 635-643.

Crocker, P.R., and Gordon, S. (1989). Mouse macrophage hemagglutinin (sheep erythrocyte receptor) with specificity for sialylated glycoconjugates characterized by a monoclonal antibody. *J. Exp. Med.* **169**, 1333-1346.

Crocker, P.R., Paulson, J.C., and Varki, A. (2007). Siglecs and their roles in the immune system. *Nat. Rev. Immunol.* **7**, 255-266.

Cyster, J.G. (2005). Chemokines, sphingosine-1-phosphate, and cell migration in secondary lymphoid organs. *Annu. Rev. Immunol.* **23**, 127-159.

Cyster, J.G. (2010). B cell follicles and antigen encounters of the third kind. *Nat. Immunol.* **11**, 989-996.

Cyster, J.G., and Schwab, S.R. (2012). Sphingosine-1-phosphate and lymphocyte egress from lymphoid organs. *Annu. Rev. Immunol.* **30**, 69-94.

Do, J.S., Fink, P.J., Li, L., Spolski, R., Robinson, J., Leonard, W.J., Letterio, J.J., and Min, B. (2010). Cutting edge: spontaneous development of IL-17-producing gamma

delta T cells in the thymus occurs via a TGF-beta 1-dependent mechanism. *J. Immunol.* **184**, 1675-1679.

Doisne, J.M., Becourt, C., Amniai, L., Duarte, N., Le Luduec, J.B., Eberl, G., and Benlagha, K. (2009). Skin and peripheral lymph node invariant NKT cells are mainly retinoic acid receptor-related orphan receptor (gamma)t+ and respond preferentially under inflammatory conditions. *J. Immunol.* **183**, 2142-2149.

Finger, E.B., Puri, K.D., Alon, R., Lawrence, M.B., von Andrian, U.H., and Springer, T.A. (1996). Adhesion through L-selectin requires a threshold hydrodynamic shear. *Nature* **379**, 266-269.

Garcia, Z., Lemaitre, F., van Rooijen, N., Albert, M.L., Levy, Y., Schwartz, O., and Bousso, P. (2012). Subcapsular sinus macrophages promote NK cell accumulation and activation in response to lymph-borne viral particles. *Blood* **120**, 4744-4750.

Gaya, M., Castello, A., Montaner, B., Rogers, N., Reis e Sousa, C., Bruckbauer, A., and Batista, F.D. (2015). Host response. Inflammation-induced disruption of SCS macrophages impairs B cell responses to secondary infection. *Science* **347**, 667-672.

Gerner, M.Y., Torabi-Parizi, P., and Germain, R.N. (2015). Strategically localized dendritic cells promote rapid T cell responses to lymph-borne particulate antigens. *Immunity* **42**, 172-185.

Gray, E.E., Friend, S., Suzuki, K., Phan, T.G., and Cyster, J.G. (2012). Subcapsular sinus macrophage fragmentation and CD169+ bleb acquisition by closely associated IL-17-committed innate-like lymphocytes. *PLoS One* **7**, e38258.

Gray, E.E., Ramirez-Valle, F., Xu, Y., Wu, S., Wu, Z., Karjalainen, K.E., and Cyster, J.G. (2013). Deficiency in IL-17-committed Vgamma4(+) gammadelta T cells in a

spontaneous Sox13-mutant CD45.1(+) congenic mouse substrain provides protection from dermatitis. *Nat. Immunol.* *14*, 584-592.

Gray, E.E., Suzuki, K., and Cyster, J.G. (2011). Cutting Edge: Identification of a Motile IL-17-Producing $\gamma\delta$ T Cell Population in the Dermis. *J. Immunol.* *186*, 6091-6095.

Grigороva, I.L., Schwab, S.R., Phan, T.G., Pham, T.H., Okada, T., and Cyster, J.G. (2009). Cortical sinus probing, S1P1-dependent entry and flow-based capture of egressing T cells. *Nat. Immunol.* *10*, 58-65.

Groom, J.R., Richmond, J., Murooka, T.T., Sorensen, E.W., Sung, J.H., Bankert, K., von Andrian, U.H., Moon, J.J., Mempel, T.R., and Luster, A.D. (2012). CXCR3 Chemokine Receptor-Ligand Interactions in the Lymph Node Optimize CD4(+) T Helper 1 Cell Differentiation. *Immunity*.

Haas, J.D., Gonzalez, F.H., Schmitz, S., Chennupati, V., Fohse, L., Kremmer, E., Forster, R., and Prinz, I. (2009). Ccr6 and NK1.1 distinguish between IL-17A and IFN- γ -producing $\gamma\delta$ effector T cells. *Eur. J. Immunol.* *39*, 3488-3497.

Heilig, J.S., and Tonegawa, S. (1986). Diversity of murine γ genes and expression in fetal and adult T lymphocytes. *Nature* *322*, 836-840.

Iannacone, M., Moseman, E.A., Tonti, E., Bosurgi, L., Junt, T., Henrickson, S.E., Whelan, S.P., Guidotti, L.G., and von Andrian, U.H. (2010). Subcapsular sinus macrophages prevent CNS invasion on peripheral infection with a neurotropic virus. *Nature* *465*, 1079-1083.

Jafarnejad, M., Woodruff, M.C., Zawieja, D.C., Carroll, M.C., and Moore, J.E., Jr. (2015). Modeling Lymph Flow and Fluid Exchange with Blood Vessels in Lymph Nodes. *Lymphat. Res. Biol.* *13*, 234-247.

Jameson, S.C., Lee, Y.J., and Hogquist, K.A. (2015). Innate memory T cells. *Adv. Immunol.* *126*, 173-213.

Jurasic, G., Iolyeva, M., Proulx, S.T., Halin, C., and Detmar, M. (2010). Thymus cell antigen 1 (Thy1, CD90) is expressed by lymphatic vessels and mediates cell adhesion to lymphatic endothelium. *Exp. Cell Res.* *316*, 2982-2992.

Kastenmuller, W., Torabi-Parizi, P., Subramanian, N., Lammermann, T., and Germain, R.N. (2012). A spatially-organized multicellular innate immune response in lymph nodes limits systemic pathogen spread. *Cell* *150*, 1235-1248.

Kisielow, J., Kopf, M., and Karjalainen, K. (2008). SCART scavenger receptors identify a novel subset of adult gammadelta T cells. *J. Immunol.* *181*, 1710-1716.

Lammermann, T., Bader, B.L., Monkley, S.J., Worbs, T., Wedlich-Soldner, R., Hirsch, K., Keller, M., Forster, R., Critchley, D.R., Fassler, R., and Sixt, M. (2008). Rapid leukocyte migration by integrin-independent flowing and squeezing. *Nature* *453*, 51-55.

Lee, M., Kiefel, H., LaJevic, M.D., Macauley, M.S., Kawashima, H., O'Hara, E., Pan, J., Paulson, J.C., and Butcher, E.C. (2014). Transcriptional programs of lymphoid tissue capillary and high endothelium reveal control mechanisms for lymphocyte homing. *Nat. Immunol.* *15*, 982-995.

Liston, A., Kohler, R.E., Townley, S., Haylock-Jacobs, S., Comerford, I., Caon, A.C., Webster, J., Harrison, J.M., Swann, J., Clark-Lewis, I., *et al.* (2009). Inhibition of Ccr6

function reduces the severity of experimental autoimmune encephalomyelitis via effects on the priming phase of the immune response. *J. Immunol.* *182*, 3121-3130.

Littman, D.R., and Rudensky, A.Y. (2010). Th17 and regulatory T cells in mediating and restraining inflammation. *Cell* *140*, 845-858.

Mabuchi, T., Singh, T.P., Takekoshi, T., Jia, G.F., Wu, X., Kao, M.C., Weiss, I., Farber, J.M., and Hwang, S.T. (2013). Ccr6 is required for epidermal trafficking of gammadelta-T cells in an IL-23-induced model of psoriasiform dermatitis. *J. Invest. Dermatol.* *133*, 164-171.

Macauley, M.S., Crocker, P.R., and Paulson, J.C. (2014). Siglec-mediated regulation of immune cell function in disease. *Nat. Rev. Immunol.* *14*, 653-666.

Miyake, Y., Asano, K., Kaise, H., Uemura, M., Nakayama, M., and Tanaka, M. (2007). Critical role of macrophages in the marginal zone in the suppression of immune responses to apoptotic cell-associated antigens. *J. Clin. Invest.* *117*, 2268-2278.

Mizui, M., Koga, T., Lieberman, L.A., Beltran, J., Yoshida, N., Johnson, M.C., Tisch, R., and Tsokos, G.C. (2014). IL-2 protects lupus-prone mice from multiple end-organ damage by limiting CD4-CD8- IL-17-producing T cells. *J. Immunol.* *193*, 2168-2177.

Nitschke, L., Floyd, H., Ferguson, D.J., and Crocker, P.R. (1999). Identification of CD22 ligands on bone marrow sinusoidal endothelium implicated in CD22-dependent homing of recirculating B cells. *J. Exp. Med.* *189*, 1513-1518.

O'Brien, R.L., and Born, W.K. (2015). Dermal gammadelta T cells--What have we learned? *Cell. Immunol.* *296*, 62-69.

Pegu, A., Flynn, J.L., and Reinhart, T.A. (2007). Afferent and efferent interfaces of lymph nodes are distinguished by expression of lymphatic endothelial markers and chemokines. *Lymphat. Res. Biol.* 5, 91-103.

Pereira, J.P., An, J., Xu, Y., Huang, Y., and Cyster, J.G. (2009). Cannabinoid receptor 2 mediates the retention of immature B cells in bone marrow sinusoids. *Nat. Immunol.* 10, 403-411.

Phan, T.G., Gray, E.E., and Cyster, J.G. (2009). The microanatomy of B cell activation. *Curr. Opin. Immunol.* 21, 258-265.

Phan, T.G., Grigorova, I., Okada, T., and Cyster, J.G. (2007). Subcapsular encounter and complement-dependent transport of immune complexes by lymph node B cells. *Nat. Immunol.* 8, 992-1000.

Qi, H., Kastenmuller, W., and Germain, R.N. (2014). Spatiotemporal basis of innate and adaptive immunity in secondary lymphoid tissue. *Annu. Rev. Cell Dev. Biol.* 30, 141-167.

Ramirez-Valle, F., Gray, E.E., and Cyster, J.G. (2015). Inflammation induces dermal Vgamma4+ gammadeltaT17 memory-like cells that travel to distant skin and accelerate secondary IL-17-driven responses. *Proc. Natl. Acad. Sci. U. S. A.* 112, 8046-8051.

Reichardt, P., Patzak, I., Jones, K., Etemire, E., Gunzer, M., and Hogg, N. (2013). A role for LFA-1 in delaying T-lymphocyte egress from lymph nodes. *EMBO J.* 32, 829-843.

Riol-Blanco, L., Lazarevic, V., Awasthi, A., Mitsdoerffer, M., Wilson, B.S., Croxford, A., Waisman, A., Kuchroo, V.K., Glimcher, L.H., and Oukka, M. (2010). IL-23 receptor regulates unconventional IL-17-producing T cells that control bacterial infections. *J. Immunol.* 184, 1710-1720.

Roark, C.L., Huang, Y., Jin, N., Aydintug, M.K., Casper, T., Sun, D., Born, W.K., and O'Brien, R.L. (2013). A canonical Vgamma4Vdelta4+ gammadelta T cell population with distinct stimulation requirements which promotes the Th17 response. *Immunol. Res.* 55, 217-230.

Rosen, S.D. (2004). Ligands for L-selectin: homing, inflammation, and beyond. *Annu. Rev. Immunol.* 22, 129-156.

Rot, A., and Von Andrian, U.H. (2004). Chemokines in Innate and Adaptive Host Defense: Basic Chemokine Grammar for Immune Cells. *Annu. Rev. Immunol.* 22, 891-928.

Saunderson, S.C., Dunn, A.C., Crocker, P.R., and McLellan, A.D. (2014). CD169 mediates the capture of exosomes in spleen and lymph node. *Blood* 123, 208-216.

Sewald, X., Ladinsky, M.S., Uchil, P.D., Beloor, J., Pi, R., Herrmann, C., Motamedi, N., Murooka, T.T., Brehm, M.A., Greiner, D.L., *et al.* (2015). Retroviruses use CD169-mediated trans-infection of permissive lymphocytes to establish infection. *Science* 350, 563-567.

Sinha, R.K., Park, C., Hwang, I.Y., Davis, M.D., and Kehrl, J.H. (2009). B lymphocytes exit lymph nodes through cortical lymphatic sinusoids by a mechanism independent of sphingosine-1-phosphate-mediated chemotaxis. *Immunity* 30, 434-446.

Smith, L.K., He, Y., Park, J.S., Bieri, G., Snethlage, C.E., Lin, K., Gontier, G., Wabl, R., Plambeck, K.E., Udeochu, J., *et al.* (2015). beta2-microglobulin is a systemic pro-aging factor that impairs cognitive function and neurogenesis. *Nat. Med.* 21, 932-937.

St John, A.L., Ang, W.X., Huang, M.N., Kunder, C.A., Chan, E.W., Gunn, M.D., and Abraham, S.N. (2014). S1P-Dependent trafficking of intracellular yersinia pestis through lymph nodes establishes Buboes and systemic infection. *Immunity* 41, 440-450.

Sung, J.H., Zhang, H., Moseman, E.A., Alvarez, D., Iannacone, M., Henrickson, S.E., de la Torre, J.C., Groom, J.R., Luster, A.D., and von Andrian, U.H. (2012). Chemokine guidance of central memory T cells is critical for antiviral recall responses in lymph nodes. *Cell* 150, 1249-1263.

Teijeira, A., Garasa, S., Pelaez, R., Azpilikueta, A., Ochoa, C., Marre, D., Rodrigues, M., Alfaro, C., Auba, C., Valitutti, S., *et al.* (2013). Lymphatic endothelium forms integrin-engaging 3D structures during DC transit across inflamed lymphatic vessels. *J. Invest. Dermatol.* 133, 2276-2285.

van den Berg, T.K., Nath, D., Ziltener, H.J., Vestweber, D., Fukuda, M., van Die, I., and Crocker, P.R. (2001). Cutting edge: CD43 functions as a T cell counterreceptor for the macrophage adhesion receptor sialoadhesin (Siglec-1). *J. Immunol.* 166, 3637-3640.

Yi, T., Wang, X., Kelly, L.M., An, J., Xu, Y., Sailer, A.W., Gustafsson, J.A., Russell, D.W., and Cyster, J.G. (2012). Oxysterol gradient generation by lymphoid stromal cells guides activated B cell movement during humoral responses. *Immunity* 37, 535-548.

Figure Legends

Figure 1. Rapid induction of IL17 expression by IL7Ra^{hi}Ccr6⁺ innate-like lymphocytes in a CD169+ macrophage-dependent manner following bacterial and fungal challenge. (A) Representative FACS plot showing IL7Ra^{hi}Ccr6⁺ staining of peripheral LN cells from a Cxcr6^{GFP/+} mouse, and Cxcr6-GFP intensity on the gated cells.. (B) Representative FACS plots showing CD3e, TCRb and TCRgd staining of the IL7Ra^{hi}Ccr6⁺ population. Bar graph shows summary frequency data (mean ± sd) for more than 10 mice. (C) Intracellular FACS showing IL17 production among LN cells after 3hr *in vitro* stimulation with IL1b and IL23 or PMA and ionomycin. Graph shows summary data from 3 experiments. (D) Representative FACS plots showing IL17 production among popliteal LN cells 3hrs after footpad challenge with heat inactivated *C. albicans*, *S. aureus* coated bioparticles, and attenuated *Y. pestis*. Summary graph shows % IL17⁺ cells among IL7Ra^{hi}Ccr6⁺ cells. (E) IL17 production by IL7Ra^{hi}Ccr6⁺ cells in control and CD169-DTR macrophage ablated mice treated with *S. aureus* bioparticles as in D, Summary graph shows % IL17⁺ cells among IL7Ra^{hi}Ccr6⁺ cells. (F) *I11b* and *I123a* mRNA level in popliteal LNs of *S. aureus* bioparticle challenged mice relative to controls, determined by qRT-PCR. (G) Summary graph to show % IL17⁺ cells among IL7Ra^{hi}Ccr6⁺ cells between control and ASC deficient mice after 3 hr *S. aureus* bioparticle challenge. ***, p < 0.001 by student's t test. Data are representative of at least two experiments for panels A-C. Data are representative of two or more experiments with at least two mice per group for panels D-G.

Figure 2. IL7Ra^{hi}Ccr6⁺ innate-like lymphocytes are mostly LN resident. (A)

Representative FACS plots showing frequency of IL7Ra^{hi}Ccr6⁺ and Vg4⁺Ccr6⁺ cells in LNs and blood. Graphs show summary data for more than 30 mice of each type. (B) FACS analysis of LN IL7Ra^{hi}Ccr6⁺ cells and naïve ab T cells in KikGR mice before, immediately after and 24 and 48 hrs after photoconversion. Summary data are pooled from three experiments and each point indicates an individual mouse. (C) FACS analysis of LN IL7Ra^{hi}Ccr6⁺ cells and naïve ab T cells in GFP-host and GFP+ host from parabiotic pairs. Summary data are pooled from two experiments and each point indicates an individual mouse. **, p < 0.01, ***, p < 0.001, by student's t test. Data are representative for at least two experiments.

Figure 3. Migration dynamics, sinus exposure and CD169⁺ macrophage

interaction of LN innate-like lymphocytes. (A) Time series of Cxcr6^{GFP/+} cell movement with respect to CD169⁺ SCS macrophages. Upper panels: white arrow indicates a Cxcr6^{GFP/+} lymphocyte in the LN parenchyma that crosses into the SCS. 300 sec time series was taken from a 46µm z stack. Lower panel: white arrow indicates a Cxcr6^{GFP/+} lymphocyte that begins in the SCS and crosses into the LN parenchyma. 360 sec time series was taken from a 34µm z stack. Green, Cxcr6-GFP⁺ lymphocytes; Red, CD169⁺ macrophages; Blue, second harmonic. White dashed line indicates boundary between SCS and LN parenchyma. (B, C) Percent tracks in SCS compartment among the total tracks enumerated (B) and frequency of tracks crossing from the parenchyma into the SCS or out of the SCS into the parenchyma (C) in Cxcr6^{GFP/+} control mice. Each point represents data from a single movie (2 independent experiments). (D) *In vivo* 5

min Thy1-PE labeling of IL7Ra^{hi}Ccr6⁺ cells, Vg4⁺Ccr6⁺ cells and ab T cells, analyzed by flow cytometry. Data are representative of at least 10 mice. (E) *In vivo* Thy1-PE labeling of cells analyzed in tissue sections. Costaining was with CD3-A488 (green) and Lyve1-A647 (blue). White arrows point out Thy1 and CD3 costained cells. (F) Frequency of IL7Ra^{hi}Ccr6⁺, Vg4⁺Ccr6⁺ and naïve αβ T cells positive for CD169. Data are representative of 10 mice. (G) *In vivo* Thy1-PE labeling and CD169 staining on IL7Ra^{hi}Ccr6⁺, Vg4⁺Ccr6⁺ and naïve ab T cells, analyzed by flow cytometry. Data are representative of at least two experiments in each panel.

Figure 4. Ccr6 promotes innate-like lymphocyte positioning near the SCS. (A) *Ccl20* mRNA abundance in sorted LN lymphatic endothelial cells (LEC), blood endothelial cells (BEC), fibroblastic reticular cells (FRC) and double negative stromal cells (DN) determined by qRT-PCR, shown relative to *Hprt*. (B) CCL20 staining of LN section (red). The control (no primary) section was stained with the secondary anti-goat-Cy3 antibody alone. B cells were detected in blue (B220). (C) Transwell migration of IL7Ra^{hi}Ccr6⁺ cells to CCL20. (D) Distribution of Cxcr6^{GFP/+} cells in LNs 3 hrs after saline or CCL20 s.c. injection. Sections were stained to detect Cxcr6-GFP (green) and Lyve1 (blue). (E) Representative FACS plots show Ccr6 surface level, *in vivo* Thy1-PE labeling and CD169 macrophage bleb level on IL7Ra^{hi}Ccr6⁺ cells from control (con) or CCL20 injected mice. Summary graph shows comparison of Thy1-PE labeling and CD169+ staining frequency of IL7Ra^{hi}Ccr6⁺ and Vg4⁺Ccr6⁺ cells from control or CCL20 injected mice. (F) LN sections from Ccr6^{GFP/+} or Ccr6^{GFP/GFP} mice stained for EGFP (green) and B220 (blue). White, SCS: white arrow indicates subcapsular sinus area; FO: B cell

follicle; T: T zone. (G) Comparison of Thy1-PE labeling on IL7Ra^{hi}Ccr6⁺ cells from WT and Ccr6^{GFP/+} or Ccr6^{GFP/GFP} mice. Ccr6 in Het and KO mice was detected based on GFP reporter expression. (H) Comparison of CD169 staining on IL7Ra^{hi}Ccr6⁺ cells from WT, Ccr6^{GFP/+} or Ccr6^{GFP/GFP} mice. (I) Representative FACS plots showing Vg4⁺Scart2⁺ cells amongst gdT cells and the fraction that are Ccr6⁺ (upper), and *in vivo* Scart2-BV605 labeling and CD169 staining (lower). Graph shows summary data. (J) LN sections from Ccr6 Het or KO mice stained for Scart2⁺ (green) and B220 (blue). White, SCS: white arrow indicates subcapsular sinus area; FO: B cell follicle; T: T zone. (K) Representative histogram plot and summary mean fluorescence intensity (MFI) data of IL17 intracellular staining in IL7Ra^{hi}Ccr6⁺ LN cells from Ccr6 Het or KO mice 3 hrs after *S. aureus* bioparticle challenge. *, p < 0.05, **, p < 0.01, ***, p < 0.001, by student's t test. Data are representative of at least two experiments for panel A-D, F, J. Data are representative of two or more experiments with at least two mice per group for panels E, G-I, K.

Figure 5. S1pr1 is required for innate-like lymphocyte movement into the SCS. (A) S1pr1 surface expression on IL7Ra^{hi}Ccr6⁺ and Vg4⁺Ccr6⁺ cells from control or FTY720 treated mice. Negative indicates samples stained with no primary antibody. (B) Transwell migration assay showing % of input cells that migrated to the indicated amounts of S1P or SDF. (C) Representative FACS plots and summary data of *in vivo* Thy1-PE labeling and CD169 staining on IL7Ra^{hi}Ccr6⁺ and Vg4⁺Ccr6⁺ LN cells from control or FTY720 treated mice. (D) Summary graph showing *in vivo* Scart2 labeling on IL7Ra^{hi}Ccr6⁺ Vg4⁺ cells from control or FTY720 treated mice. (E) Representative

histogram plot and summary data of CD169 staining on IL7Ra^{hi}Ccr6⁺ and Vg4⁺Ccr6⁺ LN cells from AUY954 treated mice. (F) GFP, Lyve1 and TCRgd staining of LN sections from control and FTY720 treated Cxcr6-GFP⁺ mice. White, SCS: white arrow indicates subcapsular sinus area; FO: B cell follicle; T: T zone. (G) Scart2 and Lyve1 staining of LN sections from FTY720 treated and control mice. White, SCS: white arrow indicates subcapsular sinus area; FO: B cell follicle; T: T zone. (H) Summary data of *in vivo* Thy1-PE labeling and CD169 staining of the indicated cells in Lyve1-Cre *Sphk1*^{fl/-} *Sphk2*^{-/-} (Sphk DKO) and control mice. (I) Representative FACS plot showing S1pr1 staining on IL7Ra^{hi}Ccr6⁺ cells from a control mouse and histogram plots of CD169 staining on the indicated cells. (J) Representative FACS plot showing S1pr1 staining on IL7Ra^{hi}Ccr6⁺ cells from a control and 5 day tamoxifen treated S1pr1^{ff} CreERt2 mouse, Graphs show summary data for frequency of Thy1-PE labeled and CD169⁺ IL7Ra^{hi}Ccr6⁺ and Vg4⁺Ccr6⁺ cells in control (con) or tamoxifen (tam) treated mice. (K) Representative FACS plots of the type in I for cells from a 2 day tamoxifen treated S1pr1^{ff} CreERt2 mouse. Graph shows CD169⁺ cell frequency amongst S1pr1-negative IL7Ra^{hi}Ccr6⁺ cells. *, p < 0.05, **, p < 0.01, ***, p < 0.001, by student's t test. Data are representative of at least two experiments for panels A-B, E-G, I and two or more experiments with at least two mice per group for panels C-D, H. Data are representative of at least 3 experiments with at least one control and one S1pr1^{ff} CreERt2 mouse for panels J and K. (L) Percent tracks in SCS compartment among the total tracks enumerated in FTY270 treated mice. Each point represents data from a single movie (3 independent experiments). Dashed line is the mean for control mice (data shown in Fig. 3B). The frequency of cells in the SCS differed significantly from the control (p<0.05 by

students t test). (M) Frequency of tracks crossing into and out of the SCS of FTY270 treated mice, enumerated as in L. Dashed lines are the means for control mice (data shown in Fig. 3C). Frequency of tracks crossing into the SCS differed significantly from the control ($p < 0.05$ by students t test).

Figure 6. LFA1 and ICAM1 control innate-like lymphocyte access to the LN parenchyma from the SCS. (A) Representative FACS histogram showing LFA1 staining of IL7R^{hi}Ccr6⁺, Vg4⁺Ccr6⁺ and naïve $\alpha\beta$ T cells. (B) ICAM1 staining of WT and ICAM1 KO LN sections. (C) Adhesion of IL7R^{hi}Ccr6⁺, Vg4⁺Ccr6⁺ cells and naïve $\alpha\beta$ T cells to ICAM1 or BSA. (D) Representative FACS plots and summary graph showing *in vivo* Thy1-PE labeling of IL7R^{hi}Ccr6⁺ cells in 6 hr control or α L blocking antibody treated mice. (E) Summary graph showing *in vivo* Thy1-PE labeling of IL7R^{hi}Ccr6⁺ cells in ICAM1 Het and KO mice. (F, G) IL7R^{hi}Ccr6⁺ and Vg4⁺Ccr6⁺ cell frequencies in LNs (F) and blood (G) from ICAM1 Het and KO mice. (H) Distribution of IL7R^{hi} cells in LN sections from control and α L antibody treated mice. White, SCS: white arrow indicates subcapsular sinus area; FO: B cell follicle; T: T zone. (I) Left panels: Time series of Cxcr6^{GFP/+} cells in LN of control or anti- α L treated mice. Mice were treated with CD11b-PE to label macrophages. Right panel: Axis ratio of Cxcr6^{GFP/+} cells in control and anti- α L treated mice. Cxcr6^{GFP/+} cells in SCS contacting CD11b⁺ macrophages were measured. Data are pooled from 2 independent experiments. *, $p < 0.05$, **, $p < 0.01$, ***, $p < 0.001$, by student's t test. Data are representative of at least two experiments for panels A-C, H-I and two or more experiments with at least two mice per group for panels D-G. (J) Percent of tracks in the SCS compartment among the total tracks

enumerated in anti-aL treated mice. Each point represents data from a single movie (3 independent experiments). Dashed line is the mean for control mice (data shown in Fig. 3B). The frequency of cells in the SCS differed significantly from the control ($p < 0.05$ by students t test). (K) Frequency of tracks crossing into and out of the SCS of anti-aL treated mice, enumerated as in J. Dashed lines are the means for control mice (data shown in Fig. 3C). Frequency of tracks crossing out of the SCS differed significantly from the control ($p < 0.05$ by students t test).

Figure 7. CD169 mediates SCS retention of innate-like lymphocytes. (A) CD169-Fc binding of innate-like lymphocytes. (B) Effect of CD169-deficiency or blocking antibody treatment on macrophage bleb acquisition by IL7Ra^{hi}Ccr6⁺ cells. Cells were stained to detect the macrophage markers CD169 and CD11b. (C) Frequency of tracks crossing into and out of the SCS of anti-CD169 treated mice. Each point represents data from a single movie (3 independent experiments). Frequency of tracks crossing into and out of the SCS differed significantly from the control ($p < 0.05$ by students t test). (D) Number of Vg4⁺Ccr6⁺ cells in LN after 30hr of CD169 blockade. (E) *In vivo* Thy1-PE labeling on Vg4⁺Ccr6⁺ cells after 6hr CD169 blockade. (F) Number and *in vivo* Thy1-PE⁺ labeled Vg4⁺Ccr6⁺ cell frequency in LNs of control (con) or CD169-DTR⁺ mice after DT treatment. (G) Change in innate-like lymphocyte frequency and Thy1-PE labeling over time after treating mice with aL and CD169 blocking antibodies. (H) Effect of 6 hr combined aL and CD169 blockade on IL7Ra^{hi}Ccr6⁺ cell frequency in LN and blood, and fraction of LN cells that are *in vivo* Thy1-PE labeled. (I) Effect of aL blocking in CD169 KO mice on IL7Ra^{hi}Ccr6⁺ cell number and *in vivo* Thy1-PE labeling. (J) IL7Ra^{hi}Ccr6⁺

cell adhesion to CD169-Fc and R97A-Fc coated plates. *, $p < 0.05$, **, $p < 0.01$, ***, $p < 0.001$, by student's t test. Data are representative of at least two experiments for panels A-B, F, I. Data are representative of two or more experiments with at least two mice per group for panels C-E, G-H.

Figure 8. Model of requirements for innate-like lymphocyte surveillance of the LN SCS. (A) Diagram of skin draining LN. (B) Model showing effect of Ccr6-deficiency on innate-like lymphocyte positioning and associated defect in ability to upregulate IL17 in response to IL1-family cytokines produced by SCS macrophages in an ASC-dependent manner. (C) Model showing role of Ccr6-CCL20 in guiding innate-like lymphocyte to lymphatic sinus, S1pr1-S1P in promoting trans-cellular migration into sinus, CD169 on macrophage (MØ) in mediating retention of CD169-ligand^{hi} lymphocyte (green) against lymph flow, and LFA1-ICAM1 in promoting adhesion and transmigration. Green arrows show cell migration and orange arrows show lymph flow.

Supplemental Figures

Figure 3-figure supplement 1. Example of automatically generated tracks for Cxcr6-GFP+ cells in a Cxcr6^{GFP/+} mouse LN. Green, Cxcr6-GFP⁺ lymphocytes; Red, CD11b⁺ macrophages. 5min~30min tracks for Cxcr6-GFP⁺ lymphocytes are shown in colored lines.

Figure 4-figure supplement 1. CCL20 distribution in inguinal LN. Serial sections were stained with anti-CCL20 (A) or without primary antibody (B, C) (red) and anti-B220

(blue). The arrows in A point to staining in the SCS region adjacent to B cell follicles. The controls show that there is non-specific staining in some regions, particularly, in the medulla, but this is minimal in the SCS. The weak staining of the T zone in A but not in the control (panel B) may reflect non-specific binding by the primary antibody since T zone stromal cells showed minimal CCL20 transcript expression (Fig. 4A).

Figure 4-figure supplement 2. Movement of Cxcr6-GFP⁺ cells to SCS location following CCL20 injection. Cxcr6^{GFP/+} mice were injected s.c. with saline (A) or CCL20 (B) and 1 hrs later inguinal LN sections were stained to detect Cxcr6-GFP (green), and Lyve1 (blue).

Figure 4-figure supplement 3. Ccr6 is required for positioning of Ccr6⁺ cells at the SCS. Inguinal LN sections from Ccr6^{GFP/+} (A) and Ccr6^{GFP/GFP} (Ccr6-deficient) (B) mice were stained to detect GFP (green) and B220 (blue). (C) GFP⁺B220⁻ cells were counted manually and percentage of cells within 100 μm of the capsule (indicated by the yellow dashed line in A, B) was calculated. Quantification was done for serial sections of LNs from 3 Ccr6^{GFP/+} and 3 Ccr6^{GFP/GFP} mice.

Figure 4-figure supplement 4. Ccr6 is required for positioning of Scart2⁺ gdT cells at the SCS. Inguinal LN sections from control (Ccr6^{+/-}) (A) and Ccr6^{-/-} (Ccr6 deficient) (B) mice were stained to detect Scart2 (green) and B220 (blue). (C) Scart2⁺ cells were counted manually and percentage of cells within 100 μm of the capsule (indicated by the yellow dashed line in A, B) was calculated. Quantification was done for serial sections of LNs from 3 Ccr6^{+/-} and 3 Ccr6^{-/-} mice.

Figure 5-figure supplement 1. FTY720 treatment depletes SCART2⁺ gdT cells from the SCS. Mice were treated i.v. with saline (A) or FTY720 (B) and 6 hrs later inguinal LN sections were stained to detect Scart2 (green) and Lyve1 (blue). SCS and medulla indicate subcapsular sinus area and medullary area.

Figure 5-figure supplement 2. Frequency of Cxcr6^{GFP/+} cells plotted against their depth from the surface of the LN capsule. Each individual cell's location was determined using the Spots tool in Imaris. The depth, or minimum distance from the cell's center as a Surface object created in Imaris to the capsule, was calculated using a custom Matlab script and the ImarisXT interface. Plots are an aggregate of all experiments for each presented condition (n=3-6 mice per condition). (A) Representative anatomy for reference against the plotted depth. The region adjacent to the LN capsule (blue in image) can be divided into the sinus (depth defined as 0-20 μ m below capsule, represented by gray bars) and the LN parenchyma (depth defined as >20 μ m below capsule, see Movie 1 for dynamics in these regions). Cxcr6⁺ cells (green in image) at the floor of the sinus (depth 15-20 μ m, dark gray bar) and close to the sinus but within the parenchyma (depth 20-28 μ m, blue bar) are both adjacent to CD11b⁺ subcapsular macrophages (red in image). (B) Sixteen hrs after FTY720 treatment, a buildup of Cxcr6^{GFP/+} cells is seen in the parenchyma adjacent to the sinus (blue bar), while a corresponding depletion of cells within the sinus is observed, compared to control mice.

Figure 6-figure supplement 1. Effects of α L blockade on innate-like lymphocyte distribution. (A) Frequency of IL7Ra^{hi}Ccr6⁺ and Vg4⁺Ccr6⁺ LN cells 6 hrs after

treatment with saline or aL blocking antibody. (B) Number of IL7Ra^{hi}Ccr6⁺ cells in peripheral LNs and blood 3 days after treatment with saline or aL blocking antibody. (C) Frequency of Cxcr6^{GFP/+} cells plotted against their depth from the surface of the LN capsule. Four hrs after treatment with aL blocking antibody (alphaL), a marked increase in the number of Cxcr6^{GFP/+} cells at the floor of the sinus (dark gray bar) is observed compared to control mice.

Figure 7-figure supplement 1. Effects of CD169 blockade on innate-like

lymphocyte properties and distribution. (A) CD169 CD11b costaining of

IL7Ra^{hi}Ccr6⁺ cells from control and CD169-deficient LNs. (B) Frequency and Thy1-PE labeling of IL7Ra^{hi}Ccr6⁺ and Vg4⁺Ccr6⁺ LN cells in control and CD169-deficient mice.

(C) Frequency of IL7Ra^{hi}Ccr6⁺ and Vg4⁺Ccr6⁺ LN cells 6 hrs after treatment with saline or CD169 blocking antibody. (D) Frequency of Cxcr6^{GFP/+} cells plotted against their

depth from the surface of the LN capsule. Only slight changes in distribution of

Cxcr6^{GFP/+} cells are observed 4 hrs following treatment with CD169 blocking antibody (CD169), or in CD169^{-/-} Cxcr6^{GFP/+} mice (CD169 KO), compared to control mice. (E)

Frequency of Cxcr6^{GFP/+} cells plotted against their depth from the surface of the LN

capsule. Mice treated for 4 hours with both aL blocking antibody and CD169 blocking

antibody (alphaL+CD169) show a marked decrease in the frequency of Cxcr6⁺ cells at

the sinus floor compared to control mice or mice treated with 4hr aL blocking antibody

(alphaL) alone.

Movie Legends

Movie 1. Cxcr6-GFP⁺ cell shuttling between parenchyma and the SCS.

Representative intravital time-lapse imaging of the popliteal LNs from two Cxcr6^{GFP/+} mice. Overhead 3D video exemplifies the dynamic movement of Cxcr6-GFP⁺ cells (green) within the LN. Two-dimensional video of a 20 μm maximal intensity projection from an orthogonal plane demonstrates the anatomy of the SCS region. An afferent lymphatic vessel (rarely visualized) drains into the SCS, bounded by the collagenous LN capsule (blue, second harmonic signal) and CD11b⁺ SCS macrophages (red). The second example further reveals the motility of Cxcr6-GFP⁺ cells both within the SCS and the LN parenchyma. Cxcr6-GFP⁺ cells are observed to cross from within the LN parenchyma into the SCS, as well as from within the SCS into the LN parenchyma (examples highlighted by circles).

Movie 2. Representative examples of individual Cxcr6-GFP⁺ cells crossing into and out of SCS.

Intravital time-lapse imaging of the popliteal LN from a Cxcr6^{GFP/+} control mouse, highlighting one cell crossing from the parenchyma into the SCS, and one crossing from the SCS into the parenchyma. Cells such as these that clearly crossed from one region were manually identified from automated tracking of all Cxcr6-GFP⁺ cells in an experiment.

Movie 3. Cxcr6-GFP⁺ cellular dynamics following FTY720 treatment.

One hr time-lapse imaging of a popliteal LN in a Cxcr6^{GFP/+} mouse 16 hrs after treatment with FTY720. Cxcr6-GFP⁺ cells (green) can be seen accumulated on the parenchymal side

of the SCS macrophages (red, CD11b⁺), and depleted from the SCS. LN capsule appears blue (second harmonic signal).

Movie 4. Cxcr6-GFP⁺ cell fluttering in the SCS following α L blockade. In Cxcr6^{GFP/+} mice four hrs after treatment with α L blocking antibody, Cxcr6-GFP⁺ cells (green) are observed to flutter at the floor of the SCS. Cxcr6-GFP⁺ cells appear attached to CD11b⁺ SCS macrophages (red) while being buffeted by bulk lymph flow in the SCS, yielding a characteristic fluttering dynamic (video inset and arrowheads). LN capsule appears blue.

Movie 5. Increased movement of SCS Cxcr6-GFP⁺ cells after CD169 blockade and in CD169^{-/-} mice. Representative time-lapse images of Cxcr6^{GFP/+} mice 4 hrs after treatment with CD169 blocking antibody, as well as Cxcr6^{GFP/+} CD169^{-/-} mice. In both conditions there appeared to be an increased frequency of Cxcr6-GFP⁺ cell (green) crossing events, both from the SCS into the LN parenchyma and from the parenchyma into the SCS. LN capsule appears blue and SCS macrophages (CD11b) red.

Movie 6. Decreased Cxcr6-GFP⁺ cell frequency in SCS following α L and CD169 double blockade. Decreased numbers of Cxcr6-GFP⁺ cells (green) are observed in the SCS and LN parenchyma following dual antibody blockade of α L and CD169. Time-lapse imaging in a Cxcr6^{GFP/+} mouse beginning 4 hrs post treatment. LN capsule appears blue and SCS macrophages (CD11b) red.

Movie 7. Addition of CD169 blockade causes release of Cxcr6-GFP⁺ cells from floor of SCS when pre-treated with α L blocking antibody. Representative time-lapse imaging beginning 5 minutes after treatment with CD169 blocking antibody in Cxcr6^{GFP/+} mice pretreated 4 hrs before with α L blocking antibody. Upon addition of CD169 blockade, Cxcr6-GFP⁺ cells (green) detached from the floor of the SCS and entered the bulk lymph flow, rapidly moving away from the field of view (inset and arrowheads). LN capsule appears blue and SCS macrophages (CD11b) red.

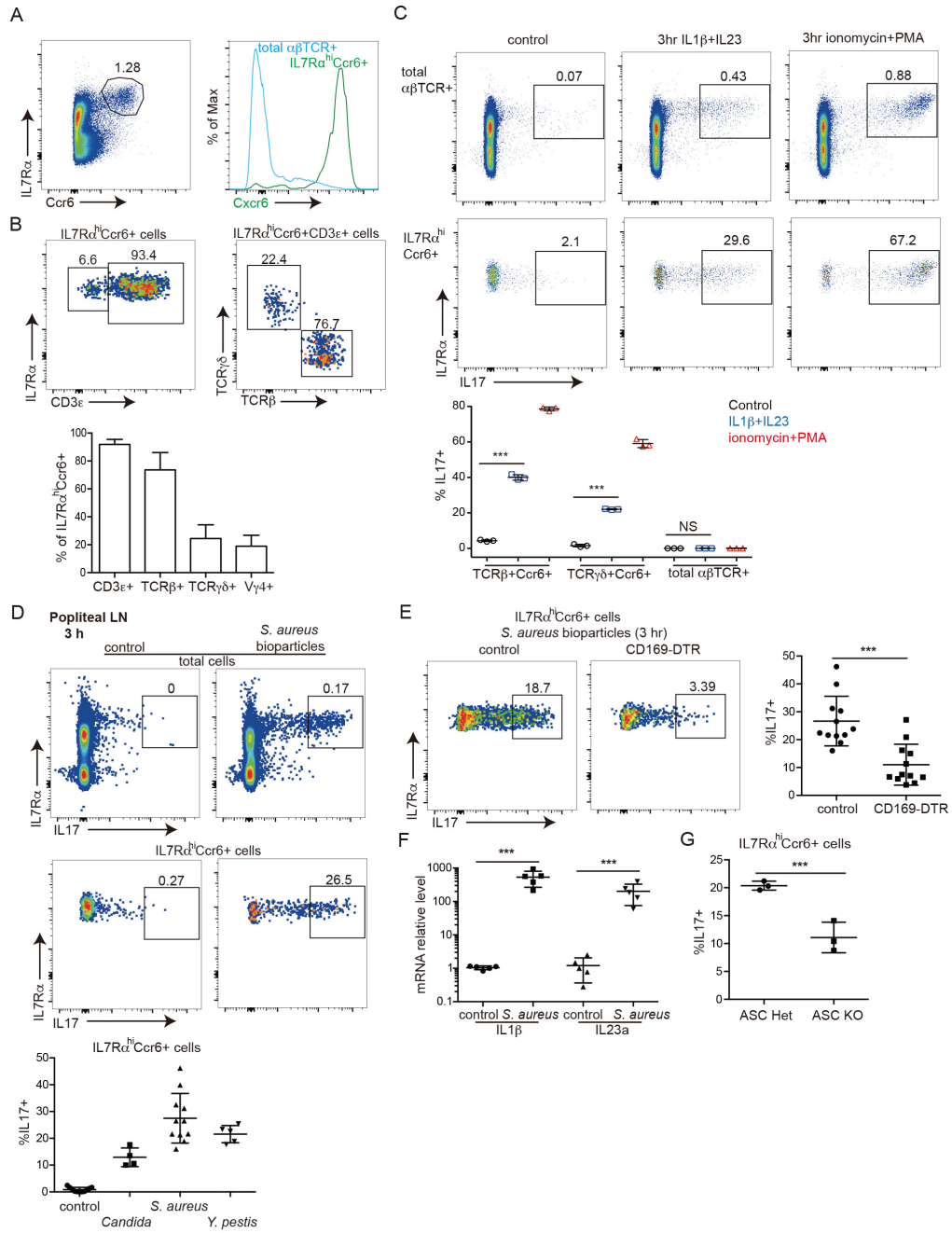


Figure 1

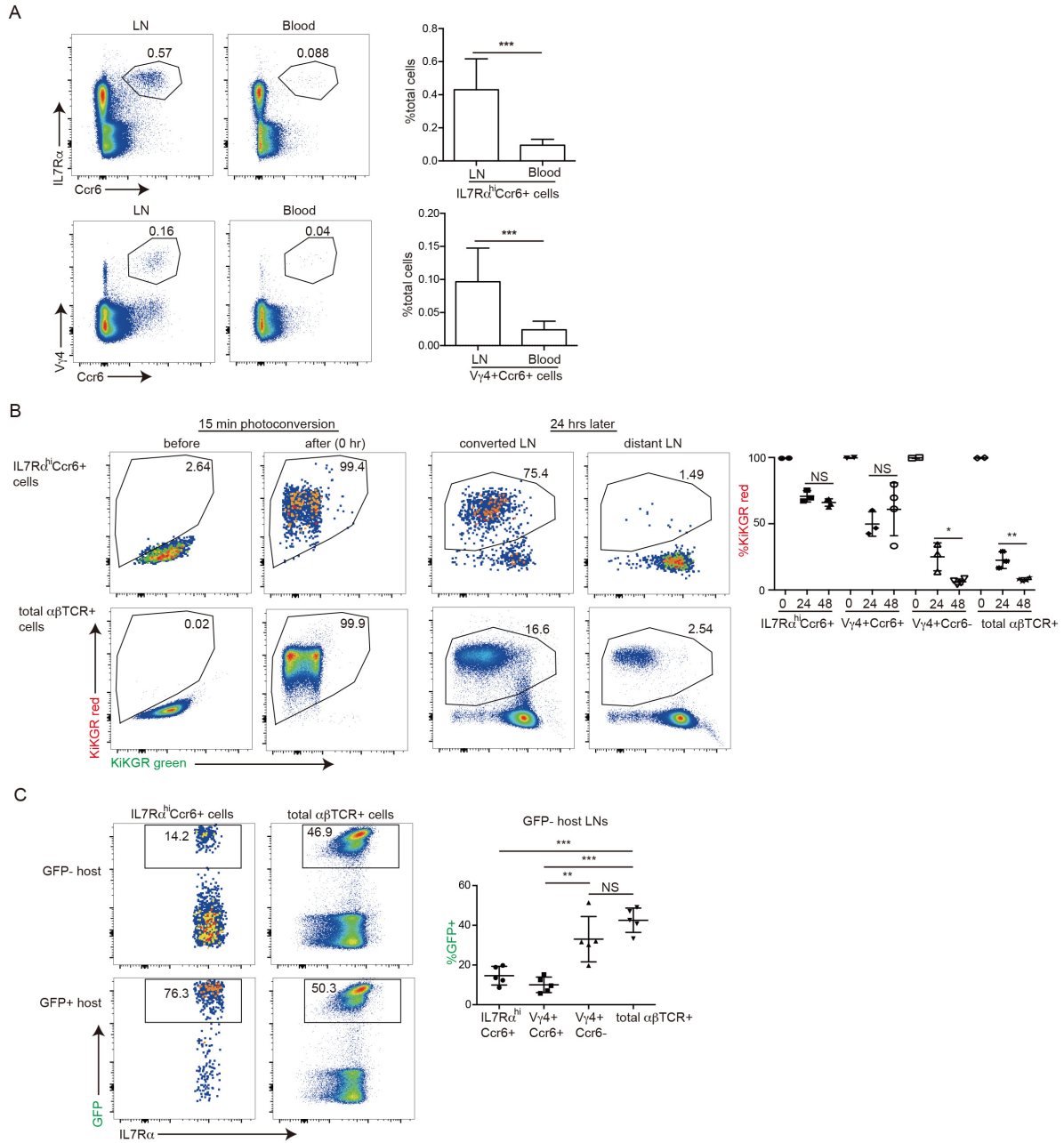


Figure 2

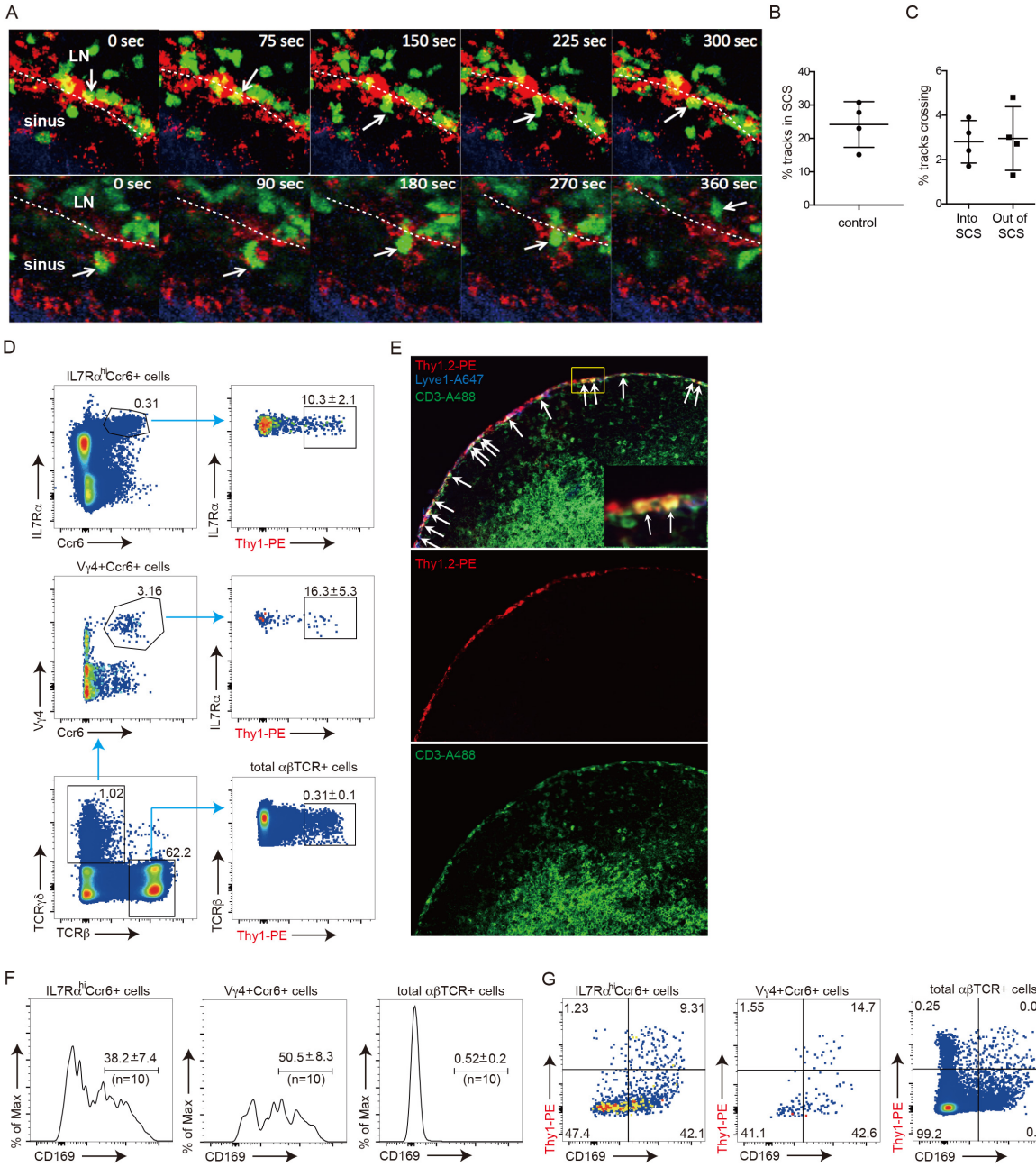


Figure 3

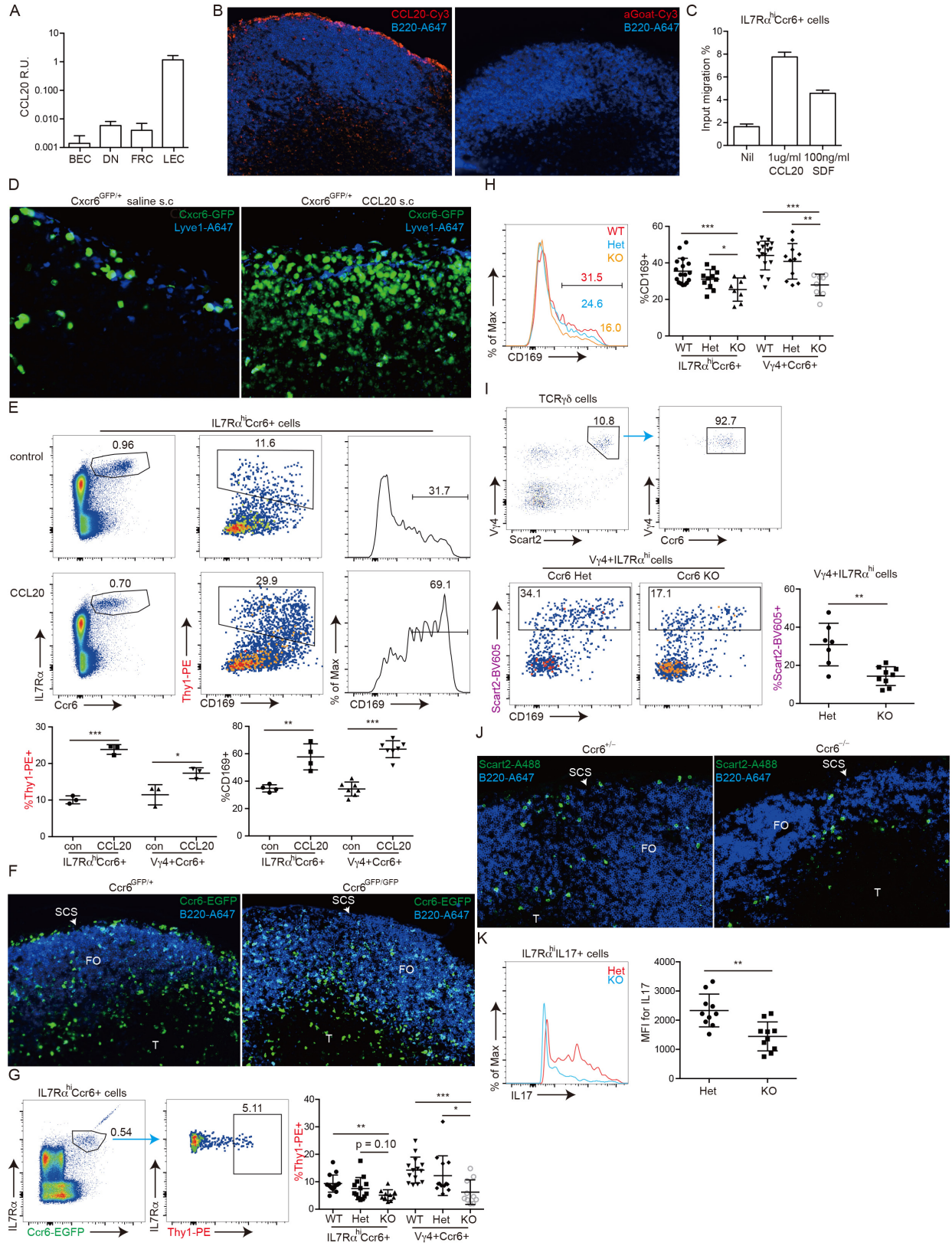


Figure 4

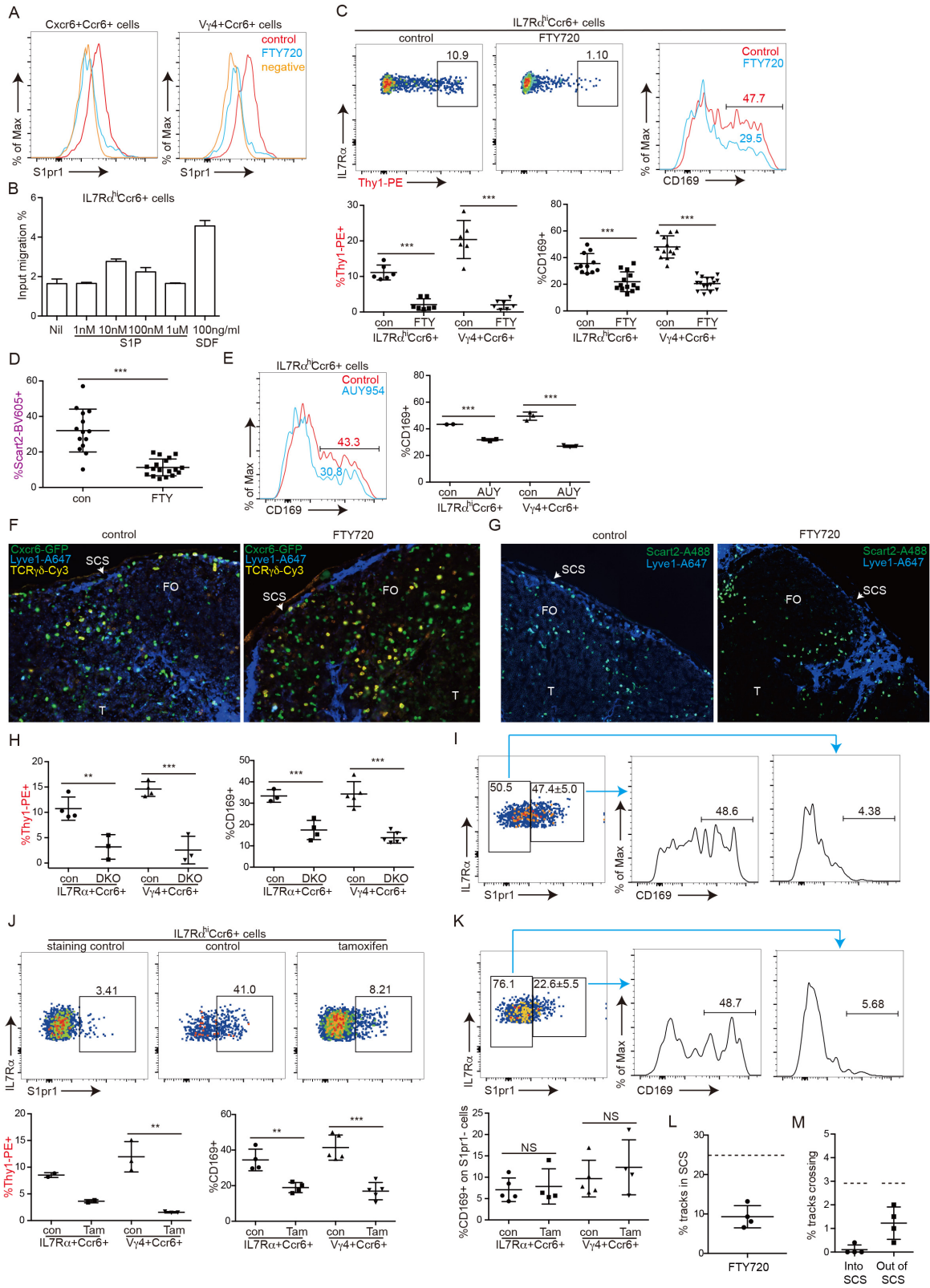


Figure 5

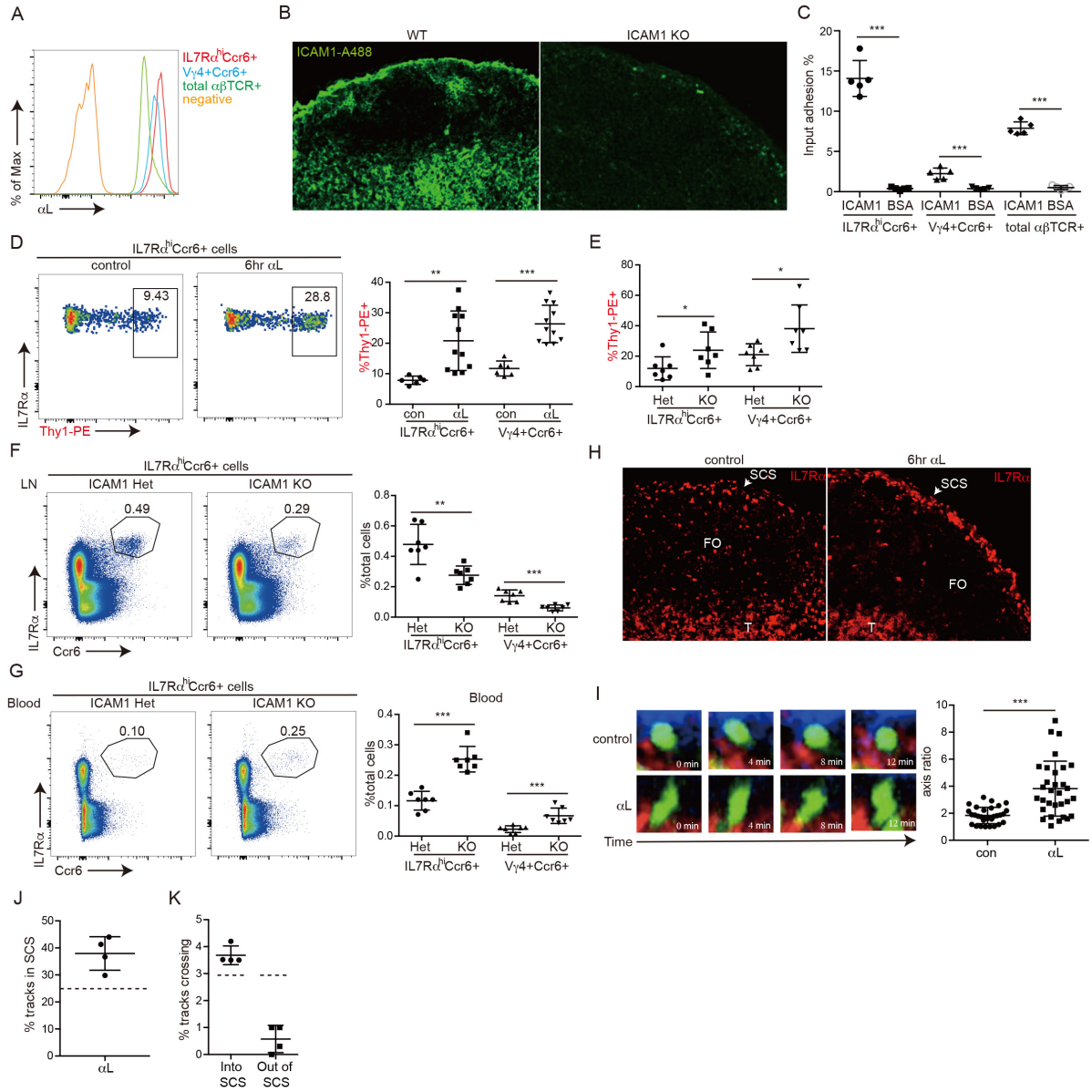


Figure 6

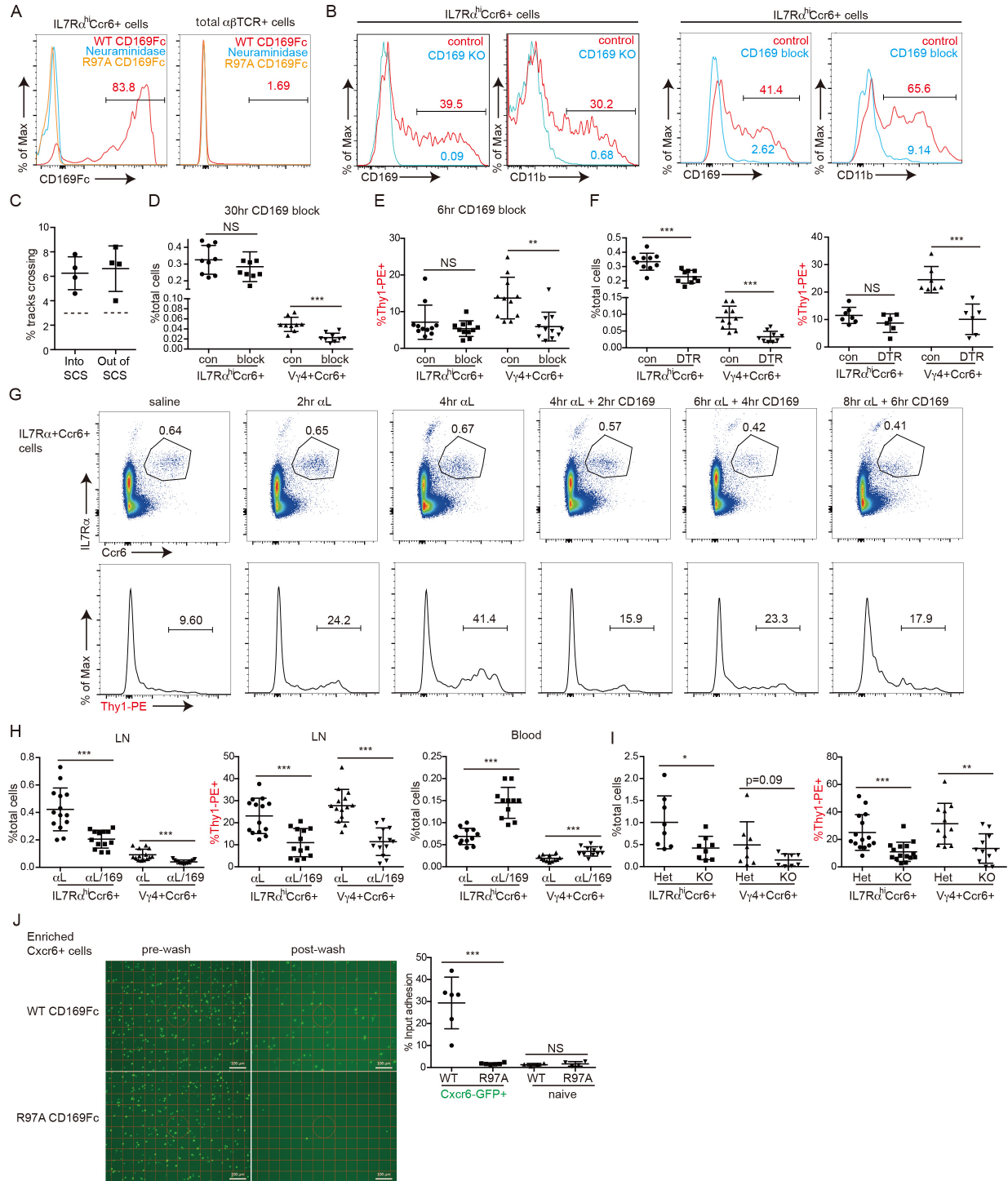


Figure 7

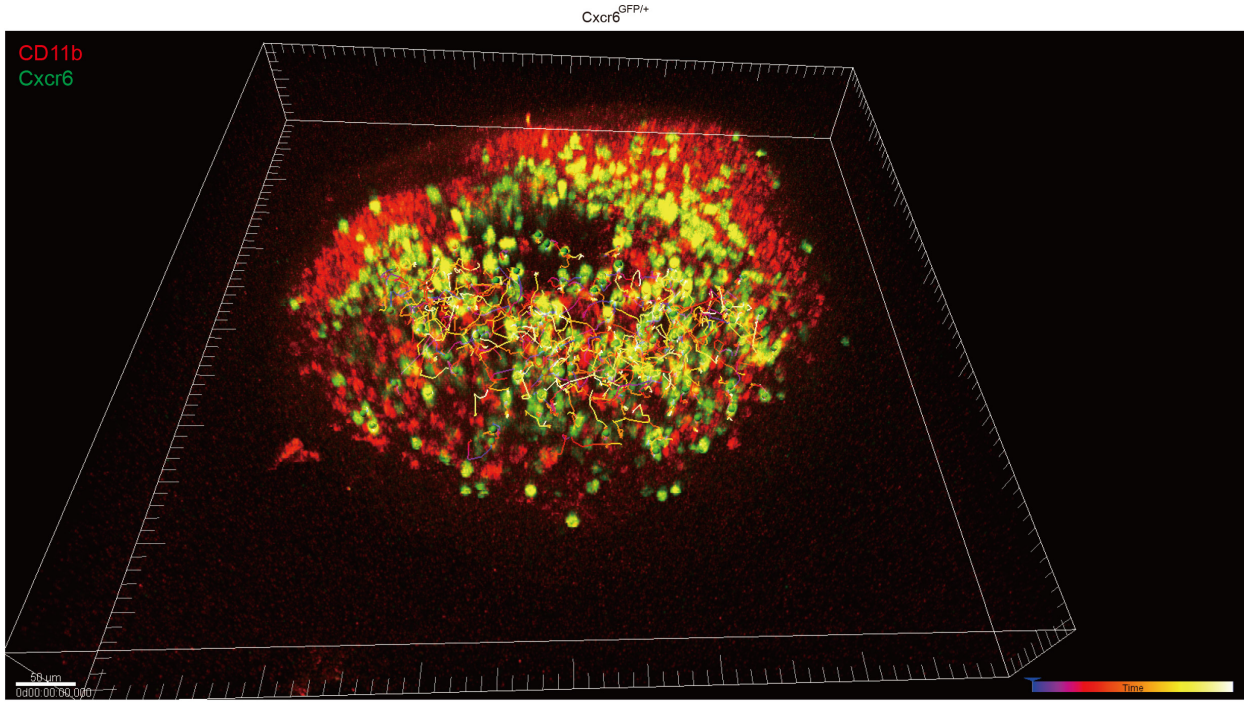


Figure 3-figure supplement 1

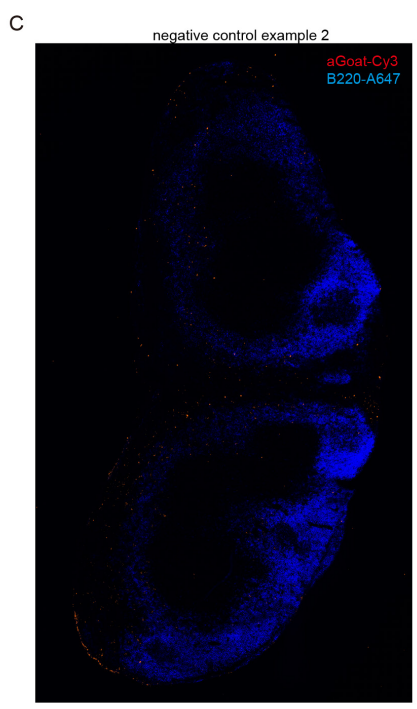
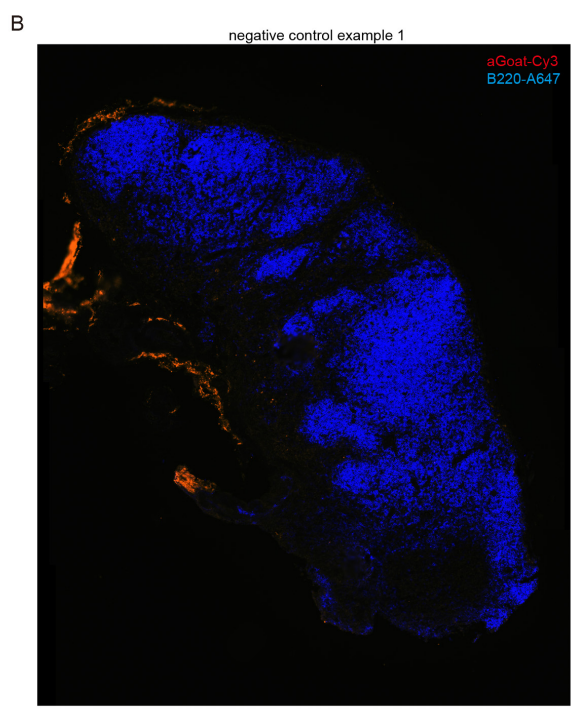
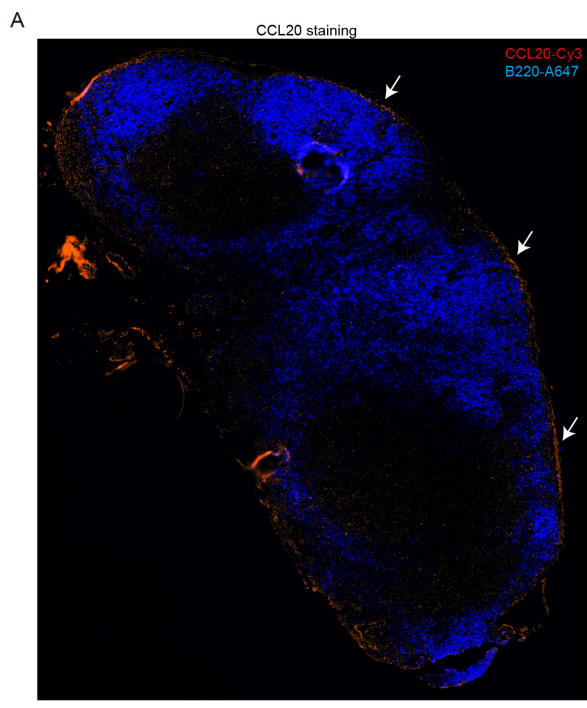
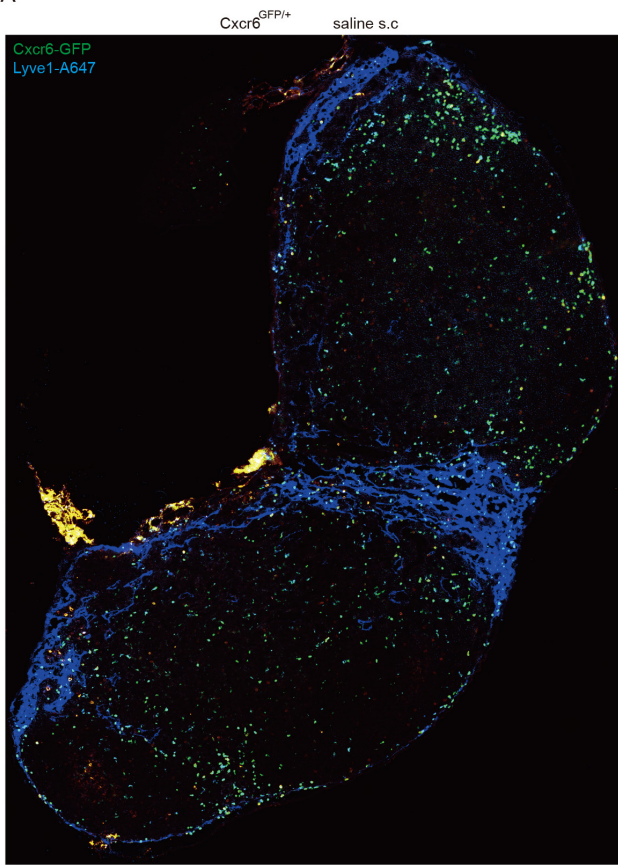


Figure 4-figure supplement 1

A



B

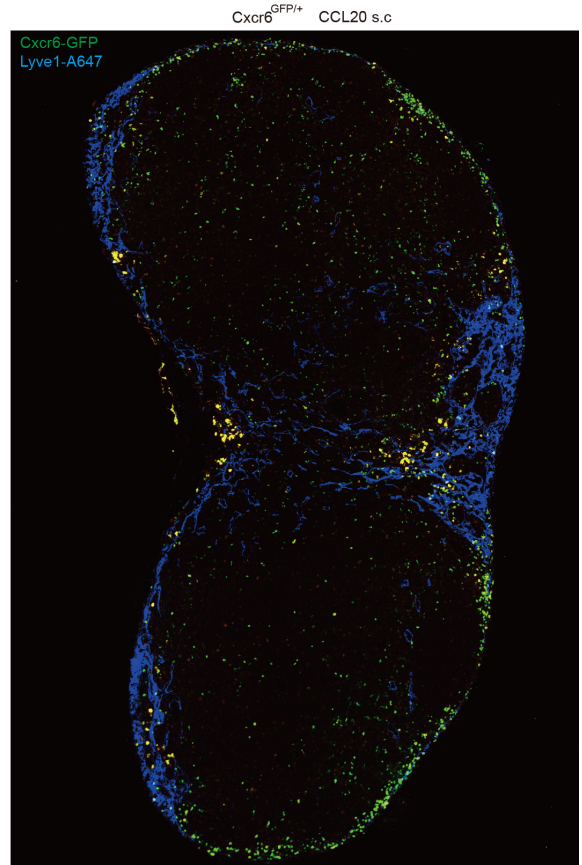


Figure 4-figure supplement 2

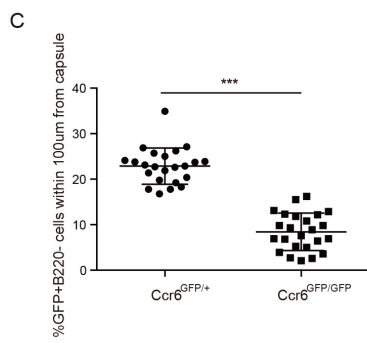
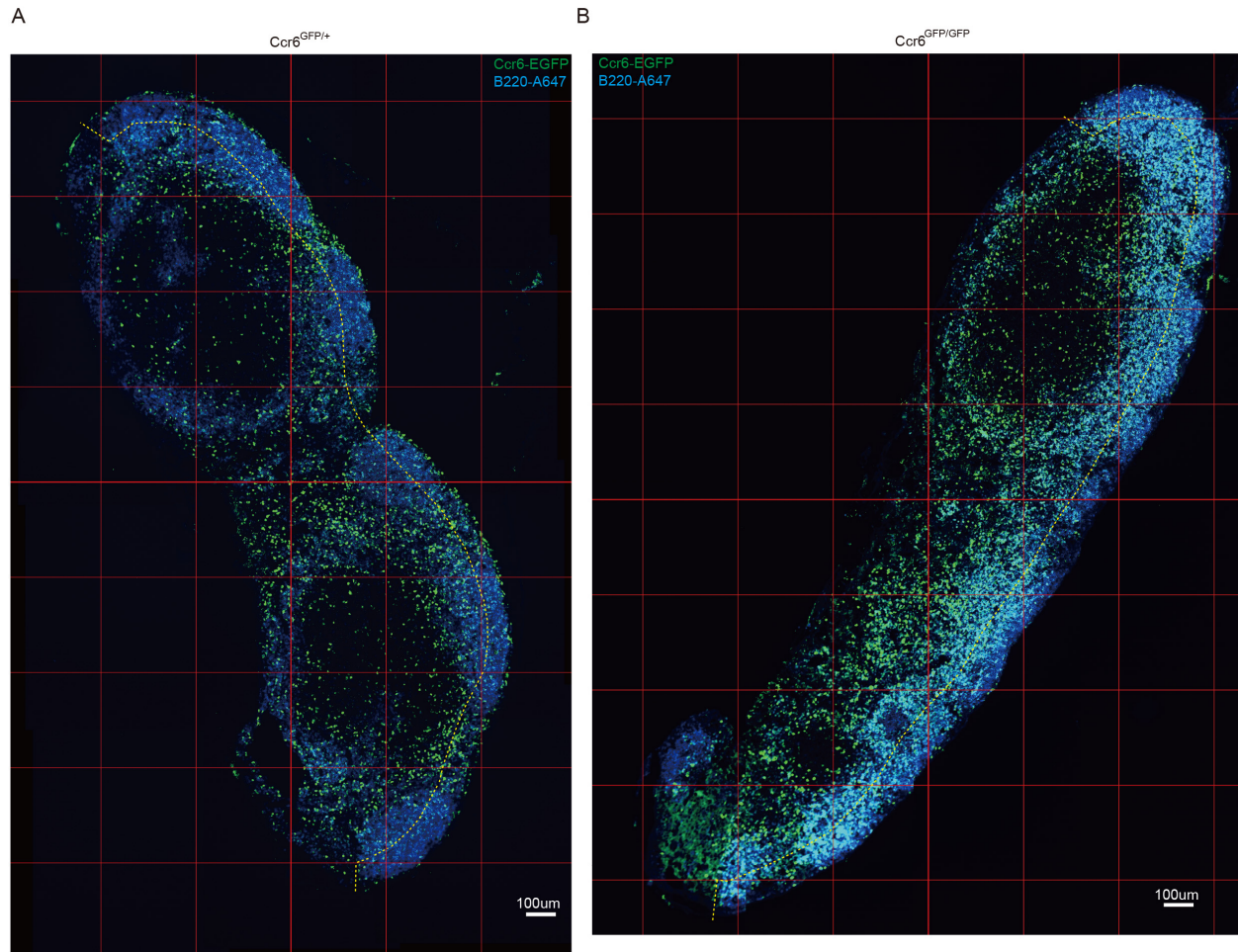
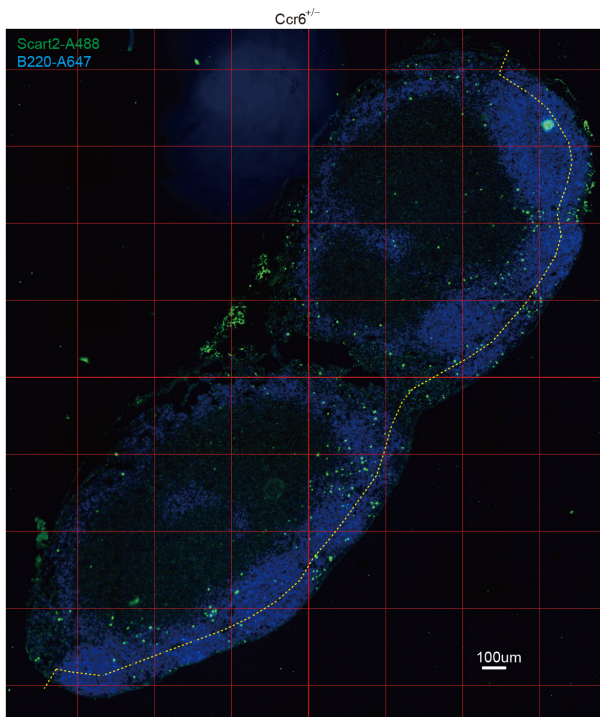
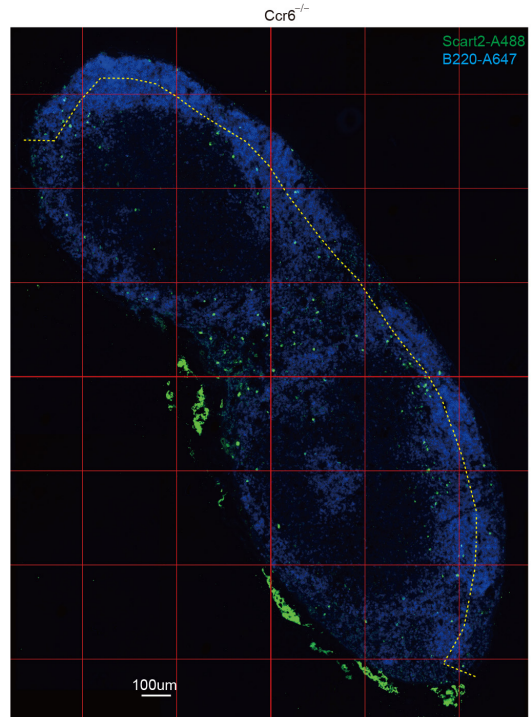


Figure 4-figure supplement 3

A



B



C

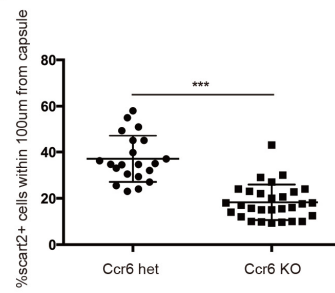
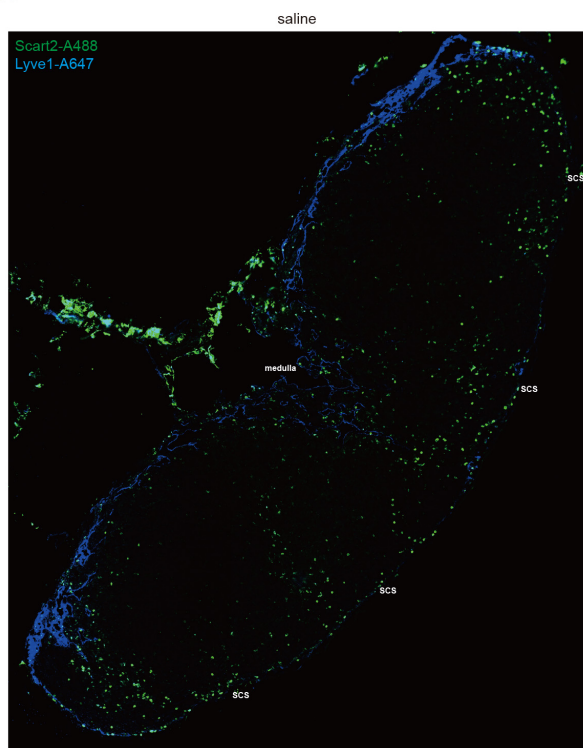


Figure 4-figure supplement 4

A

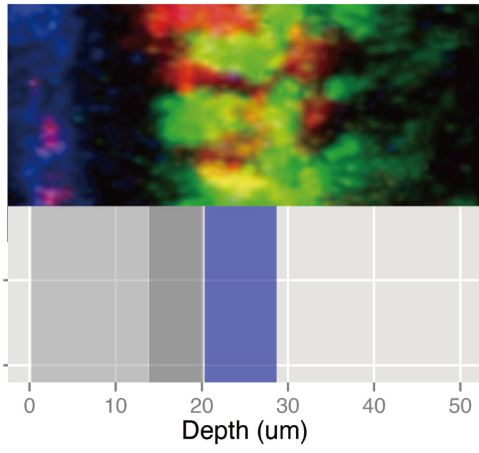


B



Figure 5-figure supplement 1

A



B

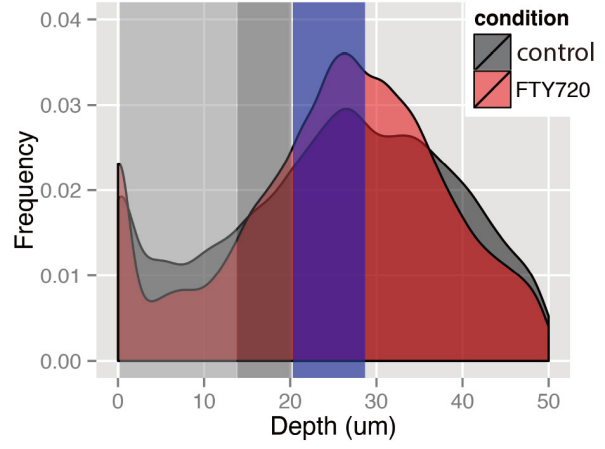


Figure 5-figure supplement 2

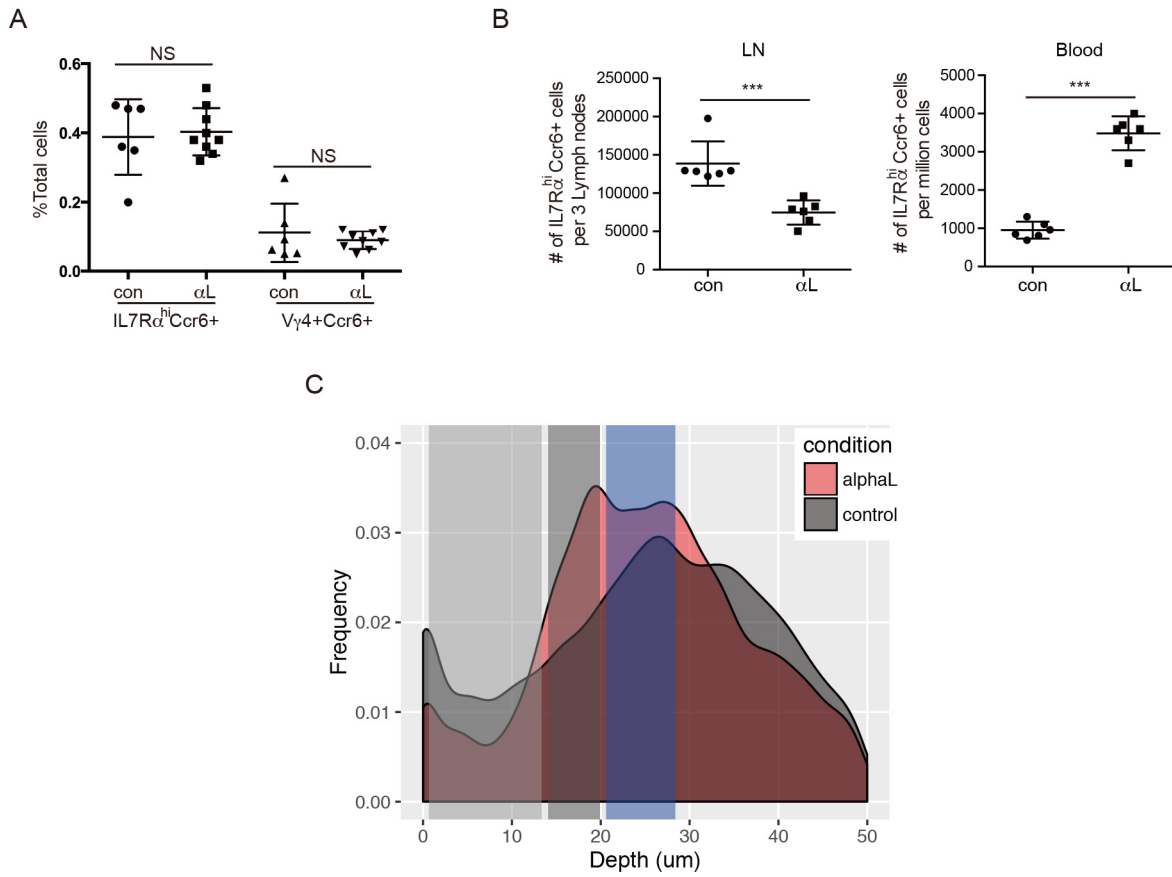


Figure 6-figure supplement 1

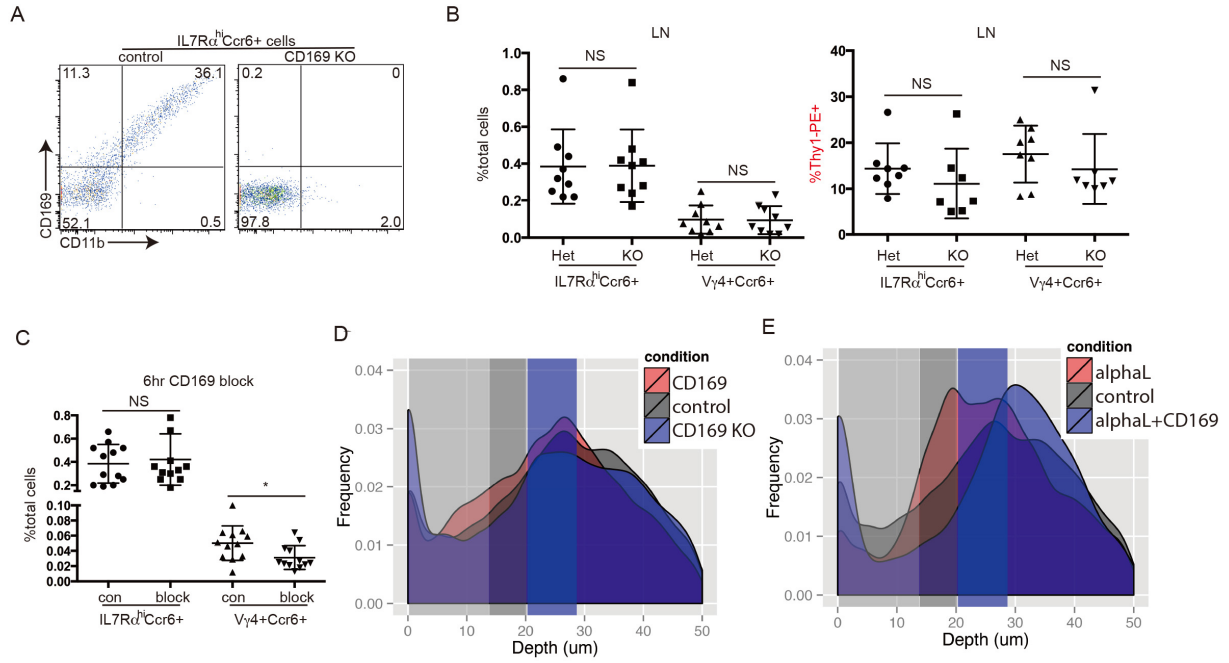


Figure 7-figure supplement 1

Chapter 3

Conclusion and Discussion

This study demonstrated that IL7R α ^{hi} CCR6⁺ innate-like lymphocytes are able to rapidly produce IL17 upon various bacterial and fungal challenges. Their production of IL17 depends on subcapsular sinus (SCS) macrophages. ASC is required for their full capacity of IL17 production. We show innate-like lymphocytes are closely associated with SCS macrophages and we observe their movement into and out of SCS. By photoconversion and parabiosis experiments, we find innate-like lymphocytes are lymph node resident. Through genetic models, immunofluorescence analysis, antibody labeling and in vivo imaging analysis, we find CCR6 promotes their position near SCS macrophages and CCR6 is required for their full capacity to produce IL17. S1PR1 promotes innate-like lymphocytes to access the SCS. LFA1 on innate-like lymphocytes and ICAM1 on lymphatic vessels are important for innate-like lymphocytes to return into the lymph node parenchyma from the SCS. In addition, innate-like lymphocytes express high level of CD169 ligands. We identify a novel role of CD169 in mediating innate-like lymphocytes sinus retention. CD169 together with LFA1 play important roles in keeping innate-like lymphocytes' resident in the lymph node.

In 2010, Gray et al identified a group of $\gamma\delta$ T cells (Gray, E. E. et al., 2011) in dermal skin that were able to produce IL17 upon in vitro stimulation. Those cells also played a pathogenic role in imiquimod induced dermatitis model. The same population (Gray, E. E. et al., 2013) was also found in the skin draining lymph node, suggesting they might be able to mediate rapid inflammatory response against acute challenge. A recent study identified a group of IL7R α^{hi} CCR6 $^{+}$ innate-like lymphocytes present in skin draining lymph nodes. Those innate-like lymphocytes included ~70% $\alpha\beta$ TCR $^{+}$ cells and ~20% $\gamma\delta$ TCR $^{+}$ cells. They exhibited an effector phenotype by expressing a high level of CD44 and a low level CD62L. They had pre-made IL17 messenger RNA (Gray, E. E. et al., 2012) and produced IL17 rapidly upon in vitro stimulation. They were positioned in close proximity to SCS macrophages and had high expression of CD169 ligand to allow for adhesive interaction with SCS macrophages. In this study, we show IL7R α^{hi} CCR6 $^{+}$ innate-like lymphocytes were able to produce IL17 3 hours post acute challenge with attenuated *Yersinia pestis*, *Candida albicans*, and *Staphylococcus aureus*. Their IL17 production required SCS macrophages and intact ASC functionality. Given the fact that they were closely positioned near SCS macrophages, a potential cytokine crosstalk between SCS macrophages and these innate-like lymphocytes could be proposed. Upon acute bacterial/fungal challenge, SCS macrophages captured the pathogen and were activated through pattern recognition receptors. A recent study has shown modified MVA virus (Sagoo, P. et al, 2016) could induce inflammasome activation in

SCS macrophages, which could lead to IL1 β and IL18 production. In our acute challenge model, presumably bacteria and fungal activated SCC macrophage through the inflammasome as well. The processed IL1 β from SCS macrophages activated innate-like lymphocytes resulting in the of IL17. In turn, IL17 could potentially feedback to macrophages to enhance their anti-bacterial, anti-fungal properties. In this study, cytokine IL1 β and IL23 were sufficient to activate innate-like lymphocytes in vitro. And in the in vivo acute challenge model, both IL1 β and IL23 mRNA in LN were unregulated more than 100 fold, so it was more likely those innate-like lymphocytes were predominantly activated through cytokines, although we did not rule out the possibility that innate-like lymphocytes could recognize specialized pathogenic ligands through their TCR under certain circumstances.

Besides IL17-producing innate-like lymphocytes, a different subset of IFN γ -producing innate-like lymphocytes have been identified in close association with SCS macrophages as well. Upon rapid challenge, SCS macrophages are activated and secrete mature IL18. Combining with other cytokines and IL18, innate-like lymphocytes then produce IFN γ to enhance anti-viral/bacterial property of SCS macrophages to mediate barrier immunity in lymph nodes (Kastenmuller, W. et al., 2012; Chapter 1, Figure 2). One future direction that can be taken is to look at the macrophage innate-like lymphocytes crosstalk in real time. This relies on using fluorescent cytokine reporter mice for key cytokines such as IL1 β and IL17 to see if positional correlation between IL1 β signal in SCS macrophages and IL17 signal in innate-like lymphocytes can be observed in real time upon acute challenge.

We next asked the question whether the IL17-producing innate-like lymphocytes were lymph node resident. By photoconversion experiments we found these cells were circulating at a slower rate compared with naïve lymphocytes. Consistent with the photoconversion experiment, 2 weeks post parabiosis also reveal a slower rate chimerism, unlike naïve T lymphocytes, which reach ~50% chimerism between donor and recipient mice in lymph nodes. The majority of the innate-like lymphocytes remained in their original lymph nodes and did not enter circulation. It would be interesting to see if IFN γ -producing innate-like lymphocytes are also lymph node resident. One important question to answer would be how those innate like lymphocytes seed in lymph nodes. Do they develop in the thymus and enter the lymph node through HEVs as naïve T cells, or do they develop in other organs and seed the skin first before arriving the lymph node?

IL17-producing innate-like lymphocytes expressed high level of CCR6 and strongly migrated towards its ligand CCL20 both in vitro and in vivo. We found subcutaneous injection of CCL20 brought innate-like lymphocytes near and into the subcapsular sinus area. Subcutaneously CCL20 injection could presumably mimic the situation of a skin draining chemokine. Keratinocytes express CCL20 and the expression level increases under inflammatory conditions (Homey, B. et al., 2000; Harper, E. G. et al., 2009). Therefore, it is likely the skin draining CCL20 could attract innate-like lymphocytes to the SCS area under both homeostatic and inflammatory conditions. In the absence of CCR6, innate-like lymphocytes were predominantly positioned between B-T boundaries, consistent with a role of CCR6 in guiding innate-like lymphocytes towards SCS. In addition, LECs isolated from LN expressed high level of CCL20 and

immunofluorescence analysis showed CCL20 was localized to lymphatics near the SCS. Similar ligand distribution has been observed in simian. In the primate study, the authors found the CCL20 chemokine ligand (Choi, Y. K. et al., 2003) was specifically localized at the afferent lymphatic but not other sites in the skin draining lymph node. A similar scenario exists in peyer's patch as well. CCL20 was exclusively expressed in the subepithelial dome in the peyer's patch and a recent study has shown activated B cells upregulate CCR6 (Reboldi, A. et al., 2016) and CCR6 promoted their migration towards subepithelial dome to interact with DC, which is important for their IgA isotype switching. In our study in the lymph nodes, we found CCR6 is important for innate-like lymphocytes to migrate towards SCS, which is important for IL17 production of those cells upon acute challenge.

Using intravital two photon microscopy analysis, innate-like lymphocytes could be found in the subcapsular sinus, and occasionally cells could be identified to cross into the SCS from the lymph node parenchyma. Combined with genetic models, in vitro migration, immunofluorescence, in vivo antibody labeling and imaging analysis, we concluded S1PR1 contributed to innate-like lymphocytes' ability to access the SCS. S1PR1 (Matloubian, M. et al., 2004) is the main regulator for naïve lymphocytes egress from the lymph node. Unlike other chemokine receptors, which can mediate long-distance migration, S1PR1 (Grigороva, L. I. et al., 2009) acted at the decision making point for naïve lymphocytes to probe and access the lymphatic sinus. S1P from Lyve1+ lymphatic endothelial cells (Pham, H. T. et al., 2009) was for naïve T cells to egress from the lymph node. Our in vivo antibody labeling and FACS analysis suggest S1P from Lyve1+ lymphatic cells are also important for innate-like lymphocytes to access

SCS. One big difference between lymphatics near the SCS and other sites in lymph node is that lymphatics near SCS are closely associated with CD169+ macrophages. So S1PR1 may not only promote innate-like lymphocytes access SCS, but also promote their interaction and surveillance of SCS macrophages. In addition, scart2 is a scavenger receptor related to bovine scavenger receptor WC1 family, which has been describe to recognize pathogenic bacteria *Leptospira spp* and *Borrelia burgdorferi* (Hsu, H. et al., 2015). Vg4+CCR6+ $\gamma\delta$ T cells, as a subset of innate-like lymphocytes described in our study, expressed high level of scart2. So by promoting their SCS accessing through S1PR1, they might be able to directly sample antigens and pathogens present in lymph through scavenger receptor scart2. Overall, S1PR1 promotes innate-like lymphocytes to access SCS, which could potentially facilitate their surveillance of SCS macrophages and direct sampling of lymph borne antigens.

Although innate-like lymphocytes can be found in the SCS, they are lymph node resident, indicating there are mechanisms allowing them to stay in the lymph node without flushing away by lymph flow. By intravital two photon microscopy, occasionally we could find innate-like lymphocytes cross back into lymph node parenchyma from SCS, which could contribute to their LN resident property. Innate-like lymphocytes expressed high level of LFA1 integrin and lymphatic endothelial cells express high level of its ligand, ICAM1. Inspired by the important finding in the mid 80s that LFA1 was critical for naïve lymphocytes to stop on blood vessel and cross into lymph node through HEV (Hamann, A. et al., 1988), we found LFA1 played a similar role in getting innate-like lymphocytes back into lymph node parenchyma from SCS. Blocking LFA1 for 6 hours caused innate-like lymphocytes to accumulate and stick in the SCS. They

became elongated and were flowing by passing lymph flow. One of the questions remained to be answered is what chemokine/chemokine receptor is involved in activation of LFA1 on innate-like lymphocytes. In naïve lymphocytes, it is well known that CCL21-CCR7 is important for LFA1 activation on naïve T cells to facilitate their lymph node homing (Andrian, H. U. et al., 2003). However, innate-like lymphocytes express low level of CCR7, and they express high level of CCR6 and EBI2. Signal through CCR6 and EBI2 may facilitate LFA1 activation to get them to cross through the lymphatic endothelial layer into the lymph node parenchyma. A recent study also reported a role of LFA1 in regulating naïve lymphocytes egress. By adoptive transfer, the authors found LFA1⁺ T cells had prolonged LN residence time compared with LFA1⁻ T cells, and LFA1⁺ T cells (Reichardt, P. et al., 2013) returned back to lymph node parenchyma more frequently compared with LFA1⁻ T cells after they probed the cortical or medullary lymphatic sinus. Consistent with our study, LFA1 plays an important role in guiding sinus-exposed lymphocytes back into lymph node.

Although LFA1 is important for innate-like lymphocytes to get back into lymph node parenchyma once they get exposed to the sinus, short-term LFA1 blocking caused innate-like lymphocytes to accumulate and stick in the SCS, indicating there existed additional adhesive players in retaining innate-like lymphocytes against lymph flow in SCS. By using genetic model, in vitro adhesion assay, in vivo antibody labeling and imaging analysis, we found innate-like lymphocytes expressed high level of CD169 ligand and identified a novel role of CD169 in mediating sinus retention. As a member of the Siglec family of sialic acid-binding lectins, CD169 has been shown to interact and internalized virus particle. Many viruses have evolved to have CD169 ligand on their

viral particle to be internalized and replicate within CD169+ macrophages, potentially protecting the virus from other immune components. It has been reported that porcine CD169 can mediate capture and internalization of porcine reproductive and respiratory syndrome virus (PRRSV) (Baere, D. M. et al., 2012), which probably could be utilized by PRRSV to replicate within CD169+ macrophages in safety. CD169 can also mediate the capture of HIV-1 virus by interacting with Ganglioside GM3, a host derived glycosphingolipid incorporated in the membrane of HIV-1 viral particle (Yu, X. et al. 2014). HIV-1 infectivity was preserved after been internalized by CD169+ macrophages or dendritic cells, which could be a potential mechanism to facilitate HIV-1 systemic spread. CD169 has also been shown as critical receptor for exosomes. B cell derived exosomes (Saunderson, C. S. et al. 2014) can be captured by marginal zone and subcapsular sinus macrophages through CD169, which can modulate macrophage proinflammatory activity. In our study, we found CD169 could also be used to mediating interaction with cells from self (in this case innate-like lymphocytes) to mediate their sinus retention. Besides subcapsular sinus, CD169 is expressed in marginal zone sinus of spleen, kidney medullary interstitium, and blood-brain barrier. The unique expression pattern of CD169 between tissue parenchyma and vasculature structure may indicate a general role of CD169 to retain certain cell types in sinus or vessels to resist against shear force. In addition, higher density of CD169+ macrophages (Saito, Y. et al. 2015) present in the draining lymph node in melanoma patients have been significantly associated with better overall survival and less tumor metastasis. In our unpublished study, we have shown various tumor cell lines express high level of CD169 ligand, so a higher density of CD169 macrophages in the draining lymph node may contribute to

retain malignant tumor cells locally without systemic spread. Overall, in this study, we identified a novel mechanism for CD169 to mediate cell-cell interaction for innate-like lymphocytes sinus retention.

In this study, we mainly defined organization cues involved in positioning IL17-producing innate-like lymphocytes near the SCS, and we found molecules involved in adhesion to keep innate-like lymphocytes resident in LNs. A few important future questions remain to be answered. First, since currently we gate on those innate-like lymphocytes based on IL7R α and CCR6 expression, it would be helpful to use fluorescent IL17 messenger reporter mice to identify them more precisely, which would facilitate imaging analysis, developmental studies and gene expression profiles for sorted populations. Second, although innate-like lymphocytes can produce IL17 rapidly after acute challenge, direct functional assay of these cells is lacking. So it may be worthwhile to make CXCR6-DTR or CCR6-DTR mice to transiently ablate them before bacterial challenge to see if they are critical for controlling bacterial and if they play a role in influencing adaptive immune response. Third, how is IL17 mRNA per-transcribed in those innate-like lymphocytes: do there exist tonic signals in the skin or in the lymph node responsible for their IL17 transcription? Does flora in skin play a role in maintaining innate-like lymphocytes maturation and homeostasis in lymph node? A lot can be learned in the future, by understanding the barrier immunity of secondary lymphoid tissues, we can better understand how innate and adaptive immunity can be coordinated and cooperated to mediate immune response against infectious agents in the same organ.

References

- Andrian, H. U., Mempel, R. T. Homing and cellular traffic in lymph nodes. *Nat Rev Immunology*. 3. 867-878. (2003)
- Baere, D. M. et al. Interaction of the european genotype porcine reproductive and respiratory syndrome virus (PRRSV) with sialoadhesin (CD169/Siglec-1) inhibits alveolar macrophage phagocytosis. *BioMed Central*. 42. 47. (2012)
- Choi, Y.K., Fallert, B.A., Murphey-Corb, M.A., and Reinhart, T.A. Simian immunodeficiency virus dramatically alters expression of homeostatic chemokines and dendritic cell markers during infection in vivo. *Blood*. 101. 1684-1691. (2003)
- Gray, E. E., Suzuki, K., Cyster, G. J. Cutting Edge: Identification of a motile IL-17-producing $\gamma\delta$ T cell population in the dermis. *J. Immunol*. 186. (2011)
- Gray, E. E., Friend, S., Suzuki, K., Phan, G. T., Cyster, G. J. Subcapsular sinus macrophages fragmentation and CD169+ bleb acquisition by closely associated IL17-committed innate-like lymphocytes. *Plos One*. 7. e38258. (2012)
- Gray, E. E. et al. Deficiency in IL-17-committed V γ 4+ $\gamma\delta$ T cells in a spontaneous Sox13-mutant CD45.1⁺ congenic mouse substrain provides protection from dermatitis. *Nature Immunology*. 14. 584-592. (2013)
- Grigorova, L. I. et al. Cortical sinus probing, S1P₁-dependent entry and flow-based capture of egressing T cells. *Nature Immunology*. 10. 58-65. (2009)
- Hamann, A. et al. Evidence for an accessory role of LFA-1 in lymphocyte-high endothelium interaction during homing. *J. Immunol*. 140. 693-699. (1988)

Harper, E. G. et al. Th17 cytokines stimulate CCL20 expression in keratinocytes in vitro and in vivo: implications for psoriasis pathogenesis. *J Invest Dermatol.* 129. 2175-2183. (2009)

Homey, B. et al. Up-regulation of Macrophage inflammatory protein-3 α /CCL20 and CC chemokine receptor 6 in psoriasis. *J. Immunol.* 164. 6621-6632. (2000)

Hsu, H. et al. WC1 is a hybrid $\gamma\delta$ TCR coreceptor and pattern recognition receptor for pathogenic bacteria. *J. Immunol.* 194. 2280-2288. (2015)

Kastenmuller, W., Torabi-Parizi, P., Subramanian, N., Lammermann, T., Germain, N. R. A spacially-organized multicellular innate immune response in lymph nodes limits systemic pathogen spread. *Cell.* 150. 1235-1248. (2012)

Matloubian, M. et al. Lymphocytes egress from thymus and peripheral lymphoid organs is dependent on S1P receptor 1. *Nature.* 427. 355-360. (2004)

Pham, H. T. et al. Lymphatic endothelial cell sphingosine kinase activity is required for lymphocyte egress and lymphatic patterning. *The Journal of Experimental Medicine.* 207. 17-27. (2009)

Reboldi, A. et al. IgA production requires B cell interaction with subepithelial dendritic cells in peyer's patches. *Science.* 352. aaf4822-1-10. (2016)

Reichardt, P. et al. A role of LFA-1 in delaying T-lymphocyte egress from lymph nodes. *The EMBO Journal.* 32. 829-843. (2013)

Sagoo, P. et al. In vivo imaging of inflammasome activation reveals a subcapsular macrophage burst response that mobilizes innate and adaptive immunity. *Nature Medicine.* 22. 64-71 (2016)

Saito, Y. et al. Prognostic significance of CD169+ lymph node sinus macrophages in patients with malignant melanoma. *Cancer Immunology Research*. 3. 1356-1363. (2015)

Saunderson, C. S. et al. CD169 mediates the capture of exosomes in spleen and lymph node. *Blood*. 123. 208-216. (2014)

Yu, X. et al. Glycosphingolipid-functionalized nanoparticles recapitulate CD169-dependent HIV-1 uptake and trafficking in dendritic cells. *Nature Communications*. 5. 4136. (2014)

Publishing Agreement

It is the policy of the University to encourage the distribution of all theses, dissertations, and manuscripts. Copies of all UCSF theses, dissertations, and manuscripts will be routed to the library via the Graduate Division. The library will make all theses, dissertations, and manuscripts accessible to the public and will preserve these to the best of their abilities, in perpetuity.

Please sign the following statement:

I hereby grant permission to the Graduate Division of the University of California, San Francisco to release copies of my thesis, dissertation, or manuscript to the Campus Library to provide access and preservation, in whole or in part, in perpetuity.

Yang Zhang
Author Signature

Aug 8, 2016
Date